



Correlated long-range mixed-harmonic fluctuations measured in pp , $p+Pb$ and low-multiplicity $Pb+Pb$ collisions with the ATLAS detector

The ATLAS Collaboration*



ARTICLE INFO

Article history:

Received 6 July 2018

Received in revised form 7 October 2018

Accepted 13 November 2018

Available online 2 January 2019

Editor: D.F. Geesaman

ABSTRACT

Correlations of two flow harmonics v_n and v_m via three- and four-particle cumulants are measured in 13 TeV pp , 5.02 TeV $p+Pb$, and 2.76 TeV peripheral $Pb+Pb$ collisions with the ATLAS detector at the LHC. The goal is to understand the multi-particle nature of the long-range collective phenomenon in these collision systems. The large non-flow background from dijet production present in the standard cumulant method is suppressed using a method of subevent cumulants involving two, three and four subevents separated in pseudorapidity. The results show a negative correlation between v_2 and v_3 and a positive correlation between v_2 and v_4 for all collision systems and over the full multiplicity range. However, the magnitudes of the correlations are found to depend on the event multiplicity, the choice of transverse momentum range and collision system. The relative correlation strength, obtained by normalisation of the cumulants with the $\langle v_f^2 \rangle$ from a two-particle correlation analysis, is similar in the three collision systems and depends weakly on the event multiplicity and transverse momentum. These results based on the subevent methods provide strong evidence of a similar long-range multi-particle collectivity in pp , $p+Pb$ and peripheral $Pb+Pb$ collisions.

© 2019 The Author. Published by Elsevier B.V. This is an open access article under the CC BY license (<http://creativecommons.org/licenses/by/4.0/>). Funded by SCOAP³.

1. Introduction

One of the goals in the studies of azimuthal correlations in high-energy nuclear collisions at the Relativistic Heavy Ion Collider (RHIC) and the Large Hadron Collider (LHC) is to understand the multi-parton dynamics of QCD in the strongly coupled non-perturbative regime [1]. Measurements of azimuthal correlations in small collision systems, such as pp , $p+A$ or $d+A$ collisions, have revealed the ridge phenomenon [2–6]: enhanced production of particle pairs at small azimuthal angle separation, $\Delta\phi$, extended over a wide range of pseudorapidity separation, $\Delta\eta$. The azimuthal structure has been related to harmonic modulation of particle densities, characterised by a Fourier expansion, $dN/d\phi \propto 1 + 2 \sum_{n=1}^{\infty} v_n \cos n(\phi - \Phi_n)$, where v_n and Φ_n represent the magnitude and the event-plane angle of the n th-order flow harmonic. They are also conveniently represented by the flow vector: $\mathbf{v}_n = v_n e^{in\Phi_n}$. The v_n are known to depend on the collision system, but have weak dependence on collision energies [6,7]. The ridge reflects multi-parton dynamics early in the collision and has generated significant interest in the high-energy physics community. A key question is whether the long-range multi-particle collectivity reflects initial momentum correlation from gluon sat-

uration effects [8], or a final-state hydrodynamic response to the initial transverse collision geometry [9].

Further insight into the ridge phenomenon is obtained via a multi-particle correlation technique, known as cumulants, involving three or more particles [10–12]. The multi-particle cumulants probe the event-by-event fluctuation of a single flow harmonic v_n , as well as the correlated fluctuations between two flow harmonics, v_n and v_m . These event-by-event fluctuations are often represented by probability density distributions $p(v_n)$ and $p(v_n, v_m)$, respectively. For instance, the four-particle cumulants $c_n\{4\} = \langle v_n^4 \rangle - 2\langle v_n^2 \rangle^2$ constrain the width of $p(v_n)$ [10], while the four-particle symmetric cumulants $sc_{n,m}\{4\} = \langle v_n^2 v_m^2 \rangle - \langle v_n^2 \rangle \langle v_m^2 \rangle$ quantify the lowest-order correlation between v_n and v_m [12]. The three-particle asymmetric cumulants such as $ac_n\{3\} = \langle \mathbf{v}_n^2 \mathbf{v}_{2n}^* \rangle = \langle v_n^2 v_{2n} \cos 2n(\Phi_n - \Phi_{2n}) \rangle$ [5,13] are sensitive to correlations involving both the flow magnitude v_n and flow phase Φ_n .

One of the challenges in the study of azimuthal correlations in small collision systems is how to distinguish the long-range ridge from “non-flow” correlations involving only a few particles, such as resonance decays, jets, or dijets. For two-particle correlations, the non-flow contribution is commonly suppressed by requiring a large $\Delta\eta$ gap between the two particles in each pair and a peripheral subtraction procedure [3–5,7,14,15]. For multi-particle cumulants, the non-flow contributions can be suppressed by requiring correlation between particles from different subevents separated in η ,

* E-mail address: atlas.publications@cern.ch.

while preserving the genuine long-range multi-particle correlations associated with the ridge. Here each subevent is a collection of particles in a given η range. This so-called “subevent method” has been demonstrated to measure reliably $c_n\{4\}$ and $sc_{n,m}\{4\}$ [13, 16]. In contrast, $c_n\{4\}$ and $sc_{n,m}\{4\}$ based on the standard cumulant method are contaminated by non-flow correlations over the full multiplicity range in pp collisions and the low multiplicity region in $p+A$ collisions [16]. In small collision systems, measurements have been performed for $c_n\{4\}$ with both the standard [15, 17] and subevent methods [18], and for $sc_{n,m}\{4\}$ with the standard method [19]. The subevent method has not yet been used to measure $sc_{n,m}\{4\}$, and no measurements of $ac_n\{3\}$ have ever been attempted in small collision systems.

This Letter presents measurements of $sc_{2,3}\{4\}$, $sc_{2,4}\{4\}$ and $ac_2\{3\}$ in pp collisions at $\sqrt{s} = 13$ TeV, $p+Pb$ collisions at $\sqrt{s_{NN}} = 5.02$ TeV and low-multiplicity $Pb+Pb$ collisions at $\sqrt{s_{NN}} = 2.76$ TeV. They are obtained using two-, three- and four-subevent cumulant methods and are compared with results from the standard cumulant method. The cumulants are normalised by the $\langle v_n^2 \rangle$ obtained from a two-particle correlation analysis [7] to quantify their relative correlation strength. The measurements suggest that the results obtained with the standard method are strongly contaminated by correlations from non-flow sources. The results obtained with the three-subevent method or the four-subevent method provide new evidence of long-range three- or four-particle azimuthal correlations.

The Letter is organised as follows. Details of the ATLAS detector, the trigger system, datasets, as well as event and track selections are provided in Sections 2 to 4. Section 5 describes the standard and subevent cumulant methods used in this analysis. The analysis procedure and systematic uncertainties are described in Sections 6 and 7, respectively. The measured cumulants are presented in Section 8. A summary is given in Section 9.

2. Detector and trigger

The ATLAS detector [20] provides nearly full solid-angle coverage around the collision point with tracking detectors, calorimeters, and muon chambers, and is well suited for measurement of multi-particle correlations over a large pseudorapidity range.¹ The measurements were performed using primarily the inner detector (ID), minimum-bias trigger scintillators (MBTS) and the zero-degree calorimeters (ZDC). The ID detects charged particles within $|\eta| < 2.5$ using a combination of a silicon pixel detector, a silicon microstrip detector (SCT), and a straw-tube transition radiation tracker, all immersed in a 2 T axial magnetic field [21]. An additional pixel layer, the “insertable B-layer” (IBL) [22] is installed between the Run-1 (2010–2013) and Run-2 (2015–2018) periods. The MBTS detects charged particles within $2.1 \lesssim |\eta| \lesssim 3.9$ using two hodoscopes of counters positioned at $z = \pm 3.6$ m. The ZDC, used only in $p+Pb$ and $Pb+Pb$ collisions, are positioned at ± 140 m from the collision point, and detect neutral particles, primarily neutrons and photons, with $|\eta| > 8.3$.

The ATLAS trigger system [23,24] consists of a first-level (L1) trigger implemented using a combination of dedicated electronics and programmable logic, and a high-level trigger (HLT) implemented in processors. The HLT reconstructs charged-particle tracks

¹ ATLAS typically uses a right-handed coordinate system with its origin at the nominal interaction point (IP) in the centre of the detector and the z -axis along the beam pipe. The x -axis points from the IP to the centre of the LHC ring, and the y -axis points upward. Cylindrical coordinates (r, ϕ) are used in the transverse plane, ϕ being the azimuthal angle around the beam pipe. By default, the pseudorapidity is defined in terms of the polar angle θ as $\eta = -\ln \tan(\theta/2)$. However, for asymmetric $p+Pb$ or $Pb+p$ collisions, the $-z$ direction is always defined as the direction of the Pb beam.

Table 1
The list of datasets used in this analysis.

	Pb+Pb	$p+Pb$	pp
Integrated luminosity (year)	$7 \mu\text{b}^{-1}$ (2010)	28 nb^{-1} (2013) 0.3 nb^{-1} (2016)	0.07 pb^{-1} (2015) 0.84 pb^{-1} (2016)

using methods similar to those applied in the offline analysis. The HLT enables the high-multiplicity track triggers (HMT) to select events according to the number of tracks having $p_T > 0.4$ GeV matched to the primary vertex, $N_{\text{ch}}^{\text{HLT}}$. The different HMT triggers apply additional requirements on either the total transverse energy (E_T) in the calorimeters or the number of hits in the MBTS found by the L1 trigger, as well as on $N_{\text{ch}}^{\text{HLT}}$ by the HLT trigger. The pp and $p+Pb$ data were collected using combinations of the minimum-bias and HMT triggers. The minimum-bias trigger required either a hit in at least one MBTS counter, or a hit in at least one MBTS counter on each side, or at least one reconstructed track at the HLT seeded by a random trigger at L1. More detailed information about the triggers used for the pp and $p+Pb$ data and their performance can be found in Refs. [7,25] and Refs. [5,26], respectively.

3. Datasets and Monte Carlo simulations

This analysis is based on ATLAS datasets corresponding to integrated luminosities of 0.9 pb^{-1} of pp data recorded at $\sqrt{s} = 13$ TeV, 28 nb^{-1} of $p+Pb$ data recorded at $\sqrt{s_{NN}} = 5.02$ TeV, and $7 \mu\text{b}^{-1}$ of $Pb+Pb$ data at $\sqrt{s_{NN}} = 2.76$ TeV. The 2.76 TeV $Pb+Pb$ data were collected in 2010. The $p+Pb$ data were mainly collected in 2013, but also include 0.3 nb^{-1} of data collected in 2016, which increase the number of events at moderate multiplicity (see Section 4). During both $p+Pb$ runs, the LHC was configured to provide a 4 TeV proton beam and a 1.57 TeV per-nucleon Pb beam, which produced collisions at $\sqrt{s_{NN}} = 5.02$ TeV, with a rapidity shift of 0.465 of the nucleon–nucleon centre-of-mass frame towards the proton beam direction relative to the ATLAS rest frame. The direction of the Pb beam is always defined to have negative pseudorapidity. The 13 TeV pp data were collected during several special runs of the LHC with low pile-up in 2015 and 2016. A summary of the datasets used in this analysis is shown in Table 1.

The track reconstruction efficiency was determined using simulated Monte Carlo (MC) event samples (Section 4). The pp events were simulated with the Pythia8 MC event generator [27] using the A2 set of tuned parameters with MSTW2008LO parton distribution functions [28]. The HIJING event generator [29] was used to produce $Pb+Pb$ and $p+Pb$ collisions with the same energy and the same boost of the centre-of-mass system as in the data. The detector response was simulated using GEANT4 [30,31] with detector conditions matching those during the data-taking. The simulated events and data events are reconstructed with the same algorithms. The MC sample for $Pb+Pb$ events in the multiplicity region of interest is very small, and so the track reconstruction efficiency for $Pb+Pb$ was taken from the larger $p+Pb$ sample reconstructed with the same reconstruction algorithm. The efficiency in $p+Pb$ events was found to be consistent with the efficiency from the $Pb+Pb$ MC simulation [17].

4. Event and track selection

The offline event selection for the pp and $p+Pb$ data requires at least one reconstructed vertex with its longitudinal position satisfying $|z_{\text{vtx}}| < 100$ mm relative to the nominal interaction point. The vertex is required to have at least two associated tracks with $p_T > 0.4$ GeV. The mean number of collisions per bunch crossing, μ , was 0.002–0.8 for the 13 TeV pp data, 0.03 for the 2013

$p+\text{Pb}$ data, and 0.001–0.006 for the 2016 $p+\text{Pb}$ data. In order to suppress additional interactions in the same bunch crossing (referred to as pile-up) in pp collisions, events containing additional vertices with at least four associated tracks are rejected. In $p+\text{Pb}$ collisions, events with more than one good vertex, defined as any vertex for which the scalar sum of the p_T of the associated tracks is greater than 5 GeV, are rejected. The remaining pile-up events are further suppressed by using the signal in the ZDC in the direction of the Pb beam. This signal is calibrated to the number of detected neutrons, N_n , by using the location of the peak corresponding to a single neutron. The distribution of N_n in events with pile-up is broader than that for the events without pile-up. Hence a simple requirement on the ZDC signal distribution is used to further suppress events with pile-up, while retaining more than 98% of events without pile-up. The impact of residual pile-up, at the level of $\lesssim 10^{-3}$, is studied by comparing the results obtained from data with different μ values.

The offline event selection for the $\text{Pb}+\text{Pb}$ data requires $|z_{\text{vtx}}| < 100$ mm. The selection also requires a time difference $|\Delta t| < 3$ ns between signals in the MBTS trigger counters on either side of the interaction point to suppress non-collision backgrounds. A coincidence between the ZDC signals at forward and backward pseudorapidity is required to reject a variety of background processes, while maintaining high efficiency for inelastic processes. The fraction of events with more than one interaction after applying these selection criteria is less than 10^{-4} .

Charged-particle tracks and collision vertices are reconstructed using algorithms optimised for improved performance for Run-2. In order to compare directly with the pp and $p+\text{Pb}$ systems using event selections based on the multiplicity of the collisions, a subset of data from low-multiplicity $\text{Pb}+\text{Pb}$ collisions, collected during the 2010 LHC heavy-ion run with a minimum-bias trigger, was analysed using the same track reconstruction algorithm as that used for $p+\text{Pb}$ collisions. For the $\text{Pb}+\text{Pb}$ and 2013 $p+\text{Pb}$ analyses, tracks are required to have a p_T -dependent minimum number of hits in the SCT. The transverse (d_0) and longitudinal ($z_0 \sin\theta$) impact parameters of the track relative to the vertex are required to be less than 1.5 mm. Additional requirements $|d_0|/\sigma_{d_0} < 3$ and $|z_0 \sin\theta|/\sigma_{z_0} < 3$ are imposed, where σ_{d_0} and σ_{z_0} are the uncertainties of the transverse and longitudinal impact parameter values, respectively. A more detailed description of the track selection for the 2010 $\text{Pb}+\text{Pb}$ data and 2013 $p+\text{Pb}$ data can be found in Refs. [5,17].

For all the data taken since the start of Run-2, the track selection criteria make use of the IBL, as described in Refs. [14,25]. For the pp and 2016 $p+\text{Pb}$ analyses, the tracks are required to satisfy $|d_0^{\text{BL}}| < 1.5$ mm and $|z_0 \sin\theta| < 1.5$ mm, where d_0^{BL} is the transverse impact parameter of the track relative to the beam line (BL).

The cumulants are calculated using tracks passing the above selection requirements, and having $|\eta| < 2.5$ and $0.3 < p_T < 3$ GeV or $0.5 < p_T < 5$ GeV. These two p_T ranges are chosen because they were often used in the previous ridge measurements at the LHC [6,7,14,15,17]. However, to count the number of reconstructed charged particles for event-class definition (denoted by $N_{\text{ch}}^{\text{rec}}$), tracks with $p_T > 0.4$ GeV and $|\eta| < 2.5$ are used for compatibility with the requirements in the HLT selections described above. Due to different trigger requirements, most of the $p+\text{Pb}$ events with $N_{\text{ch}}^{\text{rec}} > 150$ are provided by the 2013 dataset, while the 2016 dataset provides most of the events at lower $N_{\text{ch}}^{\text{rec}}$.

The efficiency of the combined track reconstruction and track selection requirements is estimated using MC samples reconstructed with the same algorithms and selection requirements as in data. Efficiencies, $\epsilon(\eta, p_T)$, are evaluated as a function of track η , p_T and the number of reconstructed charged-particle tracks, but averaged over the full range in azimuth. The efficiencies are simi-

lar for events with the same multiplicity. For all collision systems, the efficiency increases by about 4% as track p_T increases from 0.3 GeV to 0.6 GeV. Above 0.6 GeV, the efficiency is independent of p_T and reaches 86% (72%) for Run-1 pp and $p+\text{Pb}$, and 83% (70%) for $\text{Pb}+\text{Pb}$ and Run-2 $p+\text{Pb}$ collisions, at $\eta \approx 0$ ($|\eta| > 2$). The efficiency is independent of the event multiplicity for $N_{\text{ch}}^{\text{rec}} > 40$. For lower-multiplicity events the efficiency is smaller by up to 3% due to broader d_0 and $z_0 \sin\theta$ distributions [17].

The fraction of falsely reconstructed charged-particle tracks is also estimated and found to be negligibly small in all datasets. This fraction decreases with increasing track p_T , and even at the lowest transverse momenta of 0.3 GeV it is below 1% of the total number of tracks. Therefore, there is no correction for the presence of such tracks in the analysis.

In the simulated events, the reconstruction efficiency reduces the measured charged-particle multiplicity relative to the generated multiplicity for primary charged particles. A correction factor b is used to correct $N_{\text{ch}}^{\text{rec}}$ to obtain the efficiency-corrected average number of charged particles per event, $\langle N_{\text{ch}} \rangle = b \langle N_{\text{ch}}^{\text{rec}} \rangle$. The value of the correction factor is obtained from the MC samples described above, and is found to be nearly independent of $N_{\text{ch}}^{\text{rec}}$ in the range used in this analysis, $N_{\text{ch}}^{\text{rec}} < 400$. Its value and the associated uncertainties are $b = 1.29 \pm 0.05$ for the $\text{Pb}+\text{Pb}$ and 2013 $p+\text{Pb}$ collisions and $b = 1.18 \pm 0.05$ for Run-2 $p+\text{Pb}$ and pp collisions [32]. Both $\text{sc}_{n,m}\{4\}$ and $\text{ac}_2\{3\}$ are then studied as a function of $\langle N_{\text{ch}} \rangle$.

5. Cumulant method

The multi-particle cumulant method [10] has the advantage of directly reducing non-flow correlations from jets and dijets. The mathematical framework for the standard cumulant is based on the Q-cumulants discussed in Refs. [11,12,33]. It was extended recently to the case of subevent cumulants in Refs. [13,16]. These methods are briefly summarised below.

5.1. Cumulants in the standard method

The standard cumulant method calculates k -particle azimuthal correlations, $\langle \{k\} \rangle$, in one event using a complex number notation [11,12]:

$$\begin{aligned} \langle \{2\}_n \rangle &= \left\langle e^{in(\phi_1 - \phi_2)} \right\rangle, \quad \langle \{3\}_n \rangle = \left\langle e^{in(\phi_1 + \phi_2 - 2\phi_3)} \right\rangle, \\ \langle \{4\}_{n,m} \rangle &= \left\langle e^{in(\phi_1 - \phi_2) + im(\phi_3 - \phi_4)} \right\rangle, \end{aligned} \quad (1)$$

where “ $\langle \rangle$ ” denotes a single-event average over all pairs, triplets or quadruplets, respectively. The averages from Eq. (1) can be expressed in terms of per-particle normalised flow vectors $\mathbf{q}_{n;l}$ with $l = 1, 2, \dots$ in each event [11]:

$$\mathbf{q}_{n;l} \equiv \sum_j w_j^l e^{in\phi_j} \left/ \sum_j w_j^l \right., \quad (2)$$

where the sum runs over all tracks in the event and w_j is a weight assigned to the j th track. This weight is constructed to correct for both detector non-uniformity and tracking inefficiency as explained in Section 6.

The multi-particle asymmetric and symmetric cumulants are obtained from $\langle \{k\} \rangle$ as:

$$\text{ac}_n\{3\} = \langle \langle \{3\}_n \rangle \rangle, \quad \text{sc}_{n,m}\{4\} = \langle \langle \{4\}_{n,m} \rangle \rangle - \langle \langle \{2\}_n \rangle \rangle \langle \langle \{2\}_m \rangle \rangle, \quad (3)$$

where “ $\langle \langle \rangle \rangle$ ” represents a weighted average of $\langle \{k\} \rangle$ over an event ensemble with similar $N_{\text{ch}}^{\text{rec}}$. One averages first over all distinct

pairs, triplets or quadruplets in one event to obtain $\langle\{2\}_n\rangle$, $\langle\{2\}_m\rangle$, $\langle\{3\}_n\rangle$ and $\langle\{4\}_{n,m}\rangle$. Then the obtained values are averaged over an event ensemble with similar $N_{\text{ch}}^{\text{rec}}$ to obtain $\text{sc}_{n,m}\{4\}$ and $\text{ac}_n\{3\}$. In the absence of non-flow correlations, $\text{sc}_{n,m}\{4\}$ and $\text{ac}_n\{3\}$ measure the correlation between v_n and v_m or between v_n and v_{2n} :

$$\text{ac}_n\{3\} = \left\langle \mathbf{v}_n^2 \mathbf{v}_{2n}^* \right\rangle = \left\langle v_n^2 v_{2n} \cos 2n(\Phi_n - \Phi_{2n}) \right\rangle, \quad (4)$$

$$\text{sc}_{n,m}\{4\} = \left\langle v_n^2 v_m^2 \right\rangle - \left\langle v_n^2 \right\rangle \left\langle v_m^2 \right\rangle, \quad (5)$$

where the averages are taken over the events. This analysis measures three types of cumulants defined in Eq. (3): $\text{sc}_{2,3}\{4\}$, $\text{sc}_{2,4}\{4\}$ and $\text{ac}_2\{3\}$.

5.2. Cumulants in the subevent method

In the standard cumulant method described above, all k -particle multiplets involved in $\langle\{k\}_n\rangle$ and $\langle\{k\}_{n,m}\rangle$ are selected using tracks in the entire ID acceptance of $|\eta| < \eta_{\max} = 2.5$. To suppress further the non-flow correlations that typically involve a few particles within a localised region in η , the tracks are divided into several subevents, each covering a unique η interval. The multi-particle correlations are then constructed by only correlating tracks between different subevents.

In the two-subevent cumulant method, the tracks are divided into two subevents, labelled by a and b , according to $-\eta_{\max} < \eta_a < 0$ and $0 \leq \eta_b < \eta_{\max}$. The per-event k -particle azimuthal correlations are evaluated as:

$$\begin{aligned} \langle\{2\}_n\rangle_{a|b} &= \left\langle e^{in(\phi_1^a - \phi_2^b)} \right\rangle, \quad \langle\{3\}_n\rangle_{2a|b} = \left\langle e^{in(\phi_1^a + \phi_2^b - 2\phi_3^b)} \right\rangle, \\ \langle\{4\}_{n,m}\rangle_{2a|2b} &= \left\langle e^{in(\phi_1^a - \phi_2^b) + im(\phi_3^a - \phi_4^b)} \right\rangle, \end{aligned} \quad (6)$$

where the superscript or subscript a (b) indicates tracks chosen from the subevent a (b). Here the three- and four-particle cumulants are defined as:

$$\begin{aligned} \text{ac}_n^{2a|b}\{3\} &= \langle\langle\{3\}_n\rangle\rangle_{2a|b}, \\ \text{sc}_{n,m}^{2a|2b}\{4\} &= \langle\langle\{4\}_{n,m}\rangle\rangle_{2a|2b} - \langle\langle\{2\}_n\rangle\rangle_{a|b} \langle\langle\{2\}_m\rangle\rangle_{a|b}. \end{aligned}$$

The two-subevent method suppresses correlations within a single jet (intra-jet correlations), since particles from one jet usually fall in one subevent.

In the three-subevent cumulant method, tracks in each event are divided into three subevents a , b and c , each covering one third of the η range, $-\eta_{\max} < \eta_a < -\eta_{\max}/3$, $|\eta_b| \leq \eta_{\max}/3$ and $\eta_{\max}/3 < \eta_c < \eta_{\max}$. The multi-particle azimuthal correlations and cumulants are then evaluated as:

$$\begin{aligned} \langle\{3\}_n\rangle_{a,b|c} &= \left\langle e^{in(\phi_1^a + \phi_2^b - 2\phi_3^c)} \right\rangle, \\ \langle\{4\}_{n,m}\rangle_{a,b|2c} &= \left\langle e^{in(\phi_1^a - \phi_2^b) + im(\phi_3^b - \phi_4^c)} \right\rangle, \end{aligned} \quad (7)$$

and

$$\begin{aligned} \text{ac}_n^{a,b|c}\{3\} &= \langle\langle\{3\}_n\rangle\rangle_{a,b|c}, \\ \text{sc}_{n,m}^{a,b|2c}\{4\} &= \langle\langle\{4\}_{n,m}\rangle\rangle_{a,b|2c} - \langle\langle\{2\}_n\rangle\rangle_{a|c} \langle\langle\{2\}_m\rangle\rangle_{b|c}. \end{aligned} \quad (8)$$

Since a dijet event usually produces particles in at most two subevents, the three-subevent method efficiently suppresses the non-flow contribution from inter-jet correlations associated with dijets. To maximise the statistical precision, the η range for subevent a is swapped with that for subevent b or c , and the results are averaged to obtain the final values.

The four-subevent cumulant method is only relevant for the symmetric cumulants $\text{sc}_{n,m}\{4\}$. Tracks in each event are divided into four subevents a , b , c , and d , each covering one quarter of the η range: $-\eta_{\max} < \eta_a < -\eta_{\max}/2$, $-\eta_{\max}/2 \leq \eta_b < 0$, $0 \leq \eta_c < \eta_{\max}/2$, and $\eta_{\max}/2 \leq \eta_d < \eta_{\max}$. The multi-particle azimuthal correlations and cumulants are then evaluated as:

$$\langle\{4\}_{n,m}\rangle_{a,b|c,d} = \left\langle e^{in(\phi_1^a - \phi_2^c) + im(\phi_3^b - \phi_4^d)} \right\rangle, \quad (9)$$

$$\text{sc}_{n,m}^{a,b|c,d}\{4\} = \langle\langle\{4\}_{n,m}\rangle\rangle_{a,b|c,d} - \langle\langle\{2\}_n\rangle\rangle_{a|c} \langle\langle\{2\}_m\rangle\rangle_{b|d}. \quad (10)$$

The four-subevent method based on Eqs. (9) and (10) should further suppress the residual non-flow contributions, for instance when each of the two jets from the dijet falls across the boundary between two neighbouring subevents. To maximise the statistical precision, the η ranges for the four subevents are swapped with each other, and the results are averaged to obtain the final values.

5.3. Normalised cumulants

Although the cumulants reflect the nature of the correlation between v_n and v_m , their magnitudes also depend on the square of single flow harmonics v_n^2 and v_m^2 , see Eq. (4). The dependence on the single flow harmonics can be scaled out via the normalised cumulants [34,35]:

$$\text{nsc}_{2,3}\{4\} = \frac{\text{sc}_{2,3}\{4\}}{v_2\{2\}^2 v_3\{2\}^2} = \frac{\langle v_2^2 v_3^2 \rangle}{\langle v_2^2 \rangle \langle v_3^2 \rangle} - 1, \quad (11)$$

$$\text{nsc}_{2,4}\{4\} = \frac{\text{sc}_{2,4}\{4\}}{v_2\{2\}^2 v_4\{2\}^2} = \frac{\langle v_2^2 v_4^2 \rangle}{\langle v_2^2 \rangle \langle v_4^2 \rangle} - 1, \quad (12)$$

$$\begin{aligned} \text{nac}_2\{3\} &= \frac{\text{ac}_2\{3\}}{\sqrt{(2v_2\{2\}^4 + c_2\{4\}) c_4\{2\}}} \\ &= \frac{\langle v_2^2 v_4 \cos 4(\Phi_2 - \Phi_4) \rangle}{\sqrt{\langle v_2^4 \rangle \langle v_4^2 \rangle}}, \end{aligned} \quad (13)$$

where the $v_n\{2\}^2 = \langle v_n^2 \rangle$ are flow harmonics obtained using a two-particle correlation method based on a peripheral subtraction technique [7,14], and $c_2\{4\} = \langle v_2^4 \rangle - 2\langle v_2^2 \rangle^2$ are four-particle cumulant results from Refs. [17,18]. This definition for $\text{nac}_2\{3\}$ is motivated by Ref. [36].

6. Analysis procedure

The measurement of the $\text{sc}_{n,m}\{4\}$ and $\text{ac}_2\{3\}$ follows the same analysis procedure as for the four-particle cumulants $\text{c}_n\{4\}$ in Ref. [18]. The multi-particle cumulants are calculated in three steps using charged particles with $|\eta| < 2.5$. In the first step, $\langle\{2\}_n\rangle$, $\langle\{3\}_n\rangle$ and $\langle\{4\}_{n,m}\rangle$ from Eqs. (1), (6), (7) and (9) are calculated for each event from particles in one of two different p_T ranges, $0.3 < p_T < 3$ GeV and $0.5 < p_T < 5$ GeV. The numbers of reconstructed charged particles in these p_T ranges are denoted by $N_{\text{ch}}^{\text{sel}1}$ and $N_{\text{ch}}^{\text{sel}2}$, respectively.

In the second step, the correlators $\langle\langle k \rangle\rangle$ for $0.3 < p_T < 3$ GeV ($0.5 < p_T < 5$ GeV) are averaged over events with the same $N_{\text{ch}}^{\text{sel}1}$ ($N_{\text{ch}}^{\text{sel}2}$) to obtain $\langle\langle k \rangle\rangle$, and then $\text{sc}_{2,3}\{4\}$, $\text{sc}_{2,4}\{4\}$ and $\text{ac}_2\{3\}$. The $\text{sc}_{2,3}\{4\}$, $\text{sc}_{2,4}\{4\}$ and $\text{ac}_2\{3\}$ values are then averaged in broader multiplicity ranges of the event ensemble, weighted by number of events, to obtain statistically significant results.

In the third step, the $\text{sc}_{2,3}\{4\}$, $\text{sc}_{2,4}\{4\}$ and $\text{ac}_2\{3\}$ values obtained for a given $N_{\text{ch}}^{\text{sel}1}$ or $N_{\text{ch}}^{\text{sel}2}$ are mapped to $\langle N_{\text{ch}}^{\text{rec}} \rangle$, the average number of reconstructed charged particles with $p_T > 0.4$ GeV.

The mapping procedure is necessary so that $sc_{2,3}\{4\}$, $sc_{2,4}\{4\}$ and $ac_2\{3\}$ obtained for the two different p_T ranges can be compared using a common x -axis defined by $\langle N_{ch}^{rec} \rangle$. The $\langle N_{ch}^{rec} \rangle$ value is then converted to $\langle N_{ch} \rangle$, the efficiency-corrected average number of charged particles with $p_T > 0.4$ GeV, as discussed in Section 4.

In order to account for detector inefficiencies and non-uniformity, particle weights used in Eq. (2) are defined as:

$$w(\phi, \eta, p_T) = d(\phi, \eta)/\epsilon(\eta, p_T).$$

The additional weight factor $d(\phi, \eta)$ accounts for non-uniformities in the azimuthal acceptance of the detector as a function of η . All reconstructed charged particles with $p_T > 0.3$ GeV are entered into a two-dimensional histogram $N(\phi, \eta)$, and the weight factor is then obtained as $d(\phi, \eta) \equiv \langle N(\eta) \rangle / N(\phi, \eta)$, where $\langle N(\eta) \rangle$ is the track density averaged over ϕ in the given η bin. This procedure removes most of the ϕ -dependent non-uniformity in the detector acceptance [17].

In order to calculate the normalised cumulants from Eqs. (11)–(13), the flow harmonics $v_n\{2\}$ are obtained from a “template fit” of two-particle $\Delta\phi$ correlation as described in Refs. [7,14]. The $v_n\{2\}$ values are calculated identically to the procedure used in the previous ATLAS publications [7,14], but are further corrected for a bias, which exists only if $v_n\{2\}$ changes with N_{ch}^{rec} . The details of the correction procedure are given in the Appendix A and are discussed briefly below.

The standard procedure of Refs. [7,14] first constructs a $\Delta\phi$ distribution for pairs of tracks with $|\Delta\eta| > 2$: the per-trigger-particle yield $Y(\Delta\phi)$ for a given N_{ch}^{rec} range. The dominating non-flow jet peak at $\Delta\phi \sim \pi$ is estimated using low-multiplicity events with $N_{ch}^{rec} < 20$ and separated via a template fit procedure, and the harmonic modulation of the remaining component is taken as the $v_n\{2\}^2$ [7]:

$$Y(\Delta\phi) = F Y(\Delta\phi)^{\text{peri}} + G^{\text{tmp}} \left(1 + 2 \sum_{n=2}^{\infty} v_n\{2, \text{tmp}\}^2 \cos n\Delta\phi \right),$$

where superscripts “peri” and “tmp” indicate quantities for the $N_{ch}^{rec} < 20$ event class and quantities after the template fit for the event class of interest, respectively. The scale factor F and pedestal G^{tmp} are fixed by the fit, and $v_n\{2, \text{tmp}\}$ are calculated from a Fourier transform. This procedure implicitly assumes that $v_n\{2\}$ is independent of N_{ch}^{rec} , and requires a small correction if $v_n\{2\}$ does change with N_{ch}^{rec} (Appendix A). In $p+Pb$ and $Pb+Pb$ collisions, this correction in the $N_{ch}^{rec} > 100$ region amounts to a 2–6% reduction for $v_2\{2, \text{tmp}\}$ and a 4–9% reduction for $v_3\{2, \text{tmp}\}$ and $v_4\{2, \text{tmp}\}$. The correction is smaller for $v_2\{2, \text{tmp}\}$ in pp collisions as it is nearly independent of N_{ch}^{rec} [7].

7. Systematic uncertainties

The evaluation of the systematic uncertainties follows closely the procedure established for the four-particle cumulants $c_n\{4\}$ and described in Ref. [18]. The main sources of systematic uncertainties are related to the detector azimuthal non-uniformity, track selection, track reconstruction efficiency, trigger efficiency and pile-up. Due to the relatively poor statistics and larger non-flow effects, the systematic uncertainties are typically larger in pp collisions. The systematic uncertainties are also generally larger, in percentage, for four-particle cumulants $sc_{n,m}\{4\}$ than for the three-particle cumulants $ac_2\{3\}$, since the $|sc_{n,m}\{4\}|$ values are much smaller than those for $ac_2\{3\}$. The systematic uncertainties are generally similar among the two- and three- and four-subevent methods, but are different from those for the standard method, which is strongly

influenced by non-flow correlations. The following discussion focuses on the three-subevent method, which is the default method used to present the final results.

The effect of detector azimuthal non-uniformity is accounted for using the weight factor $d(\phi, \eta)$. The impact of the weighting procedure is studied by fixing the weight to unity and repeating the analysis. The results are mostly consistent with the nominal results. The corresponding uncertainties for $sc_{n,m}\{4\}$ vary in the range of 0–4%, 0–2% and 1–2% in pp , $p+Pb$ and $Pb+Pb$ collisions, respectively. The uncertainties for $ac_2\{3\}$ vary in the range of 0–2% in pp collisions, and 0–1% in $p+Pb$ and $Pb+Pb$ collisions, respectively.

The systematic uncertainty associated with the track selection is estimated by tightening the $|d_0|$ and $|z_0 \sin \theta|$ requirements. They are each varied from the default requirement of less than 1.5 mm to less than 1 mm. In $p+Pb$ and $Pb+Pb$ collisions, the requirement on the significance of impact parameters, $|d_0|/\sigma_{d_0}$ and $|z_0 \sin \theta|/\sigma_{z_0}$ are also varied from less than 3 to less than 2. For each variation, the tracking efficiency is re-evaluated and the analysis is repeated. For $ac_2\{3\}$, which has a large flow signal, the differences from the nominal results are observed to be less than 2% for all collision systems. For $sc_{n,m}\{4\}$, for which the signal is small, the differences from the nominal results are found to be in the range of 2–10% in pp collisions, 2–7% in $p+Pb$ collisions and 2–4% in $Pb+Pb$ collisions. The differences are smaller for results obtained for $0.5 < p_T < 5$ GeV than those obtained for $0.3 < p_T < 3$ GeV.

Previous measurements indicate that the azimuthal correlations (both the flow and non-flow components) have a strong dependence on p_T , but a relatively weak dependence on η [5,7]. Therefore, p_T -dependent systematic effects in the track reconstruction efficiency could affect the cumulant values. The uncertainty in the track reconstruction efficiency is mainly due to differences in the detector conditions and material description between the simulation and the data. The efficiency uncertainty varies between 1% and 4%, depending on track η and p_T [7,17]. Its impact on multi-particle cumulants is evaluated by repeating the analysis with the tracking efficiency varied up and down by its corresponding uncertainty as a function of track p_T . For the standard cumulant method, which is more sensitive to jets and dijets, the evaluated uncertainty amounts to 2–6% in pp collisions and less than 2% in $p+Pb$ collisions for $\langle N_{ch} \rangle > 100$. For the subevent methods, the evaluated uncertainty is typically less than 3% for most of the $\langle N_{ch} \rangle$ ranges.

Most events in pp and $p+Pb$ collisions are collected with the HMT triggers with several online N_{ch}^{rec} thresholds. In order to estimate the possible bias due to trigger inefficiency as a function of $\langle N_{ch} \rangle$, the offline N_{ch}^{rec} requirements are changed such that the HMT trigger efficiency is at least 50% or 80%. The results are obtained independently for each variation. These results are found to be consistent with each other for the subevent methods, and show some differences for the standard cumulant method in the low $\langle N_{ch} \rangle$ region. The nominal analysis is performed using the 50% efficiency selection and the differences between the nominal results and those from the 80% efficiency selection are included in the systematic uncertainty. The changes for pp collisions are in the range of 5–15% for $sc_{2,3}\{4\}$, 2–8% for $sc_{2,4}\{4\}$ and 1–5% for $ac_2\{3\}$. The ranges for $p+Pb$ collisions are much smaller due to the much sharper turn-on of the trigger efficiency and larger signal: they are estimated to be 1–3% for $sc_{2,3}\{4\}$, 2–4% for $sc_{2,4}\{4\}$ and 1–2% for $ac_2\{3\}$.

In this analysis, a pile-up rejection criterion is applied to reject events containing additional vertices in pp and $p+Pb$ collisions. In order to check the impact of residual pile-up, the analysis is repeated without the pile-up rejection criterion. No differences are observed in $p+Pb$ collisions, as is expected since the μ values in $p+Pb$ are modest. For the 13 TeV pp dataset, the differences with

and without pile-up rejection are in the range of 0–7% for $sc_{2,3}\{4\}$, 2–15% for $sc_{2,4}\{4\}$ and 2–3% for $ac_2\{3\}$. As a cross-check, the pp data are divided into two samples with approximately equal number of events based on the μ value: $\mu > 0.4$ and $\mu < 0.4$, and the results are compared. No systematic differences are observed between the two independent datasets.

The systematic uncertainties from different sources are added in quadrature to determine the total systematic uncertainty. In $p+Pb$ and $Pb+Pb$ collisions, the total uncertainties are in the range of 3–8% for $sc_{2,3}\{4\}$, 1–5% for $sc_{2,4}\{4\}$ and 1–4% for $ac_2\{3\}$. In pp collisions, the total uncertainties are larger, mainly due to larger non-flow contribution, larger pile-up and the less sharp turn-on of the HMT triggers. They are in the ranges of 10–20% for $sc_{2,3}\{4\}$, 10–20% for $sc_{2,4}\{4\}$ and 2–5% for $ac_2\{3\}$. The total systematic uncertainties are generally smaller than the statistical uncertainties.

The $v_n\{2\}$ values used to obtain normalised cumulants from Eqs. (11)–(13) are measured following the prescription of the previous ATLAS publications [7,14], resulting in very similar systematic uncertainties. The correction for the bias of the template fit procedure, as described in Section 6, reduces the sensitivity to the choice of the peripheral N_{ch}^{rec} bin. The uncertainties of normalised cumulants are obtained by propagation of the uncertainties from the original cumulants and $v_n\{2\}$, taking into account that the correlated systematic uncertainties partially cancel out.

8. Results

The results are presented in two parts. Section 8.1 presents a detailed comparison between the standard method and subevent methods to demonstrate the ability of the subevent methods to suppress non-flow correlations. Section 8.2 compares the cumulants among pp , $p+Pb$ and $Pb+Pb$ collisions to provide insight into the common nature of collectivity in these systems.

8.1. Comparison between standard and subevent methods

The top row of Fig. 1 compares the $sc_{2,3}\{4\}$ values obtained from the standard, two-, three- and four-subevent methods from pp collisions in $0.3 < p_T < 3$ GeV (left panel) and $0.5 < p_T < 5$ GeV (right panel). The values from the standard method are positive over the full $\langle N_{ch} \rangle$ range, and are larger at lower $\langle N_{ch} \rangle$ or in the higher p_T range. This behaviour suggests that the $sc_{2,3}\{4\}$ values from the standard method in pp collisions, including those from Ref. [19], are strongly influenced by non-flow effects in all $\langle N_{ch} \rangle$ and p_T ranges [16]. In contrast, the values from the subevent methods are negative over the full $\langle N_{ch} \rangle$ range, and they are slightly more negative at lowest $\langle N_{ch} \rangle$ and also more negative at higher p_T . The results are consistent among the various subevent methods for $0.3 < p_T < 3$ GeV. For the high p_T region of $0.5 < p_T < 5$ GeV, results from the two-subevent method are systematically lower than those from the three- and four-subevent methods, suggesting that the two-subevent method may be affected by negative non-flow contributions. Such negative non-flow correlation has been observed in a PYTHIA8 calculation [16].

The middle row of Fig. 1 shows $sc_{2,3}\{4\}$ from $p+Pb$ collisions. At $\langle N_{ch} \rangle > 140$, the values are negative and consistent among all four methods, reflecting genuine long-range collective correlations. At $\langle N_{ch} \rangle < 140$, the values are different between the standard method and the subevent methods. The $sc_{2,3}\{4\}$ from the standard method changes sign around $\langle N_{ch} \rangle \sim 80$ and remains positive at lower $\langle N_{ch} \rangle$, reflecting the contribution from non-flow correlations. In contrast, the $sc_{2,3}\{4\}$ from various subevent methods are negative and consistent with each other at $\langle N_{ch} \rangle < 140$, suggesting that they mainly reflect the genuine long-range correlations.

The bottom row of Fig. 1 shows $sc_{2,3}\{4\}$ from $Pb+Pb$ collisions. The results are consistent among all four methods across most of the $\langle N_{ch} \rangle$ range. In the low $\langle N_{ch} \rangle$ region, where the non-flow contribution is expected to be significant, the uncertainties of the results are too large to distinguish between different methods.

The results for the symmetric cumulant $sc_{2,4}\{4\}$ are presented in Fig. 2. The top row shows the $sc_{2,4}\{4\}$ obtained from the standard, two-subevent, three-subevent and four-subevent methods from pp collisions in $0.3 < p_T < 3$ GeV (left panel) and $0.5 < p_T < 5$ GeV (right panel). The values of $sc_{2,4}\{4\}$ are positive for all four methods. However, the results from the standard method are much larger than those from the subevent methods and also exhibit a much stronger increase towards the lower $\langle N_{ch} \rangle$ region. This behaviour is consistent with the expectation that the standard method is more affected by dijets. Significant differences are also observed between the two-subevent and three- or four-subevent methods at low $\langle N_{ch} \rangle$, but these differences decrease and disappear for $\langle N_{ch} \rangle > 100$. Within the statistical uncertainties of the measurement, no differences are observed between the three- and four-subevent methods. This comparison suggests that the two-subevent method may not be sufficient to reject non-flow correlations from dijets in pp collisions, and methods with three or more subevents are required to suppress the non-flow contribution over the measured $\langle N_{ch} \rangle$ range.

The middle row of Fig. 2 shows $sc_{2,4}\{4\}$ from $p+Pb$ collisions. Significant differences are observed between the standard method and the subevent methods over the full $\langle N_{ch} \rangle$ range. However, no differences are observed among the various subevent methods. These results suggest that the standard method is contaminated by large contributions from non-flow correlations at low $\langle N_{ch} \rangle$, and these contributions may not vanish even at large $\langle N_{ch} \rangle$ values. All subevent methods suggest an increase of $sc_{2,4}\{4\}$ toward lower $\langle N_{ch} \rangle$ for $\langle N_{ch} \rangle < 40$, which may reflect some residual non-flow correlations in this region.

The bottom row of Fig. 2 shows $sc_{2,4}\{4\}$ from $Pb+Pb$ collisions. The $sc_{2,4}\{4\}$ values increase gradually with $\langle N_{ch} \rangle$ for all four methods. This increase reflects the known fact that the v_2 increases with $\langle N_{ch} \rangle$ in $Pb+Pb$ collisions [37]. The values from the standard method are systematically larger than those from the subevent methods, and this difference varies slowly with $\langle N_{ch} \rangle$, similar to the behaviour observed in $p+Pb$ collisions in the high $\langle N_{ch} \rangle$ region.

The results for the asymmetric cumulant $ac_2\{3\}$ are presented in Fig. 3. The top row shows the results obtained from the standard, two-subevent, and three-subevent methods from pp collisions in $0.3 < p_T < 3$ GeV (left panel) and $0.5 < p_T < 5$ GeV (right panel). The results are positive for all methods. The results from the standard method are much larger than those from the subevent methods, consistent with the expectation that the standard method is more affected by non-flow correlations from dijets. Significant differences are also observed between the two-subevent and three-subevent methods at low $\langle N_{ch} \rangle$, but these differences decrease and disappear at $\langle N_{ch} \rangle > 100$. The $ac_2\{3\}$ values from the three-subevent method show a slight increase for $\langle N_{ch} \rangle < 40$ but are nearly constant for $\langle N_{ch} \rangle > 40$. This behaviour suggests that in the three-subevent method, the non-flow contribution may play some role at $\langle N_{ch} \rangle < 40$, but is negligible for $\langle N_{ch} \rangle > 40$. Therefore, the $ac_2\{3\}$ from the three-subevent method supports the existence of a three-particle long-range collective flow that is nearly independent of $\langle N_{ch} \rangle$ in pp collisions, consistent with the $\langle N_{ch} \rangle$ -independent behaviour of v_2 and v_4 observed previously in the two-particle correlation analysis [7].

The middle and bottom rows of Fig. 3 show $ac_2\{3\}$ from $p+Pb$ and $Pb+Pb$ collisions, respectively. The $ac_2\{3\}$ values from the standard method have a significant non-flow contribution up to

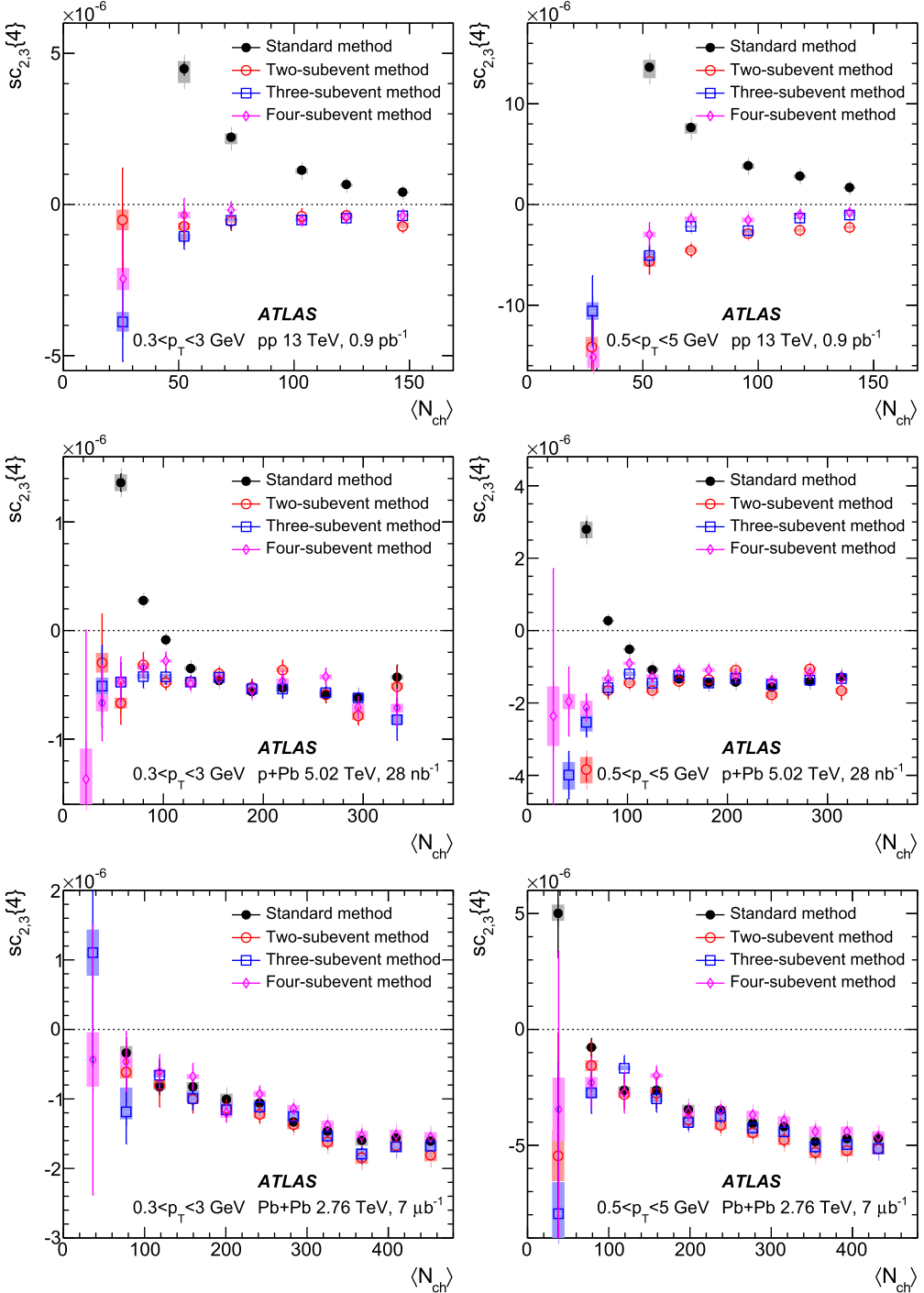


Fig. 1. The symmetric cumulant $sc_{2,3}\{4\}$ as a function of $\langle N_{ch} \rangle$ for $0.3 < p_T < 3$ GeV (left panels) and $0.5 < p_T < 5$ GeV (right panels) obtained for pp collisions (top row), $p+Pb$ collisions (middle row) and low-multiplicity $Pb+Pb$ collisions (bottom row). In each panel, the $sc_{2,3}\{4\}$ is obtained from the standard method (filled symbol), the two-subevent method (open circles), three-subevent method (open squares) and four-subevent method (open diamonds). The error bars and shaded boxes represent the statistical and systematic uncertainties.

$\langle N_{ch} \rangle \sim 200$ in $p+Pb$ collisions and $\langle N_{ch} \rangle \sim 80$ in $Pb+Pb$ collisions. In the subevent methods, the influence of non-flow contributions is very small for $\langle N_{ch} \rangle > 60$ in both collision systems, and therefore the $\langle N_{ch} \rangle$ dependence of $ac_2\{3\}$ reflects the $\langle N_{ch} \rangle$ dependence of the v_2 and v_4 . The $ac_2\{3\}$ values from the subevent methods increase with $\langle N_{ch} \rangle$, and the increase is stronger in $Pb+Pb$ collisions. This is consistent with previous observations that v_2 and v_4 increase with $\langle N_{ch} \rangle$ more strongly in $Pb+Pb$ than in $p+Pb$ collisions [17].

The values of $sc_{2,4}\{4\}$ and $ac_2\{3\}$, which are both measures of correlations between v_2 and v_4 , show significant differences between the standard method and the subevent methods, as shown in Figs. 2 and 3. The $\langle N_{ch} \rangle$ dependence of these differences decreases gradually with $\langle N_{ch} \rangle$, and is consistent with an influence of non-flow that is expected to scale as $1/\langle N_{ch} \rangle$. However, these differences seem to persist for $\langle N_{ch} \rangle > 200$ in $p+Pb$ collisions and for $\langle N_{ch} \rangle > 150$ in $Pb+Pb$ collisions, which is not compatible with the predicted behaviour of non-flow correlations. The differences at

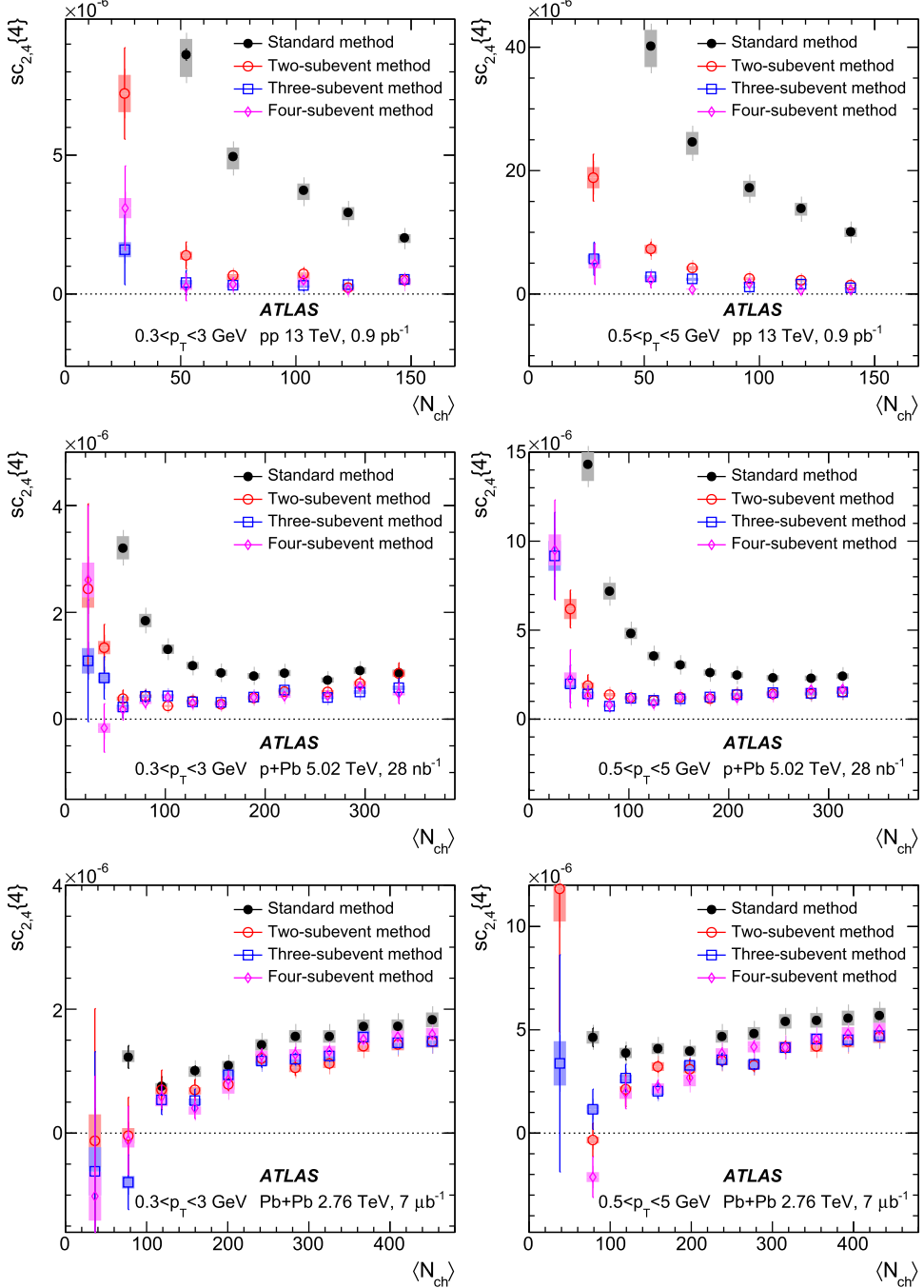


Fig. 2. The symmetric cumulant $sc_{2,4}\{4\}$ as a function of $\langle N_{ch} \rangle$ for $0.3 < p_T < 3$ GeV (left panels) and $0.5 < p_T < 5$ GeV (right panels) obtained for pp collisions (top row), $p+Pb$ collisions (middle row) and low-multiplicity $Pb+Pb$ collisions (bottom row). In each panel, the $sc_{2,4}\{4\}$ is obtained from the standard method (filled symbol), two-subevent method (open circles), three-subevent method (open squares) and four-subevent method (open diamonds). The error bars and shaded boxes represent the statistical and systematic uncertainties, respectively.

large $\langle N_{ch} \rangle$ may arise from longitudinal flow decorrelations [38,39], which have been measured by CMS [40] and ATLAS [41]. Decorrelation effects are found to be large for v_4 and strongly correlated with v_2 , and therefore they are expected to reduce the $sc_{2,4}\{4\}$ and $ac_{2,3}\{3\}$ in the subevent method. Therefore, the observed differences between the standard method and subevent method reflect the combined contribution from non-flow correlations, which dominates in the low $\langle N_{ch} \rangle$ region, and decorrelation, which is more important at large $\langle N_{ch} \rangle$ (see further discussion in the Appendix B).

The results presented above suggest that the three-subevent method is sufficient to suppress most of the non-flow effects. It is therefore used as the default method for the discussion below.

8.2. Comparison between collision systems

Fig. 4 shows a direct comparison of cumulants for the three collision systems. The three panels in the top row show the results for $sc_{2,3}\{4\}$, $sc_{2,4}\{4\}$ and $ac_{2,3}\{3\}$, respectively, for $0.3 < p_T < 3$ GeV. These results support the existence of a negative correlation between v_2 and v_3 and a positive correlation between v_2 and v_4 .

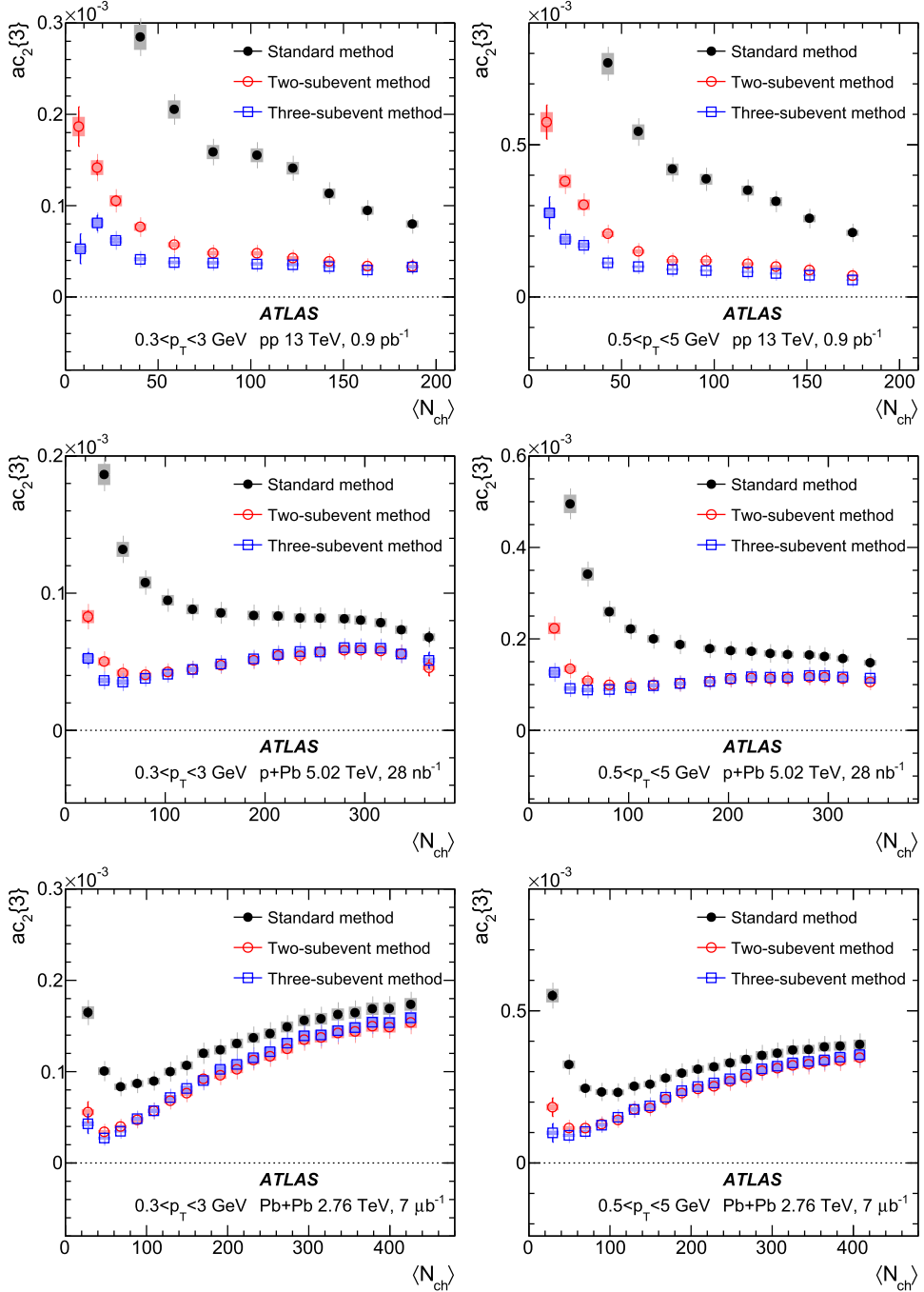


Fig. 3. The asymmetric cumulant $ac_2\{3\}$ as a function of $\langle N_{ch} \rangle$ for $0.3 < p_T < 3$ GeV (left panels) and $0.5 < p_T < 5$ GeV (right panels) obtained for pp collisions (top row), $p+Pb$ collisions (middle row) and low-multiplicity $Pb+Pb$ collisions (bottom row). In each panel, the $ac_2\{3\}$ is obtained from the standard method (filled symbol), two-subevent method (open circles), and three-subevent method (open squares). The error bars and shaded boxes represent the statistical and systematic uncertainties, respectively.

Such correlation patterns have previously been observed in large collision systems [42–44], but are now confirmed also in the small collision systems, once non-flow effects are adequately suppressed. In the multiplicity range covered by the pp collisions, $\langle N_{ch} \rangle < 150$, the results for symmetric cumulants $sc_{2,3}\{4\}$ and $sc_{2,4}\{4\}$ are similar among the three systems. In the range $\langle N_{ch} \rangle > 150$, $|sc_{2,3}\{4\}|$ and $sc_{2,4}\{4\}$ are larger in $Pb+Pb$ than in $p+Pb$ collisions. The results for $ac_2\{3\}$ are similar among the three systems at $\langle N_{ch} \rangle < 100$, but they deviate from each other at higher $\langle N_{ch} \rangle$. The pp data are approximately constant or decrease slightly with $\langle N_{ch} \rangle$, while the $p+Pb$ and $Pb+Pb$ data show significant increases as a function of

$\langle N_{ch} \rangle$. The bottom row shows the results for the higher p_T range of $0.5 < p_T < 5$ GeV, where similar trends are observed.

Fig. 5 shows the results for normalised cumulants, $nsc_{2,3}\{4\}$, $nsc_{2,4}\{4\}$ and $nac_2\{3\}$, compared among the three systems. The normalised cumulants generally show a much weaker $\langle N_{ch} \rangle$ dependence at $\langle N_{ch} \rangle > 100$, where the statistical uncertainties are small. This behaviour implies that the strong $\langle N_{ch} \rangle$ dependence of the $sc_{n,m}\{4\}$ and $ac_2\{3\}$ values reflects the $\langle N_{ch} \rangle$ dependence of the v_n values, and these dependences are removed in the normalised cumulants. The normalised cumulants are also similar among different collision systems at large $\langle N_{ch} \rangle$, although some differences

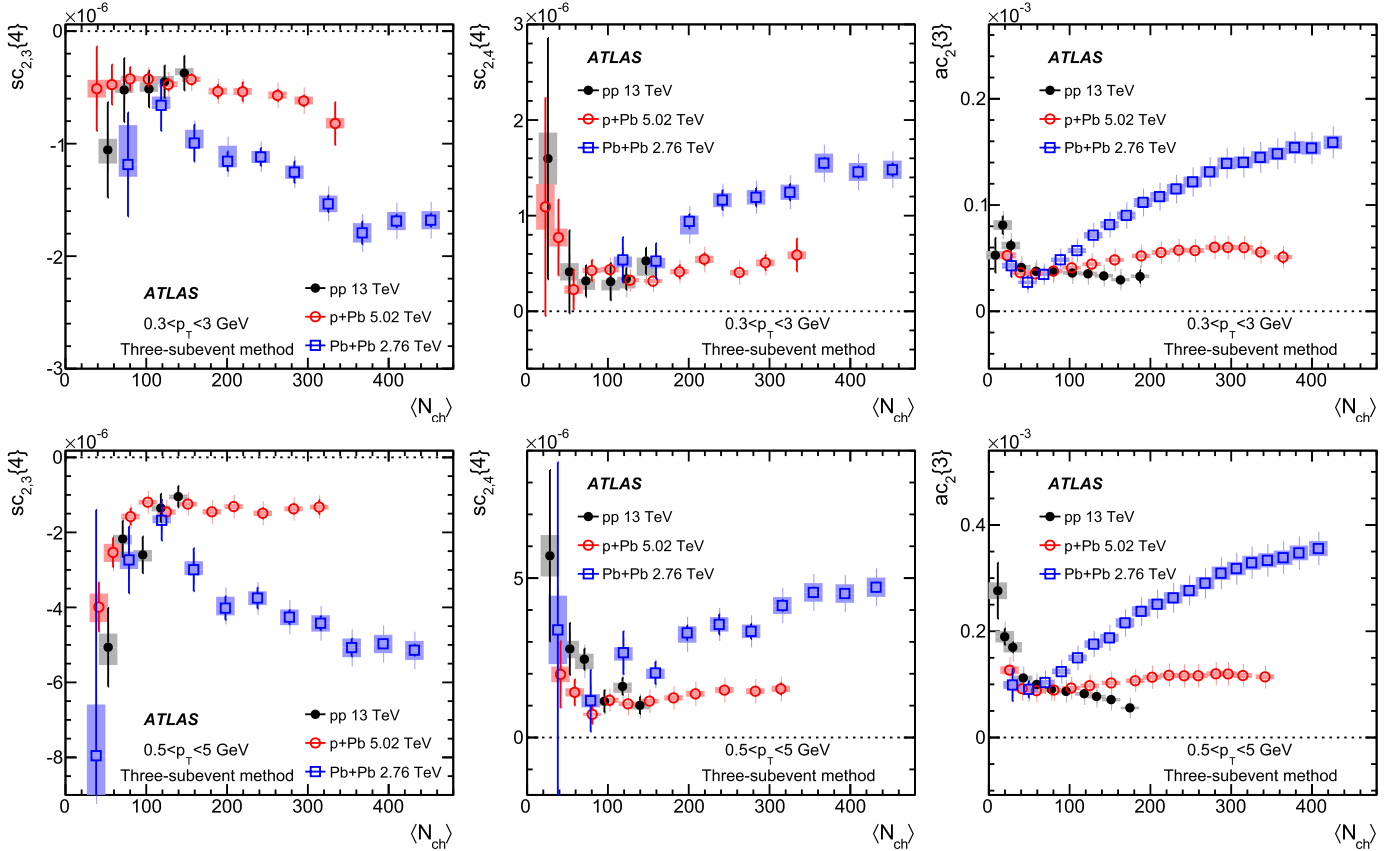


Fig. 4. The $\langle N_{\text{ch}} \rangle$ dependence of $\text{sc}_{2,3}\{4\}$ (left panels), $\text{sc}_{2,4}\{4\}$ (middle panels) and $\text{ac}_2\{3\}$ (right panels) in $0.3 < p_{\text{T}} < 3$ GeV (top row) and $0.5 < p_{\text{T}} < 5$ GeV (bottom row) obtained for pp collisions (solid circles), $p+\text{Pb}$ collisions (open circles) and low-multiplicity $\text{Pb}+\text{Pb}$ collisions (open squares). The error bars and shaded boxes represent the statistical and systematic uncertainties, respectively.

at the relative level of 20–30% are observed for smaller $\langle N_{\text{ch}} \rangle$. The only exception is $\text{nsc}_{2,3}\{4\}$, whose values in the pp collisions are very different from those in $p+\text{Pb}$ and $\text{Pb}+\text{Pb}$ collisions. In contrast, the $\text{sc}_{2,3}\{4\}$ values in Fig. 4 are close among different systems. This suggests that the $\langle v_3^2 \rangle$ values from the template fit method [7] may be significantly underestimated. As pointed out in Ref. [7] and emphasised in Appendix A, the template fit method, and other methods based on peripheral subtraction in general [5,15], tend to underestimate the odd flow harmonics, due to the presence of a large away-side peak at $\Delta\phi \sim \pi$ in the two-particle correlation function. The comparison of $\text{sc}_{2,3}\{4\}$ and $\text{nsc}_{2,3}\{4\}$ among different collision systems provides indirect evidence of this underestimation of $\langle v_3^2 \rangle$.

Fig. 5 shows that the normalised cumulants are consistent between $0.3 < p_{\text{T}} < 3$ GeV and $0.5 < p_{\text{T}} < 5$ GeV. On the other hand, the magnitudes of the cumulants in Fig. 4 differ by a large factor between the two p_{T} ranges: about a factor of three for $\text{sc}_{2,3}\{4\}$ and $\text{sc}_{2,4}\{4\}$, and a factor of two for $\text{ac}_2\{3\}$. These results suggest that the p_{T} dependence of $\text{sc}_{2,3}\{4\}$, $\text{sc}_{2,4}\{4\}$ and $\text{ac}_2\{3\}$ largely reflects the p_{T} dependence of the v_n at the single-particle level.

9. Discussion

Three- and four-particle cumulants involving correlations between two harmonics of different order v_n and v_m are measured in $\sqrt{s} = 13$ TeV pp , $\sqrt{s_{\text{NN}}} = 5.02$ TeV $p+\text{Pb}$, and low-multiplicity $\sqrt{s_{\text{NN}}} = 2.76$ TeV $\text{Pb}+\text{Pb}$ collisions with the ATLAS detector at the LHC, with total integrated luminosities of 0.9 pb^{-1} , 28 nb^{-1} , and $7 \mu\text{b}^{-1}$, respectively. The correlation between v_n and v_m is studied using four-particle symmetric cumulants, $\text{sc}_{2,3}\{4\}$ and

$\text{sc}_{2,4}\{4\}$, and the three-particle asymmetric cumulant $\text{ac}_2\{3\}$. The symmetric cumulants $\text{sc}_{n,m}\{4\} = \langle v_n^2 v_m^2 \rangle - \langle v_n^2 \rangle \langle v_m^2 \rangle$ probe the correlation of the flow magnitudes, while the asymmetric cumulant $\text{ac}_2\{3\} = \langle v_2^2 v_4 \cos 4(\Phi_2 - \Phi_4) \rangle$ is sensitive to correlations involving both the flow magnitude v_n and flow phase Φ_n . They are calculated using the standard cumulant method, as well as the two-, three- and four-subevent methods to suppress non-flow effects. The final results are presented as a function of the average number of charged particles with $p_{\text{T}} > 0.4$ GeV, $\langle N_{\text{ch}} \rangle$.

Significant differences are observed between the standard method and the subevent methods over the full $\langle N_{\text{ch}} \rangle$ range in pp collisions, as well as over the low $\langle N_{\text{ch}} \rangle$ range in $p+\text{Pb}$ and $\text{Pb}+\text{Pb}$ collisions. The differences are larger for particles at higher p_{T} or at smaller $\langle N_{\text{ch}} \rangle$. When analysed with the standard method in pp collisions, this behaviour is compatible with the dominance of the non-flow correlations rather than the long-range collective flow correlations. Systematic, but much smaller, differences are also observed in the low $\langle N_{\text{ch}} \rangle$ region between the two-subevent method and three- or four-subevent methods, which indicate that the two-subevent method may still be affected by correlations arising from jets. On the other hand no differences are observed between the three-subevent and four-subevent methods, within experimental uncertainties, suggesting that methods with three or more subevents are sufficient to reject non-flow correlations from jets. Therefore, the three-subevent method is used to present the main results in this analysis.

The three-subevent method provides a measurement of negative $\text{sc}_{2,3}\{4\}$ and positive $\text{sc}_{2,4}\{4\}$ and $\text{ac}_2\{3\}$ over nearly the full $\langle N_{\text{ch}} \rangle$ range and in all three collision systems. These results indicate a negative correlation between v_2 and v_3 and a positive

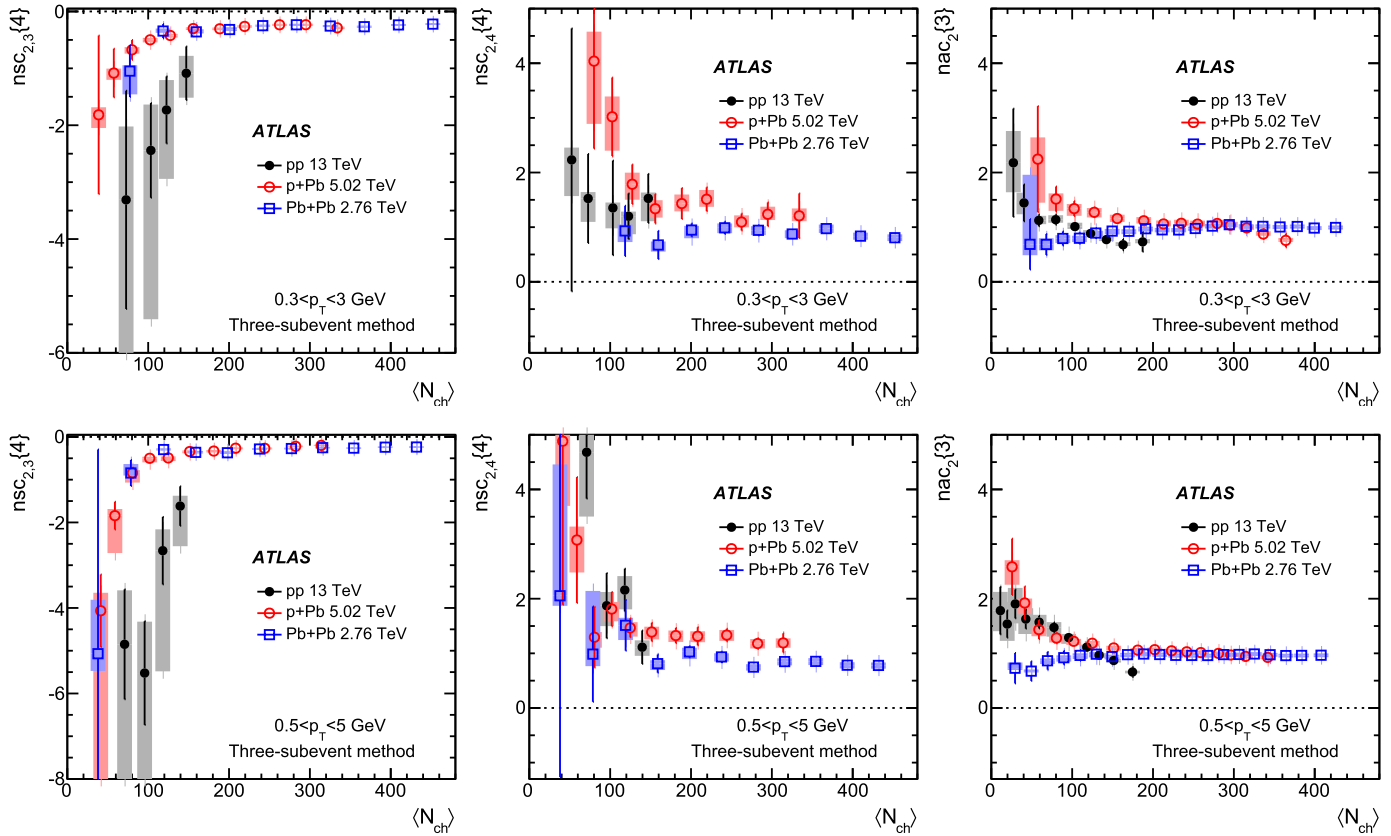


Fig. 5. The $\langle N_{\text{ch}} \rangle$ dependence of $n_{\text{sc},3,4}$ (left panels), $n_{\text{sc},2,4}$ (middle panels) and $n_{\text{ac},2}$ (right panels) in $0.3 < p_{\text{T}} < 3 \text{ GeV}$ (top row) and $0.5 < p_{\text{T}} < 5 \text{ GeV}$ (bottom row) obtained for pp collisions (solid circles), $p+\text{Pb}$ collisions (open circles) and low-multiplicity $\text{Pb}+\text{Pb}$ collisions (open squares). The error bars and shaded boxes represent the statistical and systematic uncertainties, respectively.

correlation between v_2 and v_4 . Such correlation patterns have previously been observed in large collision systems [42–44], but are now confirmed in small collision systems, once non-flow effects are adequately suppressed. The values of $n_{\text{sc},2,3}{4}$ and $n_{\text{sc},2,4}{4}$ are consistent in pp and $p+\text{Pb}$ collisions over the same $\langle N_{\text{ch}} \rangle$ range, but their magnitudes at large $\langle N_{\text{ch}} \rangle$ are much smaller than those for $\text{Pb}+\text{Pb}$ collisions. The values of $n_{\text{ac},2}{3}$ are similar at very low $\langle N_{\text{ch}} \rangle$ among the three systems, but are very different at large $\langle N_{\text{ch}} \rangle$. On the other hand, after scaling by the $\langle v_n^2 \rangle$ estimated from a two-particle analysis [7,14], the resulting normalised cumulants $n_{\text{sc},2,3}{4}$, $n_{\text{sc},2,4}{4}$ and $n_{\text{ac},2}{3}$ show a much weaker dependence on $\langle N_{\text{ch}} \rangle$, and their values are much closer to each other among the three systems. The magnitudes of the normalised cumulants are also similar to each other for $0.5 < p_{\text{T}} < 5 \text{ GeV}$ as well as $0.3 < p_{\text{T}} < 3 \text{ GeV}$. This suggests that the $\langle N_{\text{ch}} \rangle$, p_{T} and system dependence of the $n_{\text{sc},2,3}{4}$, $n_{\text{sc},2,4}{4}$ and $n_{\text{ac},2}{3}$ reflect mostly the $\langle N_{\text{ch}} \rangle$, p_{T} and system dependence of $\langle v_n^2 \rangle$, but the relative strengths of the correlations are similar for the three collision systems.

The new results obtained with the subevent cumulant technique provide further evidence that the ridge is indeed a long-range collective phenomenon involving many particles distributed across a broad rapidity interval. The similarity between different collision systems for $n_{\text{sc},2,3}{4}$, $n_{\text{sc},2,4}{4}$ and $n_{\text{ac},2}{3}$, and the weak dependence of these observables on the p_{T} range and $\langle N_{\text{ch}} \rangle$, largely free from non-flow effects, provide an important input towards understanding the space–time dynamics and the properties of the medium created in small collision systems. These results provide inputs to distinguish between models based on initial-state momentum correlations and models based on final-state hydrodynamics.

Acknowledgements

We thank CERN for the very successful operation of the LHC, as well as the support staff from our institutions without whom ATLAS could not be operated efficiently.

We acknowledge the support of ANPCyT, Argentina; YerPhI, Armenia; ARC, Australia; BMWFW and FWF, Austria; ANAS, Azerbaijan; SSTC, Belarus; CNPq and FAPESP, Brazil; NSERC, NRC and CFI, Canada; CERN; CONICYT, Chile; CAS, MOST and NSFC, China; COLCIENCIAS, Colombia; MSMT CR, MPO CR and VSC CR, Czech Republic; DNRF and DNSRC, Denmark; IN2P3-CNRS, CEA-DRF/IRFU, France; SRNSFG, Georgia; BMBF, HGF, and MPG, Germany; GSRT, Greece; RGC, Hong Kong SAR, China; ISF and Benoziyo Center, Israel; INFN, Italy; MEXT and JSPS, Japan; CNRST, Morocco; NWO, Netherlands; RCN, Norway; MNiSW and NCN, Poland; FCT, Portugal; MNE/IFA, Romania; MES of Russia and NRC KI, Russian Federation; JINR; MESTD, Serbia; MSSR, Slovakia; ARRS and MIZŠ, Slovenia; DST/NRF, South Africa; MINECO, Spain; SRC and Wallenberg Foundation, Sweden; SERI, SNSF and Cantons of Bern and Geneva, Switzerland; MOST, Taiwan; TAEK, Turkey; STFC, United Kingdom; DOE and NSF, United States of America. In addition, individual groups and members have received support from BCKDF, the Canada Council, CANARIE, CRC, Compute Canada, FQRNT, and the Ontario Innovation Trust, Canada; EPLANET, ERC, ERDF, FP7, Horizon 2020 and Marie Skłodowska-Curie Actions, European Union; Investissements d’Avenir Labex and Idex, ANR, Région Auvergne and Fondation Partager le Savoir, France; DFG and AvH Foundation, Germany; Herakleitos, Thales and Aristeia programmes co-financed by EU-ESF and the Greek NSRF; BSF, GIF and Minerva, Israel; BRF, Norway; CERCA Programme Generalitat de Catalunya, Generalitat

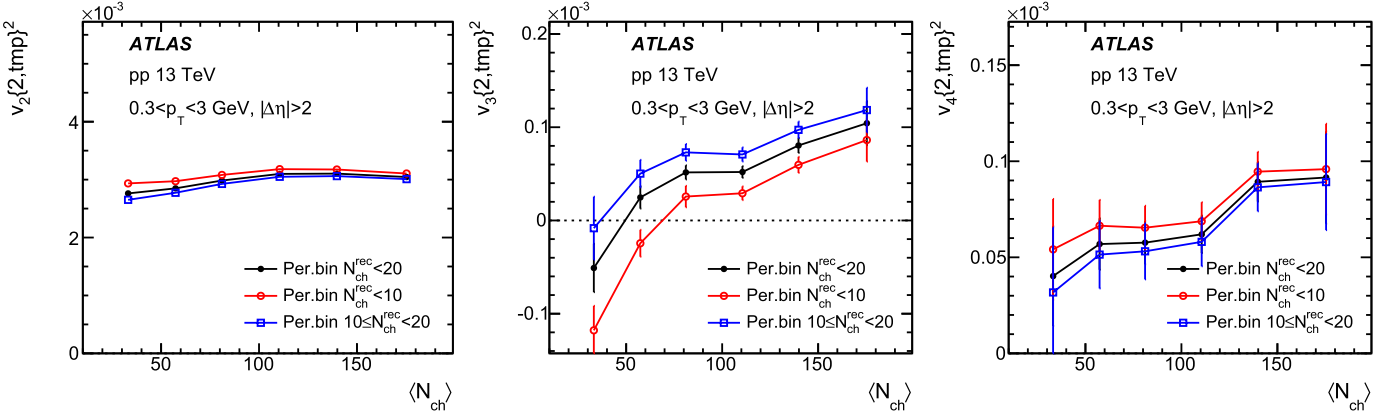


Fig. 6. The values of $v_n\{2,\text{tmp}\}^2$ obtained following the template fit procedure given in Eq. (14) [7] in pp collisions for $n = 2$ (left panel), $n = 3$ (middle panel) and $n = 4$ (right panel). In each panel, the values are calculated for three peripheral $N_{\text{ch}}^{\text{rec}}$ intervals: $N_{\text{ch}}^{\text{rec}} < 20$, $N_{\text{ch}}^{\text{rec}} < 10$ and $10 \leq N_{\text{ch}}^{\text{rec}} < 20$. Only statistical uncertainties are shown.

Valenciana, Spain; the Royal Society and Leverhulme Trust, United Kingdom.

The crucial computing support from all WLCG partners is acknowledged gratefully, in particular from CERN, the ATLAS Tier-1 facilities at TRIUMF (Canada), NDGF (Denmark, Norway, Sweden), CC-IN2P3 (France), KIT/GridKA (Germany), INFN-CNAF (Italy), NL-T1 (Netherlands), PIC (Spain), ASGC (Taiwan), RAL (UK) and BNL (USA), the Tier-2 facilities worldwide and large non-WLCG resource providers. Major contributors of computing resources are listed in Ref. [45].

Appendix A. Improvement to the template fit procedure

In order to separate the long-range ridge from other non-flow sources, especially dijets, the ATLAS Collaboration developed a template fitting procedure described in Refs. [7,14]. The first step is to construct a $\Delta\phi$ distribution of particle pairs with large pseudorapidity separation $|\Delta\eta| > 2$, the so-called “per-trigger” particle yield, $Y(\Delta\phi)$, for a given $N_{\text{ch}}^{\text{rec}}$ range. The $|\Delta\eta| > 2$ requirement suppresses the intra-jet and other short-range correlations, and in small collision systems the resulting $Y(\Delta\phi)$ distributions are known to be dominated by away-side jet correlations [4,5,14]. This away-side non-flow component is peaked at $\Delta\phi \approx \pi$, and leads to a significant bias in the flow coefficients v_n , especially for the odd harmonics.

To subtract the away-side jet correlations, the measured $Y(\Delta\phi)$ distribution in a given $N_{\text{ch}}^{\text{rec}}$ interval is assumed to be a sum of a scaled “peripheral” distribution $Y(\Delta\phi)^{\text{peri}}$, obtained for low-multiplicity events $N_{\text{ch}}^{\text{rec}} < 20$, and a constant pedestal modulated by $\cos(n\Delta\phi)$ for $n \geq 2$ [7,14]:

$$Y(\Delta\phi) = F Y(\Delta\phi)^{\text{peri}} + G^{\text{tmp}} \left(1 + 2 \sum_{n=2}^{\infty} v_n\{2,\text{tmp}\}^2 \cos n\Delta\phi \right). \quad (14)$$

The scale factor F and pedestal G^{tmp} are fixed by the fit, and $v_n\{2,\text{tmp}\}$ are calculated from a Fourier transform. On the other hand, both $Y(\Delta\phi)$ and $Y(\Delta\phi)^{\text{peri}}$ contain a dijet component and flow component:

$$Y(\Delta\phi) = Y(\Delta\phi)^{\text{cent}} + G^{\text{cent}} \left(1 + 2 \sum_{n=2}^{\infty} v_n\{2\}^2 \cos n\Delta\phi \right), \quad (15)$$

$$Y(\Delta\phi)^{\text{peri}} = Y(\Delta\phi)^{\text{jet}} + G^{\text{peri}} \left(1 + 2 \sum_{n=2}^{\infty} v_n\{2,\text{peri}\}^2 \cos n\Delta\phi \right). \quad (16)$$

With the assumption that the shape of the dijet component is independent of $N_{\text{ch}}^{\text{rec}}$, and the magnitudes of the dijet components are related by the scale factor F : $Y(\Delta\phi)^{\text{cent}} = FY(\Delta\phi)^{\text{jet}}$, Eq. (14) can be written as:

$$Y(\Delta\phi) = Y(\Delta\phi)^{\text{cent}} + (G^{\text{tmp}} + FG^{\text{peri}}) + 2 \sum_{n=2}^{\infty} (G^{\text{tmp}} v_n\{2,\text{tmp}\}^2 + FG^{\text{peri}} v_n\{2,\text{peri}\}^2) \times \cos n\Delta\phi.$$

Comparing with Eqs. (15) and (16), one obtains $G^{\text{cent}} = G^{\text{tmp}} + FG^{\text{peri}}$ and the following relation:

$$v_n\{2\}^2 = v_n\{2,\text{tmp}\}^2 - \frac{FG^{\text{peri}}}{G^{\text{cent}}} (v_n\{2,\text{tmp}\}^2 - v_n\{2,\text{peri}\}^2),$$

which shows that $v_n\{2,\text{tmp}\}$ from the template fit differs from the true $v_n\{2\}$ by a correction term that vanishes if and only if $v_n\{2\}$ is independent of $N_{\text{ch}}^{\text{rec}}$. Since the true flow harmonics in the peripheral interval $v_n\{2,\text{peri}\}$ are unknown in principle, the correction is applied starting from the third-lowest $N_{\text{ch}}^{\text{rec}}$ interval ($40 \leq N_{\text{ch}}^{\text{rec}} < 60$) in this analysis, by using $v_n\{2,\text{tmp}\}$ of the second $N_{\text{ch}}^{\text{rec}}$ interval ($20 \leq N_{\text{ch}}^{\text{rec}} < 40$) as an estimate of the true flow harmonics. Since the non-flow contribution primarily affects the odd harmonics, the $v_3\{2,\text{tmp}\}^2$ may become negative in the first few $N_{\text{ch}}^{\text{rec}}$ intervals in pp collisions. In such cases, the correction starts from the second $N_{\text{ch}}^{\text{rec}}$ interval with positive $v_3\{2,\text{tmp}\}^2$ ($60 \leq N_{\text{ch}}^{\text{rec}} < 80$) by using $v_3\{2,\text{tmp}\}$ from the previous $N_{\text{ch}}^{\text{rec}}$ interval ($40 \leq N_{\text{ch}}^{\text{rec}} < 60$).

One important feature of the template fit analysis is the assumption that the dijet component $Y(\Delta\phi)^{\text{jet}}$ is independent of $\langle N_{\text{ch}} \rangle$. In Ref. [7], the uncertainty associated with this assumption is studied by changing the default peripheral interval from $N_{\text{ch}}^{\text{rec}} < 20$ to $N_{\text{ch}}^{\text{rec}} < 10$ and $10 \leq N_{\text{ch}}^{\text{rec}} < 20$. It was found that the $v_n\{2,\text{tmp}\}$ values are relatively insensitive to the choice of peripheral interval for $n = 2$ and $n = 4$, but the sensitivity is much larger for $n = 3$. This finding is reproduced in Fig. 6 for pp collisions, which shows that the $v_3\{2,\text{tmp}\}^2$ values obtained via Eq. (14) differ substantially for the different $N_{\text{ch}}^{\text{rec}}$ ranges.

In addition to the template fit with and without the above mentioned correction procedure, the ATLAS and CMS collaborations

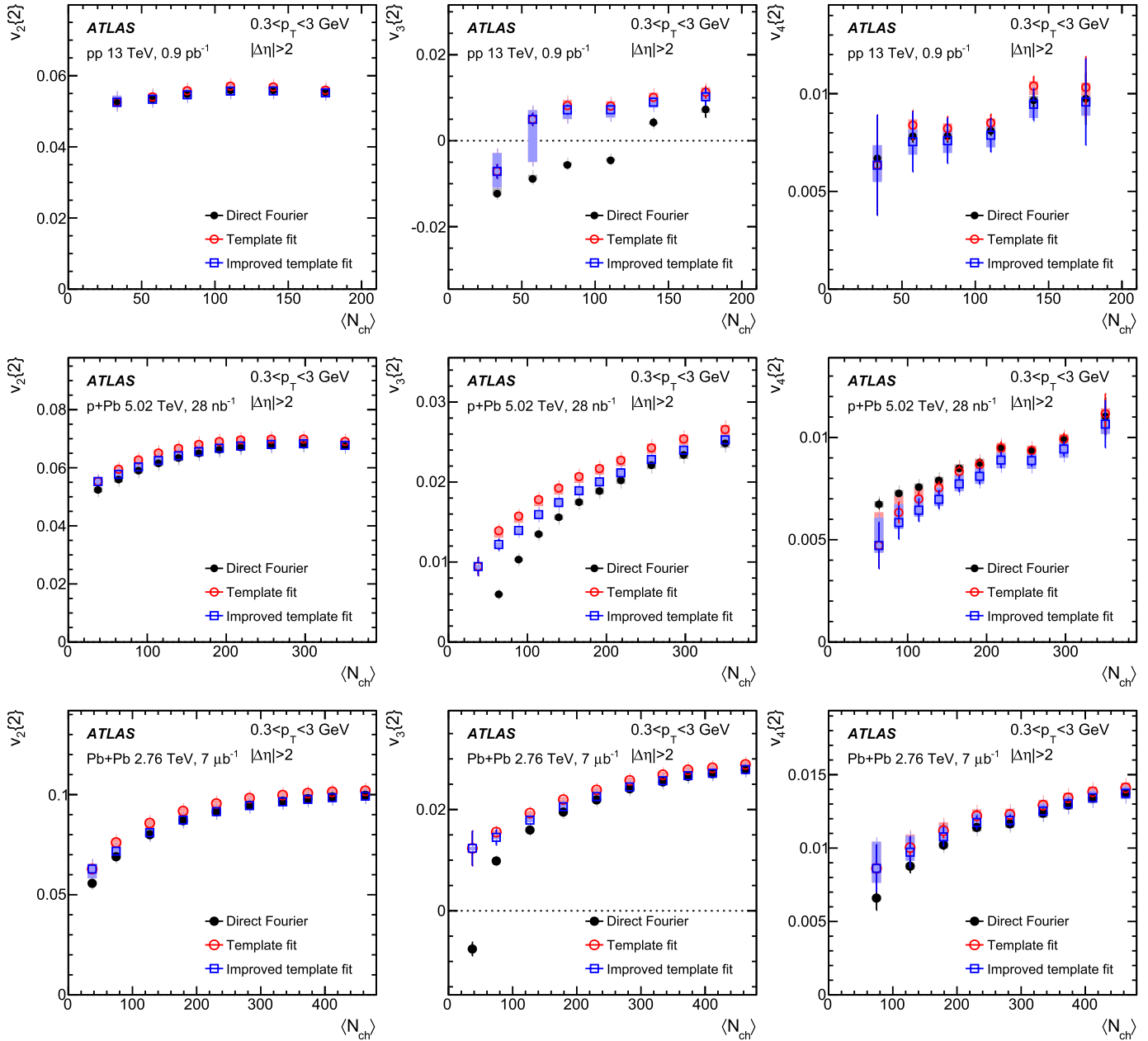


Fig. 7. The $v_2\{2\}$ (left column), $v_3\{2\}$ (middle column) and $v_4\{2\}$ (right column) obtained from two-particle correlations in $0.3 < p_T < 3$ GeV in pp (top row), $p+Pb$ (middle row) and $Pb+Pb$ (bottom row) collisions. In each panel, they are compared between three methods: direct Fourier transformation (solid circles), template fit (open circles) and the improved template fit (open squares). The error bars and shaded boxes represent the statistical and systematic uncertainties, respectively.

also calculated directly the $v_n\{2\}$ values via a Fourier transform of the $Y(\Delta\phi)$ distribution without dijet subtraction [7,19]. The differences between the direct Fourier transform and template fit reflect mainly the away-side jet contribution subtracted by the template fit procedure, and therefore give a sense of the magnitude of unknown systematic uncertainties associated with the template fit procedure. If these differences are too large, the $v_n\{2, \text{tmp}\}$ values may be sensitive to the systematic effects associated with the assumption that the shape of $Y(\Delta\phi)_{\text{jet}}$ is independent of N_{ch}^{rec} .

Fig. 7 compares the $v_n\{2\}$ in $0.3 < p_T < 3$ GeV obtained from $Y(\Delta\phi)$ using three methods: a direct Fourier transform (solid circles), a template fit (open circles) and a template fit corrected for the bias (open squares), as described above. The systematic uncertainties for the template fit results are nearly the same as those from Ref. [7]. Fig. 7 shows that the changes introduced by

the correction procedure described above are small in all cases and for all harmonics. The values of the even-order harmonics, v_2 and v_4 , are also quite similar to those obtained from the direct Fourier transformation, reflecting the fact that the dijet correlations have very little influence on the even-order harmonics. On the other hand, significant differences are observed between the direct Fourier transform and template fit for v_3 , especially in the pp collisions, due to the influence of $Y(\Delta\phi)_{\text{jet}}$, a trend observed and discussed previously in Refs. [7,15]. The template fit procedure is able to subtract the dijet correlations and change the sign of v_3 , but also introduces a large uncertainty associated with the procedure. As discussed in Section 8.2, the behaviour of the symmetric cumulants $sc_{2,3}\{4\}$ in Fig. 4 and normalised cumulants $nsc_{2,3}\{4\}$ in Fig. 5 in pp collisions, suggest that the v_3 values from the template fit procedure are significantly underestimated due to the presence

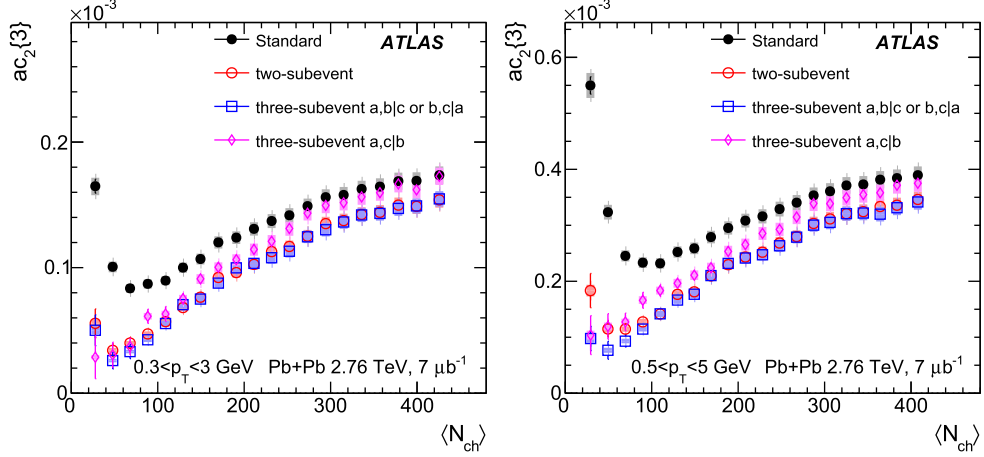


Fig. 8. The $ac_2\{3\}$ in $0.3 < p_T < 3$ GeV (left panel) and $0.5 < p_T < 5$ GeV (right panel) in $Pb+Pb$ collisions. In each panel, they are compared between the standard method (solid circles), two-subevent method (open circles), three-subevent where \mathbf{V}_4 is determined in subevent a or c (open boxes), and three-subevent where \mathbf{V}_4 is determined in subevent b (diamonds) according to Eq. (8). The error bars and shaded boxes represent the statistical and systematic uncertainties, respectively.

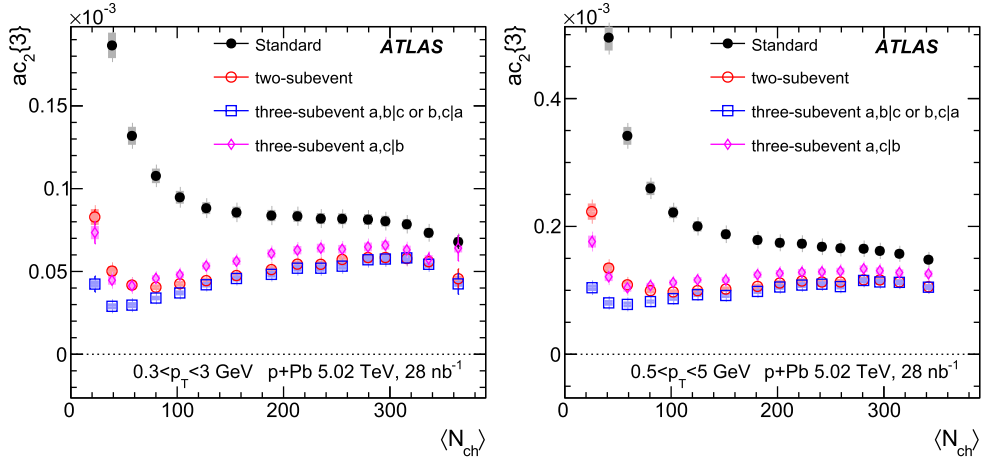


Fig. 9. The $ac_2\{3\}$ in $0.3 < p_T < 3$ GeV (left panel) and $0.5 < p_T < 5$ GeV (right panel) in $p+Pb$ collisions. In each panel, they are compared between standard method (solid circles), two-subevent method (open circles), three-subevent where \mathbf{V}_4 is determined in subevent a or c (open boxes), and three-subevent where \mathbf{V}_4 is determined in subevent b (diamonds) according to Eq. (8). The error bars and shaded boxes represent the statistical and systematic uncertainties, respectively.

of a large residual non-flow bias. In contrast, the differences of v_3 between the direct Fourier transform and the template fit are much smaller in the $p+Pb$ and the $Pb+Pb$ collisions, except in the very low $\langle N_{ch} \rangle$ region. Therefore, the v_3 values in $p+Pb$ and $Pb+Pb$ systems extracted from the template fit procedure are expected to be less affected by the dijets.

Appendix B. Effects of flow decorrelations in the subevent cumulant methods

As discussed in Section 8, the differences between the standard method and subevent methods for $ac_2\{3\}$ can be partially attributed to longitudinal flow decorrelations [38,41]. Since subevent methods correlate flow vectors obtained from different η regions, the influence of decorrelations can be studied by comparing different variants of the three-subevent method. This comparison is carried out using asymmetric cumulant $ac_2 = \langle \mathbf{V}_2^2 \mathbf{V}_4^* \rangle$, however, the statistical precision of $sc_{n,m}\{4\}$ is not sufficient for such comparison.

The three-subevent method uses flow vectors from three subevents a , b and c , covering $-2.5 < \eta_a < -2.5/3$, $|\eta_b| \leq 2.5/3$ and $2.5/3 < \eta_c < 2.5$, and have three independent definitions for asymmetric cumulant: $ac_2^{a,b|c}\{3\}$, $ac_n^{b,c|a}\{3\}$ and $ac_2^{a,c|b}\{3\}$. Because

of symmetry between subevents a and c , $ac_2^{a,b|c}\{3\}$ and $ac_n^{b,c|a}\{3\}$ measure the same physics, and are therefore averaged into a single result, denoted as $ac_2^{a,b|c} \text{ or } b,c|a\{3\}$. Fig. 8 compares the two three-subevent results with results for the standard and two-subevent methods. The results based on various subevent methods show a small decrease with $\langle N_{ch} \rangle$ in the $\langle N_{ch} \rangle < 50$ region, reflecting a modest contribution from non-flow. On the other hand, all the subevent-based results increase gradually with $\langle N_{ch} \rangle$ for $\langle N_{ch} \rangle > 50$, reflecting a dominant contribution from flow.

Fig. 8 shows that the values of $ac_2^{a,c|b}\{3\} = \langle \mathbf{V}_{2,a} \mathbf{V}_{4,b}^* \mathbf{V}_{2,c} \rangle$ are larger than $ac_2^{a,b|c} \text{ or } b,c|a\{3\}$ at larger $\langle N_{ch} \rangle$ region. This is because the subevent for \mathbf{V}_4 is in between the two subevents used to calculate \mathbf{V}_2 . This configuration has much smaller decorrelation effects [41]. For $ac_2^{a,b|c} \text{ or } b,c|a\{3\}$, the two subevents for \mathbf{V}_2 are on the same side of the subevent for \mathbf{V}_4 , leading to larger decorrelation effects. Interestingly, such configuration gives results that are very similar to those from the two-subevent method. Figs. 9 and 10 show the results for the $p+Pb$ and pp collisions, respectively. Similar observations as in $Pb+Pb$ collisions can be made, although in pp collisions the results from the two-subevent method are larger than those obtained with the three-subevent method, due to significant non-flow contribution even in the large $\langle N_{ch} \rangle$ region.

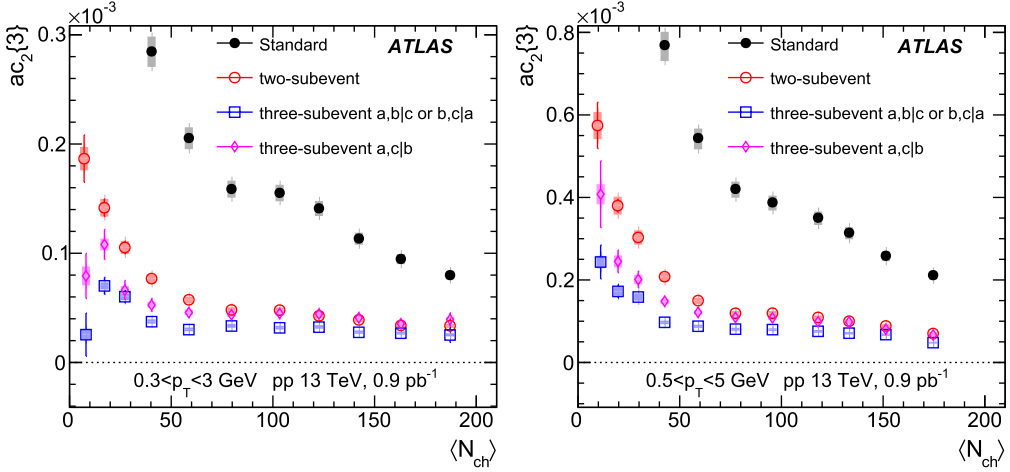


Fig. 10. The $ac_2\{3\}$ in $0.3 < p_T < 3$ GeV (left panel) and $0.5 < p_T < 5$ GeV (right panel) in pp collisions. In each panel, they are compared between standard method (solid circles), two-subevent method (open circles), three-subevent where V_4 is determined in subevent a or c (open boxes), and three-subevent where V_4 is determined in subevent b (diamonds) according to Eq. (8). The error bars and shaded boxes represent the statistical and systematic uncertainties, respectively.

References

- [1] E. Shuryak, Strongly coupled quark-gluon plasma in heavy ion collisions, *Rev. Mod. Phys.* 89 (2017) 035001, arXiv:1412.8393 [hep-ph].
- [2] CMS Collaboration, Observation of long-range near-side angular correlations in proton-lead collisions at the LHC, *Phys. Lett. B* 718 (2013) 795, arXiv:1210.5482 [nucl-ex].
- [3] ALICE Collaboration, Long-range angular correlations on the near and away side in p -Pb collisions at $\sqrt{s_{NN}} = 5.02$ TeV, *Phys. Lett. B* 719 (2013) 29, arXiv:1212.2001 [nucl-ex].
- [4] ATLAS Collaboration, Observation of associated near-side and away-side long-range correlations in $\sqrt{s_{NN}} = 5.02$ TeV proton-lead collisions with the ATLAS detector, *Phys. Rev. Lett.* 110 (2013) 182302, arXiv:1212.5198 [hep-ex].
- [5] ATLAS Collaboration, Measurement of long-range pseudorapidity correlations and azimuthal harmonics in $\sqrt{s_{NN}} = 5.02$ TeV proton-lead collisions with the ATLAS detector, *Phys. Rev. C* 90 (2014) 044906, arXiv:1409.1792 [hep-ex].
- [6] CMS Collaboration, Evidence for collective multiparticle correlations in p-Pb collisions, *Phys. Rev. Lett.* 115 (2015) 012301, arXiv:1502.05382 [nucl-ex].
- [7] ATLAS Collaboration, Measurements of long-range azimuthal anisotropies and associated Fourier coefficients for pp collisions at $\sqrt{s} = 5.02$ and 13 TeV and p -Pb collisions at $\sqrt{s_{NN}} = 5.02$ TeV with the ATLAS detector, *Phys. Rev. C* 96 (2017) 024908, arXiv:1609.06213 [nucl-ex].
- [8] K. Dusling, R. Venugopalan, Comparison of the color glass condensate to di-hadron correlations in proton-proton and proton-nucleus collisions, *Phys. Rev. D* 87 (2013) 094034, arXiv:1302.7018 [hep-ph].
- [9] P. Bozek, W. Broniowski, Collective dynamics in high-energy proton-nucleus collisions, *Phys. Rev. C* 88 (2013) 014903, arXiv:1304.3044 [nucl-th].
- [10] N. Borghini, P.M. Dinh, J.-Y. Ollitrault, New method for measuring azimuthal distributions in nucleus-nucleus collisions, *Phys. Rev. C* 63 (2001) 054906, arXiv:nucl-th/0007063 [nucl-th].
- [11] A. Bilandzic, R. Snellings, S. Voloshin, Flow analysis with cumulants: direct calculations, *Phys. Rev. C* 83 (2011) 044913, arXiv:1010.0233 [nucl-ex].
- [12] A. Bilandzic, C.H. Christensen, K. Gulbrandsen, A. Hansen, Y. Zhou, Generic framework for anisotropic flow analyses with multiparticle azimuthal correlations, *Phys. Rev. C* 89 (2014) 064904, arXiv:1312.3572 [nucl-ex].
- [13] J. Jia, M. Zhou, A. Trzupek, Revealing long-range multiparticle collectivity in small collision systems via subevent cumulants, *Phys. Rev. C* 96 (2017) 034906, arXiv:1701.03830 [nucl-th].
- [14] ATLAS Collaboration, Observation of long-range elliptic azimuthal anisotropies in $\sqrt{s} = 13$ and 2.76 TeV pp collisions with the ATLAS detector, *Phys. Rev. Lett.* 116 (2016) 172301, arXiv:1509.04776 [hep-ex].
- [15] CMS Collaboration, Evidence for collectivity in pp collisions at the LHC, *Phys. Lett. B* 765 (2017) 193–220, arXiv:1606.06198 [nucl-ex].
- [16] P. Huo, K. Gajdošová, J. Jia, Y. Zhou, Importance of non-flow in mixed-harmonic multi-particle correlations in small collision systems, *Phys. Lett. B* 777 (2018) 201, arXiv:1710.07567 [nucl-ex].
- [17] ATLAS Collaboration, Measurement of multi-particle azimuthal correlations in pp , p +Pb and low-multiplicity Pb+Pb collisions with the ATLAS detector, *Eur. Phys. J. C* 77 (2017) 428, arXiv:1705.04176 [hep-ex].
- [18] ATLAS Collaboration, Measurement of multi-particle azimuthal correlations with the subevent cumulant method in pp and p +Pb collisions with the ATLAS detector at the LHC, *Phys. Rev. C* 97 (2018) 024904, arXiv:1708.03559 [hep-ex].
- [19] CMS Collaboration, Observation of correlated azimuthal anisotropy Fourier harmonics in pp and pPb collisions at the LHC, *Phys. Rev. Lett.* 120 (2018) 092301, arXiv:1709.09189 [nucl-ex].
- [20] ATLAS Collaboration, The ATLAS experiment at the CERN Large Hadron Collider, *J. Instrum.* 3 (2008) S08003.
- [21] ATLAS Collaboration, The ATLAS inner detector commissioning and calibration, *Eur. Phys. J. C* 70 (2010) 787, arXiv:1004.5293 [physics.ins-det].
- [22] ATLAS Collaboration, ATLAS Insertable B-Layer Technical Design Report, Atlas-tdr-19, <https://cds.cern.ch/record/1291633>, 2010;
ATLAS Insertable B-Layer Technical Design Report Addendum, ATLAS-TDR-19-ADD-1, <https://cds.cern.ch/record/1451888>, 2012.
- [23] ATLAS Collaboration, Performance of the ATLAS trigger system in 2010, *Eur. Phys. J. C* 72 (2012) 1849, arXiv:1110.1530 [hep-ex].
- [24] ATLAS Collaboration, Performance of the ATLAS trigger system in 2015, *Eur. Phys. J. C* 77 (2017) 317, arXiv:1611.09661 [hep-ex].
- [25] ATLAS Collaboration, Charged-particle distributions in $\sqrt{s} = 13$ TeV pp interactions measured with the ATLAS detector at the LHC, *Phys. Lett. B* 758 (2016) 67, arXiv:1602.01633 [hep-ex].
- [26] ATLAS Collaboration, Performance of the ATLAS minimum bias and forward detector triggers in pPb collisions, ATLAS-CONF-2013-104, <https://cds.cern.ch/record/1624013>.
- [27] T. Sjöstrand, S. Mrenna, P.Z. Skands, A brief introduction to PYTHIA 8.1, *Comput. Phys. Commun.* 178 (2008) 852, arXiv:0710.3820 [hep-ph].
- [28] ATLAS Collaboration, ATLAS tunes of PYTHIA 6 and Pythia 8 for MC11, ATLAS-PHYS-PUB-2011-009, <https://cds.cern.ch/record/1363300>.
- [29] M. Gyulassy, X.-N. Wang, HIJING 1.0: a Monte Carlo program for parton and particle production in high-energy hadronic and nuclear collisions, *Comput. Phys. Commun.* 83 (1994) 307, arXiv:nucl-th/9502021.
- [30] GEANT4 Collaboration, S. Agostinelli, et al., GEANT4: a simulation toolkit, *Nucl. Instrum. Methods A* 506 (2003) 250.
- [31] ATLAS Collaboration, The ATLAS simulation infrastructure, *Eur. Phys. J. C* 70 (2010) 823, arXiv:1005.4568 [physics.ins-det].
- [32] ATLAS Collaboration, Measurement of forward-backward multiplicity correlations in lead-lead, proton-lead and proton-proton collisions with the ATLAS detector, *Phys. Rev. C* 95 (2017) 064910, arXiv:1606.08170 [hep-ex].
- [33] P. Di Francesco, M. Guillaud, M. Luzum, J.-Y. Ollitrault, Systematic procedure for analyzing cumulants at any order, *Phys. Rev. C* 95 (2017) 044911, arXiv:1612.05634 [nucl-th].
- [34] G. Giacalone, L. Yan, J. Noronha-Hostler, J.-Y. Ollitrault, Symmetric cumulants and event-plane correlations in Pb + Pb collisions, *Phys. Rev. C* 94 (2016) 014906, arXiv:1605.08303 [nucl-th].
- [35] S.J. Das, G. Giacalone, P.-A. Monard, J.-Y. Ollitrault, Relating centrality to impact parameter in nucleus-nucleus collisions, *Phys. Rev. C* 97 (2018) 014905, arXiv:1708.00081 [nucl-th].
- [36] R.S. Bhalerao, J.-Y. Ollitrault, S. Pal, Event-plane correlators, *Phys. Rev. C* 88 (2013) 024909, arXiv:1307.0980 [nucl-th].
- [37] ATLAS Collaboration, Measurement of the azimuthal anisotropy for charged particle production in $\sqrt{s_{NN}} = 2.76$ TeV lead-lead collisions with the ATLAS detector, *Phys. Rev. C* 86 (2012) 014907, arXiv:1203.3087 [hep-ex].
- [38] P. Bozek, W. Broniowski, J. Moreira, Torqued fireballs in relativistic heavy-ion collisions, *Phys. Rev. C* 83 (2011) 034911, arXiv:1011.3354 [nucl-th].
- [39] L.-G. Pang, G.-Y. Qin, V. Roy, X.-N. Wang, G.-L. Ma, Longitudinal decorrelation of anisotropic flows in heavy-ion collisions at the CERN Large Hadron Collider, *Phys. Rev. C* 91 (2015) 044904, arXiv:1410.8690 [nucl-th].

- [40] CMS Collaboration, Evidence for transverse momentum and pseudorapidity dependent event plane fluctuations in PbPb and pPb collisions, Phys. Rev. C 92 (2015) 034911, arXiv:1503.01692 [nucl-ex].
- [41] ATLAS Collaboration, Measurement of longitudinal flow de-correlations in Pb+Pb collisions at $\sqrt{s_{NN}} = 2.76$ and 5.02 TeV with the ATLAS detector, Eur. Phys. J. C 78 (2018) 142, arXiv:1709.02301 [nucl-ex].
- [42] ATLAS Collaboration, Measurement of event-plane correlations in $\sqrt{s_{NN}} = 2.76$ TeV lead-lead collisions with the ATLAS detector, Phys. Rev. C 90 (2014) 024905, arXiv:1403.0489 [hep-ex].
- [43] ATLAS Collaboration, Measurement of the correlation between flow harmonics of different order in lead-lead collisions at $\sqrt{s_{NN}} = 2.76$ TeV with the ATLAS detector, Phys. Rev. C 92 (2015) 034903, arXiv:1504.01289 [hep-ex].
- [44] ALICE Collaboration, J. Adam, et al., Correlated event-by-event fluctuations of flow harmonics in Pb+Pb collisions at $\sqrt{s_{NN}} = 2.76$ TeV, Phys. Rev. Lett. 117 (2016) 182301, arXiv:1604.07663 [nucl-ex].
- [45] ATLAS Collaboration, ATLAS computing acknowledgements, ATL-GEN-PUB-2016-002, <https://cds.cern.ch/record/2202407>.

The ATLAS Collaboration

M. Aaboud ^{34d}, G. Aad ⁹⁹, B. Abbott ¹²⁵, O. Abdinov ^{13,*}, B. Abeloos ¹²⁹, D.K. Abhayasinghe ⁹¹, S.H. Abidi ¹⁶⁴, O.S. AbouZeid ³⁹, N.L. Abraham ¹⁵³, H. Abramowicz ¹⁵⁸, H. Abreu ¹⁵⁷, Y. Abulaiti ⁶, B.S. Acharya ^{64a,64b,p}, S. Adachi ¹⁶⁰, L. Adamczyk ^{81a}, J. Adelman ¹¹⁹, M. Adersberger ¹¹², A. Adiguzel ^{12c,aj}, T. Adye ¹⁴¹, A.A. Affolder ¹⁴³, Y. Afik ¹⁵⁷, C. Agheorghiesei ^{27c}, J.A. Aguilar-Saavedra ^{137f,137a,ai}, F. Ahmadov ^{77,ag}, G. Aielli ^{71a,71b}, S. Akatsuka ⁸³, T.P.A. Åkesson ⁹⁴, E. Akilli ⁵², A.V. Akimov ¹⁰⁸, G.L. Alberghi ^{23b,23a}, J. Albert ¹⁷³, P. Albicocco ⁴⁹, M.J. Alconada Verzini ⁸⁶, S. Alderweireldt ¹¹⁷, M. Aleksić ³⁵, I.N. Aleksandrov ⁷⁷, C. Alexa ^{27b}, T. Alexopoulos ¹⁰, M. Alhroob ¹²⁵, B. Ali ¹³⁹, G. Alimonti ^{66a}, J. Alison ³⁶, S.P. Alkire ¹⁴⁵, C. Allaire ¹²⁹, B.M.M. Allbrooke ¹⁵³, B.W. Allen ¹²⁸, P.P. Allport ²¹, A. Aloisio ^{67a,67b}, A. Alonso ³⁹, F. Alonso ⁸⁶, C. Alpigiani ¹⁴⁵, A.A. Alshehri ⁵⁵, M.I. Alstaty ⁹⁹, B. Alvarez Gonzalez ³⁵, D. Álvarez Piqueras ¹⁷¹, M.G. Alvaggi ^{67a,67b}, B.T. Amadio ¹⁸, Y. Amaral Coutinho ^{78b}, L. Ambroz ¹³², C. Amelung ²⁶, D. Amidei ¹⁰³, S.P. Amor Dos Santos ^{137a,137c}, S. Amoroso ⁴⁴, C.S. Amrouche ⁵², C. Anastopoulos ¹⁴⁶, L.S. Ancu ⁵², N. Andari ¹⁴², T. Andeen ¹¹, C.F. Anders ^{59b}, J.K. Anders ²⁰, K.J. Anderson ³⁶, A. Andreazza ^{66a,66b}, V. Andrei ^{59a}, C.R. Anelli ¹⁷³, S. Angelidakis ³⁷, I. Angelozzi ¹¹⁸, A. Angerami ³⁸, A.V. Anisenkov ^{120b,120a}, A. Annovi ^{69a}, C. Antel ^{59a}, M.T. Anthony ¹⁴⁶, M. Antonelli ⁴⁹, D.J.A. Antrim ¹⁶⁸, F. Anulli ^{70a}, M. Aoki ⁷⁹, J.A. Aparisi Pozo ¹⁷¹, L. Aperio Bella ³⁵, G. Arabidze ¹⁰⁴, J.P. Araque ^{137a}, V. Araujo Ferraz ^{78b}, R. Araujo Pereira ^{78b}, A.T.H. Arce ⁴⁷, R.E. Ardell ⁹¹, F.A. Arduh ⁸⁶, J-F. Arguin ¹⁰⁷, S. Argyropoulos ⁷⁵, A.J. Armbruster ³⁵, L.J. Armitage ⁹⁰, A. Armstrong ¹⁶⁸, O. Arnaez ¹⁶⁴, H. Arnold ¹¹⁸, M. Arratia ³¹, O. Arslan ²⁴, A. Artamonov ^{109,*}, G. Artoni ¹³², S. Artz ⁹⁷, S. Asai ¹⁶⁰, N. Asbah ⁵⁷, A. Ashkenazi ¹⁵⁸, E.M. Asimakopoulou ¹⁶⁹, L. Asquith ¹⁵³, K. Assamagan ²⁹, R. Astalos ^{28a}, R.J. Atkin ^{32a}, M. Atkinson ¹⁷⁰, N.B. Atlay ¹⁴⁸, K. Augsten ¹³⁹, G. Avolio ³⁵, R. Avramidou ^{58a}, M.K. Ayoub ^{15a}, G. Azuelos ^{107,av}, A.E. Baas ^{59a}, M.J. Baca ²¹, H. Bachacou ¹⁴², K. Bachas ^{65a,65b}, M. Backes ¹³², P. Bagnaia ^{70a,70b}, M. Bahmani ⁸², H. Bahrasemani ¹⁴⁹, A.J. Bailey ¹⁷¹, J.T. Baines ¹⁴¹, M. Bajic ³⁹, C. Bakalis ¹⁰, O.K. Baker ¹⁸⁰, P.J. Bakker ¹¹⁸, D. Bakshi Gupta ⁹³, E.M. Baldin ^{120b,120a}, P. Balek ¹⁷⁷, F. Balli ¹⁴², W.K. Balunas ¹³⁴, J. Balz ⁹⁷, E. Banas ⁸², A. Bandyopadhyay ²⁴, S. Banerjee ^{178,l}, A.A.E. Bannoura ¹⁷⁹, L. Barak ¹⁵⁸, W.M. Barbe ³⁷, E.L. Barberio ¹⁰², D. Barberis ^{53b,53a}, M. Barbero ⁹⁹, T. Barillari ¹¹³, M-S. Barisits ³⁵, J. Barkeloo ¹²⁸, T. Barklow ¹⁵⁰, N. Barlow ³¹, R. Barnea ¹⁵⁷, S.L. Barnes ^{58c}, B.M. Barnett ¹⁴¹, R.M. Barnett ¹⁸, Z. Barnovska-Blenessy ^{58a}, A. Baroncelli ^{72a}, G. Barone ²⁶, A.J. Barr ¹³², L. Barranco Navarro ¹⁷¹, F. Barreiro ⁹⁶, J. Barreiro Guimarães da Costa ^{15a}, R. Bartoldus ¹⁵⁰, A.E. Barton ⁸⁷, P. Bartos ^{28a}, A. Basalaev ¹³⁵, A. Bassalat ¹²⁹, R.L. Bates ⁵⁵, S.J. Batista ¹⁶⁴, S. Batlamous ^{34e}, J.R. Batley ³¹, M. Battaglia ¹⁴³, M. Bauce ^{70a,70b}, F. Bauer ¹⁴², K.T. Bauer ¹⁶⁸, H.S. Bawa ^{150,n}, J.B. Beacham ¹²³, T. Beau ¹³³, P.H. Beauchemin ¹⁶⁷, P. Bechtle ²⁴, H.C. Beck ⁵¹, H.P. Beck ^{20,s}, K. Becker ⁵⁰, M. Becker ⁹⁷, C. Becot ⁴⁴, A. Beddall ^{12d}, A.J. Beddall ^{12a}, V.A. Bednyakov ⁷⁷, M. Bedognetti ¹¹⁸, C.P. Bee ¹⁵², T.A. Beermann ³⁵, M. Begalli ^{78b}, M. Begel ²⁹, A. Behera ¹⁵², J.K. Behr ⁴⁴, A.S. Bell ⁹², G. Bella ¹⁵⁸, L. Bellagamba ^{23b}, A. Bellerive ³³, M. Bellomo ¹⁵⁷, P. Bellos ⁹, K. Belotskiy ¹¹⁰, N.L. Belyaev ¹¹⁰, O. Benary ^{158,*}, D. Benchekroun ^{34a}, M. Bender ¹¹², N. Benekos ¹⁰, Y. Benhammou ¹⁵⁸, E. Benhar Noccioli ¹⁸⁰, J. Benitez ⁷⁵, D.P. Benjamin ⁴⁷, M. Benoit ⁵², J.R. Bensinger ²⁶, S. Bentvelsen ¹¹⁸, L. Beresford ¹³², M. Beretta ⁴⁹, D. Berge ⁴⁴, E. Bergeaas Kuutmann ¹⁶⁹, N. Berger ⁵, L.J. Bergsten ²⁶, J. Beringer ¹⁸, S. Berlendis ⁷, N.R. Bernard ¹⁰⁰, G. Bernardi ¹³³, C. Bernius ¹⁵⁰, F.U. Bernlochner ²⁴, T. Berry ⁹¹, P. Berta ⁹⁷, C. Bertella ^{15a}, G. Bertoli ^{43a,43b}, I.A. Bertram ⁸⁷, G.J. Besjes ³⁹, O. Bessidskaia Bylund ¹⁷⁹, M. Bessner ⁴⁴, N. Besson ¹⁴², A. Bethani ⁹⁸, S. Bethke ¹¹³, A. Betti ²⁴, A.J. Bevan ⁹⁰, J. Beyer ¹¹³, R.M. Bianchi ¹³⁶, O. Biebel ¹¹², D. Biedermann ¹⁹, R. Bielski ³⁵, K. Bierwagen ⁹⁷, N.V. Biesuz ^{69a,69b}, M. Biglietti ^{72a}, T.R.V. Billoud ¹⁰⁷, M. Bindi ⁵¹, A. Bingul ^{12d}, C. Bini ^{70a,70b}, S. Biondi ^{23b,23a}, M. Birman ¹⁷⁷, T. Bisanz ⁵¹, J.P. Biswal ¹⁵⁸, C. Bittrich ⁴⁶, D.M. Bjergaard ⁴⁷, J.E. Black ¹⁵⁰, K.M. Black ²⁵, T. Blazek ^{28a}, I. Bloch ⁴⁴, C. Blocker ²⁶, A. Blue ⁵⁵, U. Blumenschein ⁹⁰, Dr. Blunier ^{144a}, G.J. Bobbink ¹¹⁸, V.S. Bobrovnikov ^{120b,120a},

- S.S. Bocchetta 94, A. Bocci 47, D. Boerner 179, D. Bogavac 112, A.G. Bogdanchikov 120b,120a, C. Bohm 43a,
 V. Boisvert 91, P. Bokan 169, T. Bold 81a, A.S. Boldyrev 111, A.E. Bolz 59b, M. Bomben 133, M. Bona 90,
 J.S. Bonilla 128, M. Boonekamp 142, A. Borisov 121, G. Borissov 87, J. Bortfeldt 35, D. Bortoletto 132,
 V. Bortolotto 71a,71b, D. Boscherini 23b, M. Bosman 14, J.D. Bossio Sola 30, K. Bouaouda 34a, J. Boudreau 136,
 E.V. Bouhova-Thacker 87, D. Boumediene 37, C. Bourdarios 129, S.K. Boutle 55, A. Boveia 123, J. Boyd 35,
 D. Boye 32b, I.R. Boyko 77, A.J. Bozson 91, J. Bracinik 21, N. Brahimi 99, A. Brandt 8, G. Brandt 179,
 O. Brandt 59a, F. Braren 44, U. Bratzler 161, B. Brau 100, J.E. Brau 128, W.D. Breaden Madden 55,
 K. Brendlinger 44, L. Brenner 44, R. Brenner 169, S. Bressler 177, B. Brickwedde 97, D.L. Briglin 21,
 D. Britton 55, D. Britzger 59b, I. Brock 24, R. Brock 104, G. Brooijmans 38, T. Brooks 91, W.K. Brooks 144b,
 E. Brost 119, J.H. Broughton 21, P.A. Bruckman de Renstrom 82, D. Bruncko 28b, A. Bruni 23b, G. Bruni 23b,
 L.S. Bruni 118, S. Bruno 71a,71b, B.H. Brunt 31, M. Bruschi 23b, N. Bruscino 136, P. Bryant 36, L. Bryngemark 44,
 T. Buanes 17, Q. Buat 35, P. Buchholz 148, A.G. Buckley 55, I.A. Budagov 77, M.K. Bugge 131, F. Bührer 50,
 O. Bulekov 110, D. Bullock 8, T.J. Burch 119, S. Burdin 88, C.D. Burgard 118, A.M. Burger 5, B. Burghgrave 119,
 K. Burka 82, S. Burke 141, I. Burmeister 45, J.T.P. Burr 132, D. Büscher 50, V. Büscher 97, E. Buschmann 51,
 P. Bussey 55, J.M. Butler 25, C.M. Buttar 55, J.M. Butterworth 92, P. Butti 35, W. Buttlinger 35, A. Buzatu 155,
 A.R. Buzykaev 120b,120a, G. Cabras 23b,23a, S. Cabrera Urbán 171, D. Caforio 139, H. Cai 170, V.M.M. Cairo 2,
 O. Cakir 4a, N. Calace 52, P. Calafiura 18, A. Calandri 99, G. Calderini 133, P. Calfayan 63, G. Callea 40b,40a,
 L.P. Caloba 78b, S. Calvente Lopez 96, D. Calvet 37, S. Calvet 37, T.P. Calvet 152, M. Calvetti 69a,69b,
 R. Camacho Toro 133, S. Camarda 35, P. Camarri 71a,71b, D. Cameron 131, R. Caminal Armadans 100,
 C. Camincher 35, S. Campana 35, M. Campanelli 92, A. Camplani 39, A. Campoverde 148, V. Canale 67a,67b,
 M. Cano Bret 58c, J. Cantero 126, T. Cao 158, Y. Cao 170, M.D.M. Capeans Garrido 35, I. Caprini 27b,
 M. Caprini 27b, M. Capua 40b,40a, R.M. Carbone 38, R. Cardarelli 71a, F.C. Cardillo 146, I. Carli 140, T. Carli 35,
 G. Carlino 67a, B.T. Carlson 136, L. Carminati 66a,66b, R.M.D. Carney 43a,43b, S. Caron 117, E. Carquin 144b,
 S. Carrá 66a,66b, G.D. Carrillo-Montoya 35, D. Casadei 32b, M.P. Casado 14,g, A.F. Casha 164, D.W. Casper 168,
 R. Castelijn 118, F.L. Castillo 171, V. Castillo Gimenez 171, N.F. Castro 137a,137e, A. Catinaccio 35,
 J.R. Catmore 131, A. Cattai 35, J. Caudron 24, V. Cavalieri 29, E. Cavallaro 14, D. Cavalli 66a,
 M. Cavalli-Sforza 14, V. Cavasinni 69a,69b, E. Celebi 12b, F. Ceradini 72a,72b, L. Cerdá Alberich 171,
 A.S. Cerqueira 78a, A. Cerri 153, L. Cerrito 71a,71b, F. Cerutti 18, A. Cervelli 23b,23a, S.A. Cetin 12b,
 A. Chafaq 34a, D. Chakraborty 119, S.K. Chan 57, W.S. Chan 118, Y.L. Chan 61a, J.D. Chapman 31,
 B. Chargeishvili 156b, D.G. Charlton 21, C.C. Chau 33, C.A. Chavez Barajas 153, S. Che 123, A. Chegwidden 104,
 S. Chekanov 6, S.V. Chekulaev 165a, G.A. Chelkov 77,au, M.A. Chelstowska 35, C. Chen 58a, C.H. Chen 76,
 H. Chen 29, J. Chen 58a, J. Chen 38, S. Chen 134, S.J. Chen 15c, X. Chen 15b,at, Y. Chen 80, Y-H. Chen 44,
 H.C. Cheng 103, H.J. Cheng 15d, A. Cheplakov 77, E. Cheremushkina 121, R. Cherkaoui El Moursli 34e,
 E. Cheu 7, K. Cheung 62, L. Chevalier 142, V. Chiarella 49, G. Chiarella 69a, G. Chiodini 65a, A.S. Chisholm 35,
 A. Chitan 27b, I. Chiu 160, Y.H. Chiu 173, M.V. Chizhov 77, K. Choi 63, A.R. Chomont 129, S. Chouridou 159,
 Y.S. Chow 118, V. Christodoulou 92, M.C. Chu 61a, J. Chudoba 138, A.J. Chuinard 101, J.J. Chwastowski 82,
 L. Chytka 127, D. Cinca 45, V. Cindro 89, I.A. Cioară 24, A. Ciocio 18, F. Cirotto 67a,67b, Z.H. Citron 177,
 M. Citterio 66a, A. Clark 52, M.R. Clark 38, P.J. Clark 48, C. Clement 43a,43b, Y. Coadou 99, M. Cobal 64a,64c,
 A. Coccaro 53b,53a, J. Cochran 76, H. Cohen 158, A.E.C. Coimbra 177, L. Colasurdo 117, B. Cole 38,
 A.P. Colijn 118, J. Collot 56, P. Conde Muiño 137a,i, E. Coniavitis 50, S.H. Connell 32b, I.A. Connelly 98,
 S. Constantinescu 27b, F. Conventi 67a,aw, A.M. Cooper-Sarkar 132, F. Cormier 172, K.J.R. Cormier 164,
 M. Corradi 70a,70b, E.E. Corrigan 94, F. Corriveau 101,ae, A. Cortes-Gonzalez 35, M.J. Costa 171,
 D. Costanzo 146, G. Cottin 31, G. Cowan 91, B.E. Cox 98, J. Crane 98, K. Cranmer 122, S.J. Crawley 55,
 R.A. Creager 134, G. Cree 33, S. Crépé-Renaudin 56, F. Crescioli 133, M. Cristinziani 24, V. Croft 122,
 G. Crosetti 40b,40a, A. Cueto 96, T. Cuhadar Donszelmann 146, A.R. Cukierman 150, J. Cúth 97, S. Czekierda 82,
 P. Czodrowski 35, M.J. Da Cunha Sargedas De Sousa 58b, C. Da Via 98, W. Dabrowski 81a, T. Dado 28a,z,
 S. Dahbi 34e, T. Dai 103, F. Dallaire 107, C. Dallapiccola 100, M. Dam 39, G. D'amen 23b,23a, J. Damp 97,
 J.R. Dandoy 134, M.F. Daneri 30, N.P. Dang 178,l, N.D. Dann 98, M. Danninger 172, V. Dao 35, G. Darbo 53b,
 S. Darmora 8, O. Dartsi 5, A. Dattagupta 128, T. Daubney 44, S. D'Auria 55, W. Davey 24, C. David 44,
 T. Davidek 140, D.R. Davis 47, E. Dawe 102, I. Dawson 146, K. De 8, R. De Asmundis 67a, A. De Benedetti 125,
 M. De Beurs 118, S. De Castro 23b,23a, S. De Cecco 70a,70b, N. De Groot 117, P. de Jong 118, H. De la Torre 104,
 F. De Lorenzi 76, A. De Maria 51,u, D. De Pedis 70a, A. De Salvo 70a, U. De Sanctis 71a,71b,

- M. De Santis 71a,71b, A. De Santo 153, K. De Vasconcelos Corga 99, J.B. De Vie De Regie 129,
 C. Debenedetti 143, D.V. Dedovich 77, N. Dehghanian 3, M. Del Gaudio 40b,40a, J. Del Peso 96,
 Y. Delabat Diaz 44, D. Delgove 129, F. Deliot 142, C.M. Delitzsch 7, M. Della Pietra 67a,67b, D. Della Volpe 52,
 A. Dell'Acqua 35, L. Dell'Asta 25, M. Delmastro 5, C. Delporte 129, P.A. Delsart 56, D.A. DeMarco 164,
 S. Demers 180, M. Demichev 77, S.P. Denisov 121, D. Denysiuk 118, L. D'Eramo 133, D. Derendarz 82,
 J.E. Derkaoui 34d, F. Derue 133, P. Dervan 88, K. Desch 24, C. Deterre 44, K. Dette 164, M.R. Devesa 30,
 P.O. Deviveiros 35, A. Dewhurst 141, S. Dhaliwal 26, F.A. Di Bello 52, A. Di Ciaccio 71a,71b, L. Di Ciaccio 5,
 W.K. Di Clemente 134, C. Di Donato 67a,67b, A. Di Girolamo 35, B. Di Micco 72a,72b, R. Di Nardo 100,
 K.F. Di Petrillo 57, R. Di Sipio 164, D. Di Valentino 33, C. Diaconu 99, M. Diamond 164, F.A. Dias 39,
 T. Dias Do Vale 137a, M.A. Diaz 144a, J. Dickinson 18, E.B. Diehl 103, J. Dietrich 19, S. Díez Cornell 44,
 A. Dimitrievska 18, J. Dingfelder 24, F. Dittus 35, F. Djama 99, T. Djobava 156b, J.I. Djuvsland 59a,
 M.A.B. Do Vale 78c, M. Dobre 27b, D. Dodsworth 26, C. Doglioni 94, J. Dolejsi 140, Z. Dolezal 140,
 M. Donadelli 78d, J. Donini 37, A. D'onofrio 90, M. D'Onofrio 88, J. Dopke 141, A. Doria 67a, M.T. Dova 86,
 A.T. Doyle 55, E. Drechsler 51, E. Dreyer 149, T. Dreyer 51, Y. Du 58b, J. Duarte-Campderros 158, F. Dubinin 108,
 M. Dubovsky 28a, A. Dubreuil 52, E. Duchovni 177, G. Duckeck 112, A. Ducourthial 133, O.A. Ducu 107,y,
 D. Duda 113, A. Dudarev 35, A.C. Dudder 97, E.M. Duffield 18, L. Duflot 129, M. Dührssen 35, C. Dülsen 179,
 M. Dumancic 177, A.E. Dumitriu 27b,e, A.K. Duncan 55, M. Dunford 59a, A. Duperrin 99, H. Duran Yildiz 4a,
 M. Düren 54, A. Durglishvili 156b, D. Duschinger 46, B. Dutta 44, D. Duvnjak 1, M. Dyndal 44, S. Dysch 98,
 B.S. Dziedzic 82, C. Eckardt 44, K.M. Ecker 113, R.C. Edgar 103, T. Eifert 35, G. Eigen 17, K. Einsweiler 18,
 T. Ekelof 169, M. El Kacimi 34c, R. El Kosseifi 99, V. Ellajosyula 99, M. Ellert 169, F. Ellinghaus 179,
 A.A. Elliot 90, N. Ellis 35, J. Elmsheuser 29, M. Elsing 35, D. Emeliyanov 141, Y. Enari 160, J.S. Ennis 175,
 M.B. Epland 47, J. Erdmann 45, A. Ereditato 20, S. Errede 170, M. Escalier 129, C. Escobar 171,
 O. Estrada Pastor 171, A.I. Etienne 142, E. Etzion 158, H. Evans 63, A. Ezhilov 135, M. Ezzi 34e, F. Fabbri 55,
 L. Fabbri 23b,23a, V. Fabiani 117, G. Facini 92, R.M. Faisca Rodrigues Pereira 137a, R.M. Fakhrutdinov 121,
 S. Falciano 70a, P.J. Falke 5, S. Falke 5, J. Faltova 140, Y. Fang 15a, M. Fanti 66a,66b, A. Farbin 8, A. Farilla 72a,
 E.M. Farina 68a,68b, T. Farooque 104, S. Farrell 18, S.M. Farrington 175, P. Farthouat 35, F. Fassi 34e,
 P. Fassnacht 35, D. Fassouliotis 9, M. Facci Giannelli 48, A. Favareto 53b,53a, W.J. Fawcett 31, L. Fayard 129,
 O.L. Fedin 135,q, W. Fedorko 172, M. Feickert 41, S. Feigl 131, L. Feligioni 99, C. Feng 58b, E.J. Feng 35,
 M. Feng 47, M.J. Fenton 55, A.B. Fenyuk 121, L. Feremenga 8, J. Ferrando 44, A. Ferrari 169, P. Ferrari 118,
 R. Ferrari 68a, D.E. Ferreira de Lima 59b, A. Ferrer 171, D. Ferrere 52, C. Ferretti 103, F. Fiedler 97, A. Filipčič 89,
 F. Filthaut 117, K.D. Finelli 25, M.C.N. Fiolhais 137a,137c,a, L. Fiorini 171, C. Fischer 14, W.C. Fisher 104,
 N. Flaschel 44, I. Fleck 148, P. Fleischmann 103, R.R.M. Fletcher 134, T. Flick 179, B.M. Flierl 112, L.M. Flores 134,
 L.R. Flores Castillo 61a, F.M. Follega 73a,73b, N. Fomin 17, G.T. Forcolin 98, A. Formica 142, F.A. Förster 14,
 A.C. Forti 98, A.G. Foster 21, D. Fournier 129, H. Fox 87, S. Fracchia 146, P. Francavilla 69a,69b,
 M. Franchini 23b,23a, S. Franchino 59a, D. Francis 35, L. Franconi 131, M. Franklin 57, M. Frate 168,
 M. Frernali 68a,68b, A.N. Fray 90, D. Freeborn 92, S.M. Fressard-Batraneanu 35, B. Freund 107,
 W.S. Freund 78b, D.C. Frizzell 125, D. Froidevaux 35, J.A. Frost 132, C. Fukunaga 161, E. Fullana Torregrosa 171,
 T. Fusayasu 114, J. Fuster 171, O. Gabizon 157, A. Gabrielli 23b,23a, A. Gabrielli 18, G.P. Gach 81a,
 S. Gadatsch 52, P. Gadow 113, G. Gagliardi 53b,53a, L.G. Gagnon 107, C. Galea 27b, B. Galhardo 137a,137c,
 E.J. Gallas 132, B.J. Gallop 141, P. Gallus 139, G. Galster 39, R. Gamboa Goni 90, K.K. Gan 123, S. Ganguly 177,
 J. Gao 58a, Y. Gao 88, Y.S. Gao 150,n, C. García 171, J.E. García Navarro 171, J.A. García Pascual 15a,
 M. Garcia-Sciveres 18, R.W. Gardner 36, N. Garelli 150, V. Garonne 131, K. Gasnikova 44, A. Gaudiello 53b,53a,
 G. Gaudio 68a, I.L. Gavrilenko 108, A. Gavriluk 109, C. Gay 172, G. Gaycken 24, E.N. Gazis 10, C.N.P. Gee 141,
 J. Geisen 51, M. Geisen 97, M.P. Geisler 59a, K. Gellerstedt 43a,43b, C. Gemme 53b, M.H. Genest 56, C. Geng 103,
 S. Gentile 70a,70b, S. George 91, D. Gerbaudo 14, G. Gessner 45, S. Ghasemi 148, M. Ghasemi Bostanabad 173,
 M. Ghneimat 24, B. Giacobbe 23b, S. Giagu 70a,70b, N. Giangiocomi 23b,23a, P. Giannetti 69a,
 A. Giannini 67a,67b, S.M. Gibson 91, M. Gignac 143, D. Gillberg 33, G. Gilles 179, D.M. Gingrich 3,av,
 M.P. Giordani 64a,64c, F.M. Giorgi 23b, P.F. Giraud 142, P. Giromini 57, G. Giugliarelli 64a,64c, D. Giugni 66a,
 F. Giuli 132, M. Giulini 59b, S. Gkaitatzis 159, I. Gkialas 9,k, E.L. Gkougkousis 14, P. Gkountoumis 10,
 L.K. Gladilin 111, C. Glasman 96, J. Glatzer 14, P.C.F. Glaysher 44, A. Glazov 44, M. Goblirsch-Kolb 26,
 J. Godlewski 82, S. Goldfarb 102, T. Golling 52, D. Golubkov 121, A. Gomes 137a,137b, R. Goncalves Gama 78a,
 R. Gonçalo 137a, G. Gonella 50, L. Gonella 21, A. Gongadze 77, F. Gonnella 21, J.L. Gonski 57,

- S. González de la Hoz ¹⁷¹, S. Gonzalez-Sevilla ⁵², L. Goossens ³⁵, P.A. Gorbounov ¹⁰⁹, H.A. Gordon ²⁹,
 B. Gorini ³⁵, E. Gorini ^{65a,65b}, A. Gorišek ⁸⁹, A.T. Goshaw ⁴⁷, C. Gössling ⁴⁵, M.I. Gostkin ⁷⁷, C.A. Gottardo ²⁴,
 C.R. Goudet ¹²⁹, D. Goujdami ^{34c}, A.G. Goussiou ¹⁴⁵, N. Govender ^{32b,c}, C. Goy ⁵, E. Gozani ¹⁵⁷,
 I. Grabowska-Bold ^{81a}, P.O.J. Gradin ¹⁶⁹, E.C. Graham ⁸⁸, J. Gramling ¹⁶⁸, E. Gramstad ¹³¹, S. Grancagnolo ¹⁹,
 V. Gratchev ¹³⁵, P.M. Gravila ^{27f}, F.G. Gravili ^{65a,65b}, C. Gray ⁵⁵, H.M. Gray ¹⁸, Z.D. Greenwood ^{93,al},
 C. Grefe ²⁴, K. Gregersen ⁹⁴, I.M. Gregor ⁴⁴, P. Grenier ¹⁵⁰, K. Grevtsov ⁴⁴, N.A. Grieser ¹²⁵, J. Griffiths ⁸,
 A.A. Grillo ¹⁴³, K. Grimm ^{150,b}, S. Grinstein ^{14,aa}, Ph. Gris ³⁷, J.-F. Grivaz ¹²⁹, S. Groh ⁹⁷, E. Gross ¹⁷⁷,
 J. Grosse-Knetter ⁵¹, G.C. Grossi ⁹³, Z.J. Grout ⁹², C. Grud ¹⁰³, A. Grummer ¹¹⁶, L. Guan ¹⁰³, W. Guan ¹⁷⁸,
 J. Guenther ³⁵, A. Guerguichon ¹²⁹, F. Guescini ^{165a}, D. Guest ¹⁶⁸, R. Gugel ⁵⁰, B. Gui ¹²³, T. Guillemin ⁵,
 S. Guindon ³⁵, U. Gul ⁵⁵, C. Gumpert ³⁵, J. Guo ^{58c}, W. Guo ¹⁰³, Y. Guo ^{58a,t}, Z. Guo ⁹⁹, R. Gupta ⁴¹,
 S. Gurbuz ^{12c}, G. Gustavino ¹²⁵, B.J. Gutelman ¹⁵⁷, P. Gutierrez ¹²⁵, C. Gutschow ⁹², C. Guyot ¹⁴²,
 M.P. Guzik ^{81a}, C. Gwenlan ¹³², C.B. Gwilliam ⁸⁸, A. Haas ¹²², C. Haber ¹⁸, H.K. Hadavand ⁸, N. Haddad ^{34e},
 A. Hadef ^{58a}, S. Hageböck ²⁴, M. Hagihara ¹⁶⁶, H. Hakobyan ^{181,*}, M. Haleem ¹⁷⁴, J. Haley ¹²⁶,
 G. Halladjian ¹⁰⁴, G.D. Hallewell ⁹⁹, K. Hamacher ¹⁷⁹, P. Hamal ¹²⁷, K. Hamano ¹⁷³, A. Hamilton ^{32a},
 G.N. Hamity ¹⁴⁶, K. Han ^{58a,ak}, L. Han ^{58a}, S. Han ^{15d}, K. Hanagaki ^{79,w}, M. Hance ¹⁴³, D.M. Handl ¹¹²,
 B. Haney ¹³⁴, R. Hankache ¹³³, P. Hanke ^{59a}, E. Hansen ⁹⁴, J.B. Hansen ³⁹, J.D. Hansen ³⁹, M.C. Hansen ²⁴,
 P.H. Hansen ³⁹, K. Hara ¹⁶⁶, A.S. Hard ¹⁷⁸, T. Harenberg ¹⁷⁹, S. Harkusha ¹⁰⁵, P.F. Harrison ¹⁷⁵,
 N.M. Hartmann ¹¹², Y. Hasegawa ¹⁴⁷, A. Hasib ⁴⁸, S. Hassani ¹⁴², S. Haug ²⁰, R. Hauser ¹⁰⁴, L. Hauswald ⁴⁶,
 L.B. Havener ³⁸, M. Havranek ¹³⁹, C.M. Hawkes ²¹, R.J. Hawkings ³⁵, D. Hayden ¹⁰⁴, C. Hayes ¹⁵²,
 C.P. Hays ¹³², J.M. Hays ⁹⁰, H.S. Hayward ⁸⁸, S.J. Haywood ¹⁴¹, M.P. Heath ⁴⁸, V. Hedberg ⁹⁴, L. Heelan ⁸,
 S. Heer ²⁴, K.K. Heidegger ⁵⁰, J. Heilman ³³, S. Heim ⁴⁴, T. Heim ¹⁸, B. Heinemann ^{44,ag}, J.J. Heinrich ¹¹²,
 L. Heinrich ¹²², C. Heinz ⁵⁴, J. Hejbal ¹³⁸, L. Helary ³⁵, A. Held ¹⁷², S. Hellesund ¹³¹, S. Hellman ^{43a,43b},
 C. Helsens ³⁵, R.C.W. Henderson ⁸⁷, Y. Heng ¹⁷⁸, S. Henkelmann ¹⁷², A.M. Henriques Correia ³⁵,
 G.H. Herbert ¹⁹, H. Herde ²⁶, V. Herget ¹⁷⁴, Y. Hernández Jiménez ^{32c}, H. Herr ⁹⁷, M.G. Herrmann ¹¹²,
 G. Herten ⁵⁰, R. Hertenberger ¹¹², L. Hervas ³⁵, T.C. Herwig ¹³⁴, G.G. Hesketh ⁹², N.P. Hessey ^{165a},
 J.W. Hetherly ⁴¹, S. Higashino ⁷⁹, E. Higón-Rodriguez ¹⁷¹, K. Hildebrand ³⁶, E. Hill ¹⁷³, J.C. Hill ³¹,
 K.K. Hill ²⁹, K.H. Hiller ⁴⁴, S.J. Hillier ²¹, M. Hils ⁴⁶, I. Hinchliffe ¹⁸, M. Hirose ¹³⁰, D. Hirschbuehl ¹⁷⁹,
 B. Hiti ⁸⁹, O. Hladík ¹³⁸, D.R. Hlaluku ^{32c}, X. Hoad ⁴⁸, J. Hobbs ¹⁵², N. Hod ^{165a}, M.C. Hodgkinson ¹⁴⁶,
 A. Hoecker ³⁵, M.R. Hoeferkamp ¹¹⁶, F. Hoenig ¹¹², D. Hohn ²⁴, D. Hohov ¹²⁹, T.R. Holmes ³⁶,
 M. Holzbock ¹¹², M. Homann ⁴⁵, S. Honda ¹⁶⁶, T. Honda ⁷⁹, T.M. Hong ¹³⁶, A. Höngle ¹¹³,
 B.H. Hooberman ¹⁷⁰, W.H. Hopkins ¹²⁸, Y. Horii ¹¹⁵, P. Horn ⁴⁶, A.J. Horton ¹⁴⁹, L.A. Horyn ³⁶,
 J-Y. Hostachy ⁵⁶, A. Hostiuc ¹⁴⁵, S. Hou ¹⁵⁵, A. Hoummada ^{34a}, J. Howarth ⁹⁸, J. Hoya ⁸⁶, M. Hrabovsky ¹²⁷,
 J. Hrdinka ³⁵, I. Hristova ¹⁹, J. Hrivnac ¹²⁹, A. Hrynevich ¹⁰⁶, T. Hrynevich ⁵, P.J. Hsu ⁶², S.-C. Hsu ¹⁴⁵,
 Q. Hu ²⁹, S. Hu ^{58c}, Y. Huang ^{15a}, Z. Hubacek ¹³⁹, F. Hubaut ⁹⁹, M. Huebner ²⁴, F. Huegging ²⁴,
 T.B. Huffman ¹³², E.W. Hughes ³⁸, M. Huhtinen ³⁵, R.F.H. Hunter ³³, P. Huo ¹⁵², A.M. Hupe ³³,
 N. Huseynov ^{77,ag}, J. Huston ¹⁰⁴, J. Huth ⁵⁷, R. Hyneman ¹⁰³, G. Iacobucci ⁵², G. Iakovidis ²⁹,
 I. Ibragimov ¹⁴⁸, L. Iconomidou-Fayard ¹²⁹, Z. Idrissi ^{34e}, P. Iengo ³⁵, R. Ignazzi ³⁹, O. Igonkina ^{118,ac},
 R. Iguchi ¹⁶⁰, T. Iizawa ⁵², Y. Ikegami ⁷⁹, M. Ikeno ⁷⁹, D. Iliadis ¹⁵⁹, N. Ilic ¹¹⁷, F. Iltzsche ⁴⁶,
 G. Introzzi ^{68a,68b}, M. Iodice ^{72a}, K. Iordanidou ³⁸, V. Ippolito ^{70a,70b}, M.F. Isacson ¹⁶⁹, N. Ishijima ¹³⁰,
 M. Ishino ¹⁶⁰, M. Ishitsuka ¹⁶², W. Islam ¹²⁶, C. Issever ¹³², S. Istin ¹⁵⁷, F. Ito ¹⁶⁶, J.M. Iturbe Ponce ^{61a},
 R. Iuppa ^{73a,73b}, A. Ivina ¹⁷⁷, H. Iwasaki ⁷⁹, J.M. Izen ⁴², V. Izzo ^{67a}, P. Jacka ¹³⁸, P. Jackson ¹, R.M. Jacobs ²⁴,
 V. Jain ², G. Jäkel ¹⁷⁹, K.B. Jakobi ⁹⁷, K. Jakobs ⁵⁰, S. Jakobsen ⁷⁴, T. Jakoubek ¹³⁸, D.O. Jamin ¹²⁶, D.K. Jana ⁹³,
 R. Jansky ⁵², J. Janssen ²⁴, M. Janus ⁵¹, P.A. Janus ^{81a}, G. Jarlskog ⁹⁴, N. Javadov ^{77,ag}, T. Javůrek ³⁵,
 M. Javurkova ⁵⁰, F. Jeanneau ¹⁴², L. Jeanty ¹⁸, J. Jejelava ^{156a,ah}, A. Jelinskas ¹⁷⁵, P. Jenni ^{50,d}, J. Jeong ⁴⁴,
 S. Jézéquel ⁵, H. Ji ¹⁷⁸, J. Jia ¹⁵², H. Jiang ⁷⁶, Y. Jiang ^{58a}, Z. Jiang ^{150,r}, S. Jiggins ⁵⁰, F.A. Jimenez Morales ³⁷,
 J. Jimenez Pena ¹⁷¹, S. Jin ^{15c}, A. Jinaru ^{27b}, O. Jinnouchi ¹⁶², H. Jivan ^{32c}, P. Johansson ¹⁴⁶, K.A. Johns ⁷,
 C.A. Johnson ⁶³, W.J. Johnson ¹⁴⁵, K. Jon-And ^{43a,43b}, R.W.L. Jones ⁸⁷, S.D. Jones ¹⁵³, S. Jones ⁷, T.J. Jones ⁸⁸,
 J. Jongmanns ^{59a}, P.M. Jorge ^{137a,137b}, J. Jovicevic ^{165a}, X. Ju ¹⁸, J.J. Junggeburth ¹¹³, A. Juste Rozas ^{14,aa},
 A. Kaczmarska ⁸², M. Kado ¹²⁹, H. Kagan ¹²³, M. Kagan ¹⁵⁰, T. Kaji ¹⁷⁶, E. Kajomovitz ¹⁵⁷, C.W. Kalderon ⁹⁴,
 A. Kaluza ⁹⁷, S. Kama ⁴¹, A. Kamenshchikov ¹²¹, L. Kanjir ⁸⁹, Y. Kano ¹⁶⁰, V.A. Kantserov ¹¹⁰, J. Kanzaki ⁷⁹,
 B. Kaplan ¹²², L.S. Kaplan ¹⁷⁸, D. Kar ^{32c}, M.J. Kareem ^{165b}, E. Karentzos ¹⁰, S.N. Karpov ⁷⁷, Z.M. Karpova ⁷⁷,
 V. Kartvelishvili ⁸⁷, A.N. Karyukhin ¹²¹, L. Kashif ¹⁷⁸, R.D. Kass ¹²³, A. Kastanas ¹⁵¹, Y. Kataoka ¹⁶⁰,

- C. Kato 58d, 58c, J. Katzy 44, K. Kawade 80, K. Kawagoe 85, T. Kawamoto 160, G. Kawamura 51, E.F. Kay 88, V.F. Kazanin 120b, 120a, R. Keeler 173, R. Kehoe 41, J.S. Keller 33, E. Kellermann 94, J.J. Kempster 21, J. Kendrick 21, O. Kepka 138, S. Kersten 179, B.P. Kerševan 89, R.A. Keyes 101, M. Khader 170, F. Khalil-Zada 13, A. Khanov 126, A.G. Kharlamov 120b, 120a, T. Kharlamova 120b, 120a, E.E. Khoda 172, A. Khodinov 163, T.J. Khoo 52, E. Khramov 77, J. Khubua 156b, S. Kido 80, M. Kiehn 52, C.R. Kilby 91, Y.K. Kim 36, N. Kimura 64a, 64c, O.M. Kind 19, B.T. King 88, D. Kirchmeier 46, J. Kirk 141, A.E. Kiryunin 113, T. Kishimoto 160, D. Kisielewska 81a, V. Kitali 44, O. Kivernyk 5, E. Kladiva 28b, *, T. Klapdor-Kleingrothaus 50, M.H. Klein 103, M. Klein 88, U. Klein 88, K. Kleinknecht 97, P. Klimek 119, A. Klimentov 29, R. Klingenberg 45, *, T. Klingl 24, T. Klioutchnikova 35, F.F. Klitzner 112, P. Kluit 118, S. Kluth 113, E. Kneringer 74, E.B.F.G. Knoops 99, A. Knue 50, A. Kobayashi 160, D. Kobayashi 85, T. Kobayashi 160, M. Kobel 46, M. Kocian 150, P. Kodys 140, P.T. Koenig 24, T. Koffas 33, E. Koffeman 118, N.M. Köhler 113, T. Koi 150, M. Kolb 59b, I. Koletsou 5, T. Kondo 79, N. Kondrashova 58c, K. Köneke 50, A.C. König 117, T. Kono 79, R. Konoplich 122, an, V. Konstantinides 92, N. Konstantinidis 92, B. Konya 94, R. Kopeliansky 63, S. Koperny 81a, K. Korcyl 82, K. Kordas 159, G. Koren 158, A. Korn 92, I. Korolkov 14, E.V. Korolkova 146, N. Korotkova 111, O. Kortner 113, S. Kortner 113, T. Kosek 140, V.V. Kostyukhin 24, A. Kotwal 47, A. Koulouris 10, A. Kourkoumeli-Charalampidi 68a, 68b, C. Kourkoumelis 9, E. Kourlitis 146, V. Kouskoura 29, A.B. Kowalewska 82, R. Kowalewski 173, T.Z. Kowalski 81a, C. Kozakai 160, W. Kozanecki 142, A.S. Kozhin 121, V.A. Kramarenko 111, G. Kramberger 89, D. Krasnopevtsev 58a, M.W. Krasny 133, A. Krasznahorkay 35, D. Krauss 113, J.A. Kremer 81a, J. Kretzschmar 88, P. Krieger 164, K. Krizka 18, K. Kroeninger 45, H. Kroha 113, J. Kroll 138, J. Kroll 134, J. Krstic 16, U. Kruchonak 77, H. Krüger 24, N. Krumnack 76, M.C. Kruse 47, T. Kubota 102, S. Kuday 4b, J.T. Kuechler 179, S. Kuehn 35, A. Kugel 59a, F. Kuger 174, T. Kuhl 44, V. Kukhtin 77, R. Kukla 99, Y. Kulchitsky 105, S. Kuleshov 144b, Y.P. Kulnich 170, M. Kuna 56, T. Kunigo 83, A. Kupco 138, T. Kupfer 45, O. Kuprash 158, H. Kurashige 80, L.L. Kurchaninov 165a, Y.A. Kurochkin 105, M.G. Kurth 15d, E.S. Kuwertz 35, M. Kuze 162, J. Kvita 127, T. Kwan 101, A. La Rosa 113, J.L. La Rosa Navarro 78d, L. La Rotonda 40b, 40a, F. La Ruffa 40b, 40a, C. Lacasta 171, F. Lacava 70a, 70b, J. Lacey 44, D.P.J. Lack 98, H. Lacker 19, D. Lacour 133, E. Ladygin 77, R. Lafaye 5, B. Laforge 133, T. Lagouri 32c, S. Lai 51, S. Lammers 63, W. Lampl 7, E. Lançon 29, U. Landgraf 50, M.P.J. Landon 90, M.C. Lanfermann 52, V.S. Lang 44, J.C. Lange 14, R.J. Langenberg 35, A.J. Lankford 168, F. Lanni 29, K. Lantzsch 24, A. Lanza 68a, A. Lapertosa 53b, 53a, S. Laplace 133, J.F. Laporte 142, T. Lari 66a, F. Lasagni Manghi 23b, 23a, M. Lassnig 35, T.S. Lau 61a, A. Laudrain 129, M. Lavorgna 67a, 67b, A.T. Law 143, P. Laycock 88, M. Lazzaroni 66a, 66b, B. Le 102, O. Le Dortz 133, E. Le Guiriec 99, E.P. Le Quillec 142, M. LeBlanc 7, T. LeCompte 6, F. Ledroit-Guillon 56, C.A. Lee 29, G.R. Lee 144a, L. Lee 57, S.C. Lee 155, B. Lefebvre 101, M. Lefebvre 173, F. Legger 112, C. Leggett 18, K. Lehmann 149, N. Lehmann 179, G. Lehmann Miotto 35, W.A. Leight 44, A. Leisos 159, x, M.A.L. Leite 78d, R. Leitner 140, D. Lelloch 177, B. Lemmer 51, K.J.C. Leney 92, T. Lenz 24, B. Lenzi 35, R. Leone 7, S. Leone 69a, C. Leonidopoulos 48, G. Lerner 153, C. Leroy 107, R. Les 164, A.A.J. Lesage 142, C.G. Lester 31, M. Levchenko 135, J. Levêque 5, D. Levin 103, L.J. Levinson 177, D. Lewis 90, B. Li 103, C-Q. Li 58a, am, H. Li 58b, L. Li 58c, Q. Li 15d, Q.Y. Li 58a, S. Li 58d, 58c, X. Li 58c, Y. Li 148, Z. Liang 15a, B. Liberti 71a, A. Liblong 164, K. Lie 61c, S. Liem 118, A. Limosani 154, C.Y. Lin 31, K. Lin 104, T.H. Lin 97, R.A. Linck 63, J.H. Lindon 21, B.E. Lindquist 152, A.L. Lionti 52, E. Lipeles 134, A. Lipniacka 17, M. Lisovskyi 59b, T.M. Liss 170, as, A. Lister 172, A.M. Litke 143, J.D. Little 8, B. Liu 76, B.L. Liu 6, H.B. Liu 29, H. Liu 103, J.B. Liu 58a, J.K.K. Liu 132, K. Liu 133, M. Liu 58a, P. Liu 18, Y. Liu 15a, Y.L. Liu 58a, Y.W. Liu 58a, M. Livan 68a, 68b, A. Lleres 56, J. Llorente Merino 15a, S.L. Lloyd 90, C.Y. Lo 61b, F. Lo Sterzo 41, E.M. Lobodzinska 44, P. Loch 7, T. Lohse 19, K. Lohwasser 146, M. Lokajicek 138, B.A. Long 25, J.D. Long 170, R.E. Long 87, L. Longo 65a, 65b, K.A.Looper 123, J.A. Lopez 144b, I. Lopez Paz 14, A. Lopez Solis 146, J. Lorenz 112, N. Lorenzo Martinez 5, M. Losada 22, P.J. Lösel 112, A. Lösle 50, X. Lou 44, X. Lou 15a, A. Lounis 129, J. Love 6, P.A. Love 87, J.J. Lozano Bahilo 171, H. Lu 61a, M. Lu 58a, N. Lu 103, Y.J. Lu 62, H.J. Lubatti 145, C. Luci 70a, 70b, A. Lucotte 56, C. Luedtke 50, F. Luehring 63, I. Luise 133, L. Luminari 70a, B. Lund-Jensen 151, M.S. Lutz 100, P.M. Luzi 133, D. Lynn 29, R. Lysak 138, E. Lytken 94, F. Lyu 15a, V. Lyubushkin 77, H. Ma 29, L.L. Ma 58b, Y. Ma 58b, G. Maccarrone 49, A. Macchiolo 113, C.M. Macdonald 146, J. Machado Miguens 134, 137b, D. Madaffari 171, R. Madar 37, W.F. Mader 46, A. Madsen 44, N. Madysa 46, J. Maeda 80, K. Maekawa 160, S. Maeland 17, T. Maeno 29, A.S. Maevskiy 111, V. Magerl 50, C. Maidantchik 78b, T. Maier 112, A. Maio 137a, 137b, 137d, O. Majersky 28a, S. Majewski 128, Y. Makida 79, N. Makovec 129, B. Malaescu 133, Pa. Malecki 82, V.P. Maleev 135, F. Malek 56,

- U. Mallik 75, D. Malon 6, C. Malone 31, S. Maltezos 10, S. Malyukov 35, J. Mamuzic 171, G. Mancini 49, I. Mandić 89, J. Maneira 137a, L. Manhaes de Andrade Filho 78a, J. Manjarres Ramos 46, K.H. Mankinen 94, A. Mann 112, A. Manousos 74, B. Mansoulie 142, J.D. Mansour 15a, M. Mantoani 51, S. Manzoni 66a, 66b, G. Marceca 30, L. March 52, L. Marchese 132, G. Marchiori 133, M. Marcisovsky 138, C.A. Marin Tobon 35, M. Marjanovic 37, D.E. Marley 103, F. Marroquin 78b, Z. Marshall 18, M.U.F Martensson 169, S. Marti-Garcia 171, C.B. Martin 123, T.A. Martin 175, V.J. Martin 48, B. Martin dit Latour 17, M. Martinez 14,aa, V.I. Martinez Outschoorn 100, S. Martin-Haugh 141, V.S. Martoiu 27b, A.C. Martyniuk 92, A. Marzin 35, L. Masetti 97, T. Mashimo 160, R. Mashinistov 108, J. Masik 98, A.L. Maslennikov 120b, 120a, L.H. Mason 102, L. Massa 71a, 71b, P. Massarotti 67a, 67b, P. Mastrandrea 5, A. Mastroberardino 40b, 40a, T. Masubuchi 160, P. Mättig 179, J. Maurer 27b, B. Maček 89, S.J. Maxfield 88, D.A. Maximov 120b, 120a, R. Mazini 155, I. Maznas 159, S.M. Mazza 143, N.C. Mc Fadden 116, G. Mc Goldrick 164, S.P. Mc Kee 103, A. McCarn 103, T.G. McCarthy 113, L.I. McClymont 92, E.F. McDonald 102, J.A. McFayden 35, G. Mchedlidze 51, M.A. McKay 41, K.D. McLean 173, S.J. McMahon 141, P.C. McNamara 102, C.J. McNicol 175, R.A. McPherson 173,ae, J.E. Mdhluli 32c, Z.A. Meadows 100, S. Meehan 145, T.M. Megy 50, S. Mehlhase 112, A. Mehta 88, T. Meideck 56, B. Meirose 42, D. Melini 171,h, B.R. Mellado Garcia 32c, J.D. Mellenthin 51, M. Melo 28a, F. Meloni 44, A. Melzer 24, S.B. Menary 98, E.D. Mendes Gouveia 137a, L. Meng 88, X.T. Meng 103, A. Mengarelli 23b, 23a, S. Menke 113, E. Meoni 40b, 40a, S. Mergelmeyer 19, C. Merlassino 20, P. Mermod 52, L. Merola 67a, 67b, C. Meroni 66a, F.S. Merritt 36, A. Messina 70a, 70b, J. Metcalfe 6, A.S. Mete 168, C. Meyer 134, J. Meyer 157, J-P. Meyer 142, H. Meyer Zu Theenhausen 59a, F. Miano 153, R.P. Middleton 141, L. Mijović 48, G. Mikenberg 177, M. Mikestikova 138, M. Mikuž 89, M. Milesi 102, A. Milic 164, D.A. Millar 90, D.W. Miller 36, A. Milov 177, D.A. Milstead 43a, 43b, A.A. Minaenko 121, M. Miñano Moya 171, I.A. Minashvili 156b, A.I. Mincer 122, B. Mindur 81a, M. Mineev 77, Y. Minegishi 160, Y. Ming 178, L.M. Mir 14, A. Mirta 65a, 65b, K.P. Mistry 134, T. Mitani 176, J. Mitrevski 112, V.A. Mitsou 171, A. Miucci 20, P.S. Miyagawa 146, A. Mizukami 79, J.U. Mjörnmark 94, T. Mkrtchyan 181, M. Mlynarikova 140, T. Moa 43a, 43b, K. Mochizuki 107, P. Mogg 50, S. Mohapatra 38, S. Molander 43a, 43b, R. Moles-Valls 24, M.C. Mondragon 104, K. Mönig 44, J. Monk 39, E. Monnier 99, A. Montalbano 149, J. Montejo Berlingen 35, F. Monticelli 86, S. Monzani 66a, N. Morange 129, D. Moreno 22, M. Moreno Llácer 35, P. Morettini 53b, M. Morgenstern 118, S. Morgenstern 46, D. Mori 149, M. Morii 57, M. Morinaga 176, V. Morisbak 131, A.K. Morley 35, G. Mornacchi 35, A.P. Morris 92, J.D. Morris 90, L. Morvaj 152, P. Moschovakos 10, M. Mosidze 156b, H.J. Moss 146, J. Moss 150,o, K. Motohashi 162, R. Mount 150, E. Mountricha 35, E.J.W. Moyse 100, S. Muanza 99, F. Mueller 113, J. Mueller 136, R.S.P. Mueller 112, D. Muenstermann 87, G.A. Mullier 20, F.J. Munoz Sanchez 98, P. Murin 28b, W.J. Murray 175, 141, A. Murrone 66a, 66b, M. Muškinja 89, C. Mwewa 32a, A.G. Myagkov 121,ao, J. Myers 128, M. Myska 139, B.P. Nachman 18, O. Nackenhorst 45, K. Nagai 132, K. Nagano 79, Y. Nagasaka 60, M. Nagel 50, E. Nagy 99, A.M. Nairz 35, Y. Nakahama 115, K. Nakamura 79, T. Nakamura 160, I. Nakano 124, H. Nanjo 130, F. Napolitano 59a, R.F. Naranjo Garcia 44, R. Narayan 11, D.I. Narrias Villar 59a, I. Naryshkin 135, T. Naumann 44, G. Navarro 22, R. Nayyar 7, H.A. Neal 103,*, P.Y. Nechaeva 108, T.J. Neep 142, A. Negri 68a, 68b, M. Negrini 23b, S. Nektarijevic 117, C. Nellist 51, M.E. Nelson 132, S. Nemecek 138, P. Nemethy 122, M. Nessi 35,f, M.S. Neubauer 170, M. Neumann 179, P.R. Newman 21, T.Y. Ng 61c, Y.S. Ng 19, H.D.N. Nguyen 99, T. Nguyen Manh 107, E. Nibigira 37, R.B. Nickerson 132, R. Nicolaidou 142, J. Nielsen 143, N. Nikiforou 11, V. Nikolaenko 121,ao, I. Nikolic-Audit 133, K. Nikolopoulos 21, P. Nilsson 29, Y. Ninomiya 79, A. Nisati 70a, N. Nishu 58c, R. Nisius 113, I. Nitsche 45, T. Nitta 176, T. Nobe 160, Y. Noguchi 83, M. Nomachi 130, I. Nomidis 133, M.A. Nomura 29, T. Nooney 90, M. Nordberg 35, N. Norjoharuddeen 132, T. Novak 89, O. Novgorodova 46, R. Novotny 139, L. Nozka 127, K. Ntekas 168, E. Nurse 92, F. Nuti 102, F.G. Oakham 33,av, H. Oberlack 113, T. Obermann 24, J. Ocariz 133, A. Ochi 80, I. Ochoa 38, J.P. Ochoa-Ricoux 144a, K. O'Connor 26, S. Oda 85, S. Odaka 79, S. Oerdekk 51, A. Oh 98, S.H. Oh 47, C.C. Ohm 151, H. Oide 53b, 53a, M.L. Ojeda 164, H. Okawa 166, Y. Okazaki 83, Y. Okumura 160, T. Okuyama 79, A. Olariu 27b, L.F. Oleiro Seabra 137a, S.A. Olivares Pino 144a, D. Oliveira Damazio 29, J.L. Oliver 1, M.J.R. Olsson 36, A. Olszewski 82, J. Olszowska 82, D.C. O'Neil 149, A. Onofre 137a, 137e, K. Onogi 115, P.U.E. Onyisi 11, H. Oppen 131, M.J. Oreglia 36, Y. Oren 158, D. Orestano 72a, 72b, E.C. Orgill 98, N. Orlando 61b, A.A. O'Rourke 44, R.S. Orr 164, B. Osculati 53b, 53a,*, V. O'Shea 55, R. Ospanov 58a, G. Otero y Garzon 30, H. Otono 85, M. Ouchrif 34d, F. Ould-Saada 131, A. Ouraou 142, Q. Ouyang 15a, M. Owen 55, R.E. Owen 21, V.E. Ozcan 12c, N. Ozturk 8, J. Pacalt 127,

- H.A. Pacey ³¹, K. Pachal ¹⁴⁹, A. Pacheco Pages ¹⁴, L. Pacheco Rodriguez ¹⁴², C. Padilla Aranda ¹⁴, S. Pagan Griso ¹⁸, M. Paganini ¹⁸⁰, G. Palacino ⁶³, S. Palazzo ^{40b,40a}, S. Palestini ³⁵, M. Palka ^{81b}, D. Pallin ³⁷, I. Panagoulias ¹⁰, C.E. Pandini ³⁵, J.G. Panduro Vazquez ⁹¹, P. Pani ³⁵, G. Panizzo ^{64a,64c}, L. Paolozzi ⁵², T.D. Papadopoulou ¹⁰, K. Papageorgiou ^{9,k}, A. Paramonov ⁶, D. Paredes Hernandez ^{61b}, S.R. Paredes Saenz ¹³², B. Parida ^{58c}, A.J. Parker ⁸⁷, K.A. Parker ⁴⁴, M.A. Parker ³¹, F. Parodi ^{53b,53a}, J.A. Parsons ³⁸, U. Parzefall ⁵⁰, V.R. Pascuzzi ¹⁶⁴, J.M.P. Pasner ¹⁴³, E. Pasqualucci ^{70a}, S. Passaggio ^{53b}, F. Pastore ⁹¹, P. Paswan ^{43a,43b}, S. Pataria ⁹⁷, J.R. Pater ⁹⁸, A. Pathak ^{178,l}, T. Pauly ³⁵, B. Pearson ¹¹³, M. Pedersen ¹³¹, L. Pedraza Diaz ¹¹⁷, R. Pedro ^{137a,137b}, S.V. Peleganchuk ^{120b,120a}, O. Penc ¹³⁸, C. Peng ^{15d}, H. Peng ^{58a}, B.S. Peralva ^{78a}, M.M. Perego ¹⁴², A.P. Pereira Peixoto ^{137a}, D.V. Perepelitsa ²⁹, F. Peri ¹⁹, L. Perini ^{66a,66b}, H. Pernegger ³⁵, S. Perrella ^{67a,67b}, V.D. Peshekhonov ^{77,*}, K. Peters ⁴⁴, R.F.Y. Peters ⁹⁸, B.A. Petersen ³⁵, T.C. Petersen ³⁹, E. Petit ⁵⁶, A. Petridis ¹, C. Petridou ¹⁵⁹, P. Petroff ¹²⁹, M. Petrov ¹³², F. Petrucci ^{72a,72b}, M. Pettee ¹⁸⁰, N.E. Pettersson ¹⁰⁰, A. Peyaud ¹⁴², R. Pezoa ^{144b}, T. Pham ¹⁰², F.H. Phillips ¹⁰⁴, P.W. Phillips ¹⁴¹, G. Piacquadio ¹⁵², E. Pianori ¹⁸, A. Picazio ¹⁰⁰, M.A. Pickering ¹³², R.H. Pickles ⁹⁸, R. Piegaia ³⁰, J.E. Pilcher ³⁶, A.D. Pilkington ⁹⁸, M. Pinamonti ^{71a,71b}, J.L. Pinfold ³, M. Pitt ¹⁷⁷, M.-A. Pleier ²⁹, V. Pleskot ¹⁴⁰, E. Plotnikova ⁷⁷, D. Pluth ⁷⁶, P. Podberezko ^{120b,120a}, R. Poettgen ⁹⁴, R. Poggi ⁵², L. Poggiali ¹²⁹, I. Pogrebnyak ¹⁰⁴, D. Pohl ²⁴, I. Pokharel ⁵¹, G. Polesello ^{68a}, A. Poley ¹⁸, A. Policicchio ^{70a,70b}, R. Polifka ³⁵, A. Polini ^{23b}, C.S. Pollard ⁴⁴, V. Polychronakos ²⁹, D. Ponomarenko ¹¹⁰, L. Pontecorvo ³⁵, G.A. Popeneciu ^{27d}, D.M. Portillo Quintero ¹³³, S. Pospisil ¹³⁹, K. Potamianos ⁴⁴, I.N. Potrap ⁷⁷, C.J. Potter ³¹, H. Potti ¹¹, T. Poulsen ⁹⁴, J. Poveda ³⁵, T.D. Powell ¹⁴⁶, M.E. Pozo Astigarraga ³⁵, P. Pralavorio ⁹⁹, S. Prell ⁷⁶, D. Price ⁹⁸, M. Primavera ^{65a}, S. Prince ¹⁰¹, N. Proklova ¹¹⁰, K. Prokofiev ^{61c}, F. Prokoshin ^{144b}, S. Protopopescu ²⁹, J. Proudfoot ⁶, M. Przybycien ^{81a}, A. Puri ¹⁷⁰, P. Puzo ¹²⁹, J. Qian ¹⁰³, Y. Qin ⁹⁸, A. Quadt ⁵¹, M. Queitsch-Maitland ⁴⁴, A. Qureshi ¹, P. Rados ¹⁰², F. Ragusa ^{66a,66b}, G. Rahal ⁹⁵, J.A. Raine ⁵², S. Rajagopalan ²⁹, A. Ramirez Morales ⁹⁰, T. Rashid ¹²⁹, S. Raspopov ⁵, M.G. Ratti ^{66a,66b}, D.M. Rauch ⁴⁴, F. Rauscher ¹¹², S. Rave ⁹⁷, B. Ravina ¹⁴⁶, I. Ravinovich ¹⁷⁷, J.H. Rawling ⁹⁸, M. Raymond ³⁵, A.L. Read ¹³¹, N.P. Readioff ⁵⁶, M. Reale ^{65a,65b}, D.M. Rebuzzi ^{68a,68b}, A. Redelbach ¹⁷⁴, G. Redlinger ²⁹, R. Reece ¹⁴³, R.G. Reed ^{32c}, K. Reeves ⁴², L. Rehnisch ¹⁹, J. Reichert ¹³⁴, A. Reiss ⁹⁷, C. Rembser ³⁵, H. Ren ^{15d}, M. Rescigno ^{70a}, S. Resconi ^{66a}, E.D. Resseguei ¹³⁴, S. Rettie ¹⁷², E. Reynolds ²¹, O.L. Rezanova ^{120b,120a}, P. Reznicek ¹⁴⁰, E. Ricci ^{73a,73b}, R. Richter ¹¹³, S. Richter ⁹², E. Richter-Was ^{81b}, O. Ricken ²⁴, M. Ridel ¹³³, P. Rieck ¹¹³, C.J. Riegel ¹⁷⁹, O. Rifki ⁴⁴, M. Rijssenbeek ¹⁵², A. Rimoldi ^{68a,68b}, M. Rimoldi ²⁰, L. Rinaldi ^{23b}, G. Ripellino ¹⁵¹, B. Ristić ⁸⁷, E. Ritsch ³⁵, I. Riu ¹⁴, J.C. Rivera Vergara ^{144a}, F. Rizatdinova ¹²⁶, E. Rizvi ⁹⁰, C. Rizzi ¹⁴, R.T. Roberts ⁹⁸, S.H. Robertson ^{101,ae}, D. Robinson ³¹, J.E.M. Robinson ⁴⁴, A. Robson ⁵⁵, E. Rocco ⁹⁷, C. Roda ^{69a,69b}, Y. Rodina ⁹⁹, S. Rodriguez Bosca ¹⁷¹, A. Rodriguez Perez ¹⁴, D. Rodriguez Rodriguez ¹⁷¹, A.M. Rodríguez Vera ^{165b}, S. Roe ³⁵, C.S. Rogan ⁵⁷, O. Røhne ¹³¹, R. Röhrlig ¹¹³, C.P.A. Roland ⁶³, J. Roloff ⁵⁷, A. Romanikou ¹¹⁰, M. Romano ^{23b,23a}, N. Rompotis ⁸⁸, M. Ronzani ¹²², L. Roos ¹³³, S. Rosati ^{70a}, K. Rosbach ⁵⁰, P. Rose ¹⁴³, N-A. Rosien ⁵¹, E. Rossi ⁴⁴, E. Rossi ^{67a,67b}, L.P. Rossi ^{53b}, L. Rossini ^{66a,66b}, J.H.N. Rosten ³¹, R. Rosten ¹⁴, M. Rotaru ^{27b}, J. Rothberg ¹⁴⁵, D. Rousseau ¹²⁹, D. Roy ^{32c}, A. Rozanova ⁹⁹, Y. Rozen ¹⁵⁷, X. Ruan ^{32c}, F. Rubbo ¹⁵⁰, F. Rühr ⁵⁰, A. Ruiz-Martinez ¹⁷¹, Z. Rurikova ⁵⁰, N.A. Rusakovich ⁷⁷, H.L. Russell ¹⁰¹, J.P. Rutherford ⁷, E.M. Rüttinger ^{44,m}, Y.F. Ryabov ¹³⁵, M. Rybar ¹⁷⁰, G. Rybkin ¹²⁹, S. Ryu ⁶, A. Ryzhov ¹²¹, G.F. Rzehorz ⁵¹, P. Sabatini ⁵¹, G. Sabato ¹¹⁸, S. Sacerdoti ¹²⁹, H.F-W. Sadrozinski ¹⁴³, R. Sadykov ⁷⁷, F. Safai Tehrani ^{70a}, P. Saha ¹¹⁹, M. Sahinsoy ^{59a}, A. Sahu ¹⁷⁹, M. Saimpert ⁴⁴, M. Saito ¹⁶⁰, T. Saito ¹⁶⁰, H. Sakamoto ¹⁶⁰, A. Sakharov ^{122,an}, D. Salamani ⁵², G. Salamanna ^{72a,72b}, J.E. Salazar Loyola ^{144b}, D. Salek ¹¹⁸, P.H. Sales De Bruin ¹⁶⁹, D. Salihagic ¹¹³, A. Salnikov ¹⁵⁰, J. Salt ¹⁷¹, D. Salvatore ^{40b,40a}, F. Salvatore ¹⁵³, A. Salvucci ^{61a,61b,61c}, A. Salzburger ³⁵, J. Samarati ³⁵, D. Sammel ⁵⁰, D. Sampsonidis ¹⁵⁹, D. Sampsonidou ¹⁵⁹, J. Sánchez ¹⁷¹, A. Sanchez Pineda ^{64a,64c}, H. Sandaker ¹³¹, C.O. Sander ⁴⁴, M. Sandhoff ¹⁷⁹, C. Sandoval ²², D.P.C. Sankey ¹⁴¹, M. Sannino ^{53b,53a}, Y. Sano ¹¹⁵, A. Sansoni ⁴⁹, C. Santoni ³⁷, H. Santos ^{137a}, I. Santoyo Castillo ¹⁵³, A. Santra ¹⁷¹, A. Sapronov ⁷⁷, J.G. Saraiva ^{137a,137d}, O. Sasaki ⁷⁹, K. Sato ¹⁶⁶, E. Sauvan ⁵, P. Savard ^{164,av}, N. Savic ¹¹³, R. Sawada ¹⁶⁰, C. Sawyer ¹⁴¹, L. Sawyer ^{93,al}, C. Sbarra ^{23b}, A. Sbrizzi ^{23a}, T. Scanlon ⁹², J. Schaarschmidt ¹⁴⁵, P. Schacht ¹¹³, B.M. Schachtner ¹¹², D. Schaefer ³⁶, L. Schaefer ¹³⁴, J. Schaeffer ⁹⁷, S. Schaepe ³⁵, U. Schäfer ⁹⁷, A.C. Schaffer ¹²⁹, D. Schaile ¹¹², R.D. Schamberger ¹⁵², N. Scharmberg ⁹⁸, V.A. Schegelsky ¹³⁵, D. Scheirich ¹⁴⁰, F. Schenck ¹⁹, M. Schernau ¹⁶⁸, C. Schiavi ^{53b,53a}, S. Schier ¹⁴³, L.K. Schildgen ²⁴,

- Z.M. Schillaci ²⁶, E.J. Schioppa ³⁵, M. Schioppa ^{40b,40a}, K.E. Schleicher ⁵⁰, S. Schlenker ³⁵,
 K.R. Schmidt-Sommerfeld ¹¹³, K. Schmieden ³⁵, C. Schmitt ⁹⁷, S. Schmitt ⁴⁴, S. Schmitz ⁹⁷,
 J.C. Schmoekel ⁴⁴, U. Schnoor ⁵⁰, L. Schoeffel ¹⁴², A. Schoening ^{59b}, E. Schopf ²⁴, M. Schott ⁹⁷,
 J.F.P. Schouwenberg ¹¹⁷, J. Schovancova ³⁵, S. Schramm ⁵², A. Schulte ⁹⁷, H-C. Schultz-Coulon ^{59a},
 M. Schumacher ⁵⁰, B.A. Schumm ¹⁴³, Ph. Schune ¹⁴², A. Schwartzman ¹⁵⁰, T.A. Schwarz ¹⁰³,
 H. Schweiger ⁹⁸, Ph. Schwemling ¹⁴², R. Schwienhorst ¹⁰⁴, A. Sciandra ²⁴, G. Sciolla ²⁶,
 M. Scornajenghi ^{40b,40a}, F. Scuri ^{69a}, F. Scutti ¹⁰², L.M. Scyboz ¹¹³, J. Searcy ¹⁰³, C.D. Sebastiani ^{70a,70b},
 P. Seema ²⁴, S.C. Seidel ¹¹⁶, A. Seiden ¹⁴³, T. Seiss ³⁶, J.M. Seixas ^{78b}, G. Sekhniaidze ^{67a}, K. Sekhon ¹⁰³,
 S.J. Sekula ⁴¹, N. Semprini-Cesari ^{23b,23a}, S. Sen ⁴⁷, S. Senkin ³⁷, C. Serfon ¹³¹, L. Serin ¹²⁹, L. Serkin ^{64a,64b},
 M. Sessa ^{72a,72b}, H. Severini ¹²⁵, F. Sforza ¹⁶⁷, A. Sfyrla ⁵², E. Shabalina ⁵¹, J.D. Shahinian ¹⁴³,
 N.W. Shaikh ^{43a,43b}, L.Y. Shan ^{15a}, R. Shang ¹⁷⁰, J.T. Shank ²⁵, M. Shapiro ¹⁸, A.S. Sharma ¹, A. Sharma ¹³²,
 P.B. Shatalov ¹⁰⁹, K. Shaw ¹⁵³, S.M. Shaw ⁹⁸, A. Shcherbakova ¹³⁵, Y. Shen ¹²⁵, N. Sherafati ³³,
 A.D. Sherman ²⁵, P. Sherwood ⁹², L. Shi ^{155,ar}, S. Shimizu ⁷⁹, C.O. Shimmin ¹⁸⁰, M. Shimojima ¹¹⁴,
 I.P.J. Shipsey ¹³², S. Shirabe ⁸⁵, M. Shiyakova ⁷⁷, J. Shlomi ¹⁷⁷, A. Shmeleva ¹⁰⁸, D. Shoaleh Saadi ¹⁰⁷,
 M.J. Shochet ³⁶, S. Shojaii ¹⁰², D.R. Shope ¹²⁵, S. Shrestha ¹²³, E. Shulga ¹¹⁰, P. Sicho ¹³⁸, A.M. Sickles ¹⁷⁰,
 P.E. Sidebo ¹⁵¹, E. Sideras Haddad ^{32c}, O. Sidiropoulou ³⁵, A. Sidoti ^{23b,23a}, F. Siegert ⁴⁶, Dj. Sijacki ¹⁶,
 J. Silva ^{137a}, M. Silva Jr. ¹⁷⁸, M.V. Silva Oliveira ^{78a}, S.B. Silverstein ^{43a}, L. Simic ⁷⁷, S. Simion ¹²⁹,
 E. Simioni ⁹⁷, M. Simon ⁹⁷, R. Simonello ⁹⁷, P. Sinervo ¹⁶⁴, N.B. Sinev ¹²⁸, M. Sioli ^{23b,23a}, G. Siragusa ¹⁷⁴,
 I. Siral ¹⁰³, S.Yu. Sivoklokov ¹¹¹, J. Sjölin ^{43a,43b}, P. Skubic ¹²⁵, M. Slater ²¹, T. Slavicek ¹³⁹, M. Slawinska ⁸²,
 K. Sliwa ¹⁶⁷, R. Slovak ¹⁴⁰, V. Smakhtin ¹⁷⁷, B.H. Smart ⁵, J. Smiesko ^{28a}, N. Smirnov ¹¹⁰, S.Yu. Smirnov ¹¹⁰,
 Y. Smirnov ¹¹⁰, L.N. Smirnova ¹¹¹, O. Smirnova ⁹⁴, J.W. Smith ⁵¹, M.N.K. Smith ³⁸, M. Smizanska ⁸⁷,
 K. Smolek ¹³⁹, A. Smykiewicz ⁸², A.A. Snesarev ¹⁰⁸, I.M. Snyder ¹²⁸, S. Snyder ²⁹, R. Sobie ^{173,ae},
 A.M. Soffa ¹⁶⁸, A. Soffer ¹⁵⁸, A. Søgaard ⁴⁸, D.A. Soh ¹⁵⁵, G. Sokhrannyi ⁸⁹, C.A. Solans Sanchez ³⁵,
 M. Solar ¹³⁹, E.Yu. Soldatov ¹¹⁰, U. Soldevila ¹⁷¹, A.A. Solodkov ¹²¹, A. Soloshenko ⁷⁷, O.V. Solovyanov ¹²¹,
 V. Solovyev ¹³⁵, P. Sommer ¹⁴⁶, H. Son ¹⁶⁷, W. Song ¹⁴¹, W.Y. Song ^{165b}, A. Sopczak ¹³⁹, F. Sopkova ^{28b},
 D. Sosa ^{59b}, C.L. Sotiropoulou ^{69a,69b}, S. Sottocornola ^{68a,68b}, R. Soualah ^{64a,64c,j}, A.M. Soukharev ^{120b,120a},
 D. South ⁴⁴, B.C. Sowden ⁹¹, S. Spagnolo ^{65a,65b}, M. Spalla ¹¹³, M. Spangenberg ¹⁷⁵, F. Spanò ⁹¹,
 D. Sperlich ¹⁹, F. Spettel ¹¹³, T.M. Spieker ^{59a}, R. Spighi ^{23b}, G. Spigo ³⁵, L.A. Spiller ¹⁰², D.P. Spiteri ⁵⁵,
 M. Spousta ¹⁴⁰, A. Stabile ^{66a,66b}, R. Stamen ^{59a}, S. Stamm ¹⁹, E. Stanecka ⁸², R.W. Stanek ⁶, C. Stanescu ^{72a},
 B. Stanislaus ¹³², M.M. Stanitzki ⁴⁴, B. Stapf ¹¹⁸, S. Stapnes ¹³¹, E.A. Starchenko ¹²¹, G.H. Stark ³⁶, J. Stark ⁵⁶,
 S.H. Stark ³⁹, P. Staroba ¹³⁸, P. Starovoitov ^{59a}, S. Stärz ³⁵, R. Staszewski ⁸², M. Stegler ⁴⁴, P. Steinberg ²⁹,
 B. Stelzer ¹⁴⁹, H.J. Stelzer ³⁵, O. Stelzer-Chilton ^{165a}, H. Stenzel ⁵⁴, T.J. Stevenson ⁹⁰, G.A. Stewart ³⁵,
 M.C. Stockton ¹²⁸, G. Stoica ^{27b}, P. Stolte ⁵¹, S. Stonjek ¹¹³, A. Straessner ⁴⁶, J. Strandberg ¹⁵¹,
 S. Strandberg ^{43a,43b}, M. Strauss ¹²⁵, P. Strizenec ^{28b}, R. Ströhmer ¹⁷⁴, D.M. Strom ¹²⁸, R. Stroynowski ⁴¹,
 A. Strubig ⁴⁸, S.A. Stucci ²⁹, B. Stugu ¹⁷, J. Stupak ¹²⁵, N.A. Styles ⁴⁴, D. Su ¹⁵⁰, J. Su ¹³⁶, S. Suchek ^{59a},
 Y. Sugaya ¹³⁰, M. Suk ¹³⁹, V.V. Sulin ¹⁰⁸, D.M.S. Sultan ⁵², S. Sultansoy ^{4c}, T. Sumida ⁸³, S. Sun ¹⁰³, X. Sun ³,
 K. Suruliz ¹⁵³, C.J.E. Suster ¹⁵⁴, M.R. Sutton ¹⁵³, S. Suzuki ⁷⁹, M. Svatos ¹³⁸, M. Swiatlowski ³⁶, S.P. Swift ²,
 A. Sydorenko ⁹⁷, I. Sykora ^{28a}, T. Sykora ¹⁴⁰, D. Ta ⁹⁷, K. Tackmann ^{44,ab}, J. Taenzer ¹⁵⁸, A. Taffard ¹⁶⁸,
 R. Tafirout ^{165a}, E. Tahirovic ⁹⁰, N. Taiblum ¹⁵⁸, H. Takai ²⁹, R. Takashima ⁸⁴, E.H. Takasugi ¹¹³, K. Takeda ⁸⁰,
 T. Takeshita ¹⁴⁷, Y. Takubo ⁷⁹, M. Talby ⁹⁹, A.A. Talyshев ^{120b,120a}, J. Tanaka ¹⁶⁰, M. Tanaka ¹⁶²,
 R. Tanaka ¹²⁹, B.B. Tannenwald ¹²³, S. Tapia Araya ^{144b}, S. Tapprogge ⁹⁷, A. Tarek Abouelfadl Mohamed ¹³³,
 S. Tarem ¹⁵⁷, G. Tarna ^{27b,e}, G.F. Tartarelli ^{66a}, P. Tas ¹⁴⁰, M. Tasevsky ¹³⁸, T. Tashiro ⁸³, E. Tassi ^{40b,40a},
 A. Tavares Delgado ^{137a,137b}, Y. Tayalati ^{34e}, A.C. Taylor ¹¹⁶, A.J. Taylor ⁴⁸, G.N. Taylor ¹⁰², P.T.E. Taylor ¹⁰²,
 W. Taylor ^{165b}, A.S. Tee ⁸⁷, P. Teixeira-Dias ⁹¹, H. Ten Kate ³⁵, P.K. Teng ¹⁵⁵, J.J. Teoh ¹¹⁸, F. Tepel ¹⁷⁹,
 S. Terada ⁷⁹, K. Terashi ¹⁶⁰, J. Terron ⁹⁶, S. Terzo ¹⁴, M. Testa ⁴⁹, R.J. Teuscher ^{164,ae}, S.J. Thais ¹⁸⁰,
 T. Theveneaux-Pelzer ⁴⁴, F. Thiele ³⁹, D.W. Thomas ⁹¹, J.P. Thomas ²¹, A.S. Thompson ⁵⁵, P.D. Thompson ²¹,
 L.A. Thomsen ¹⁸⁰, E. Thomson ¹³⁴, Y. Tian ³⁸, R.E. Ticse Torres ⁵¹, V.O. Tikhomirov ^{108,ap},
 Yu.A. Tikhonov ^{120b,120a}, S. Timoshenko ¹¹⁰, P. Tipton ¹⁸⁰, S. Tisserant ⁹⁹, K. Todome ¹⁶²,
 S. Todorova-Nova ⁵, S. Todt ⁴⁶, J. Tojo ⁸⁵, S. Tokár ^{28a}, K. Tokushuku ⁷⁹, E. Tolley ¹²³, K.G. Tomiwa ^{32c},
 M. Tomoto ¹¹⁵, L. Tompkins ^{150,r}, K. Toms ¹¹⁶, B. Tong ⁵⁷, P. Tornambe ⁵⁰, E. Torrence ¹²⁸, H. Torres ⁴⁶,
 E. Torró Pastor ¹⁴⁵, C. Tosciri ¹³², J. Toth ^{99,ad}, F. Touchard ⁹⁹, D.R. Tovey ¹⁴⁶, C.J. Treado ¹²², T. Trefzger ¹⁷⁴,
 F. Tresoldi ¹⁵³, A. Tricoli ²⁹, I.M. Trigger ^{165a}, S. Trincaz-Duvold ¹³³, M.F. Tripiana ¹⁴, W. Trischuk ¹⁶⁴,

- B. Trocmé ⁵⁶, A. Trofymov ¹²⁹, C. Troncon ^{66a}, M. Trovatelli ¹⁷³, F. Trovato ¹⁵³, L. Truong ^{32b},
 M. Trzebinski ⁸², A. Trzupek ⁸², F. Tsai ⁴⁴, J.-C.-L. Tseng ¹³², P.V. Tsiareshka ¹⁰⁵, A. Tsirigotis ¹⁵⁹,
 N. Tsirintanis ⁹, V. Tsiskaridze ¹⁵², E.G. Tskhadadze ^{156a}, I.I. Tsukerman ¹⁰⁹, V. Tsulaia ¹⁸, S. Tsuno ⁷⁹,
 D. Tsybychev ^{152,163}, Y. Tu ^{61b}, A. Tudorache ^{27b}, V. Tudorache ^{27b}, T.T. Tulbure ^{27a}, A.N. Tuna ⁵⁷,
 S. Turchikhin ⁷⁷, D. Turgeman ¹⁷⁷, I. Turk Cakir ^{4b,v}, R. Turra ^{66a}, P.M. Tuts ³⁸, E. Tzovara ⁹⁷,
 G. Ucchielli ^{23b,23a}, I. Ueda ⁷⁹, M. Ughetto ^{43a,43b}, F. Ukegawa ¹⁶⁶, G. Unal ³⁵, A. Undrus ²⁹, G. Unel ¹⁶⁸,
 F.C. Ungaro ¹⁰², Y. Unno ⁷⁹, K. Uno ¹⁶⁰, J. Urban ^{28b}, P. Urquijo ¹⁰², P. Urrejola ⁹⁷, G. Usai ⁸, J. Usui ⁷⁹,
 L. Vacavant ⁹⁹, V. Vacek ¹³⁹, B. Vachon ¹⁰¹, K.O.H. Vadla ¹³¹, A. Vaidya ⁹², C. Valderanis ¹¹²,
 E. Valdes Santurio ^{43a,43b}, M. Valente ⁵², S. Valentineti ^{23b,23a}, A. Valero ¹⁷¹, L. Valéry ⁴⁴, R.A. Vallance ²¹,
 A. Vallier ⁵, J.A. Valls Ferrer ¹⁷¹, T.R. Van Daalen ¹⁴, H. Van der Graaf ¹¹⁸, P. Van Gemmeren ⁶,
 J. Van Nieuwkoop ¹⁴⁹, I. Van Vulpen ¹¹⁸, M. Vanadia ^{71a,71b}, W. Vandelli ³⁵, A. Vaniachine ¹⁶³,
 P. Vankov ¹¹⁸, R. Vari ^{70a}, E.W. Varnes ⁷, C. Varni ^{53b,53a}, T. Varol ⁴¹, D. Varouchas ¹²⁹, K.E. Varvell ¹⁵⁴,
 G.A. Vasquez ^{144b}, J.G. Vasquez ¹⁸⁰, F. Vazeille ³⁷, D. Vazquez Furelos ¹⁴, T. Vazquez Schroeder ¹⁰¹,
 J. Veatch ⁵¹, V. Vecchio ^{72a,72b}, L.M. Veloce ¹⁶⁴, F. Veloso ^{137a,137c}, S. Veneziano ^{70a}, A. Ventura ^{65a,65b},
 M. Venturi ¹⁷³, N. Venturi ³⁵, V. Vercesi ^{68a}, M. Verducci ^{72a,72b}, C.M. Vergel Infante ⁷⁶, C. Vergis ²⁴,
 W. Verkerke ¹¹⁸, A.T. Vermeulen ¹¹⁸, J.C. Vermeulen ¹¹⁸, M.C. Vetterli ^{149,av}, N. Viaux Maira ^{144b},
 M. Vicente Barreto Pinto ⁵², I. Vichou ^{170,*}, T. Vickey ¹⁴⁶, O.E. Vickey Boeriu ¹⁴⁶, G.H.A. Viehhauser ¹³²,
 S. Viel ¹⁸, L. Vigani ¹³², M. Villa ^{23b,23a}, M. Villaplana Perez ^{66a,66b}, E. Vilucchi ⁴⁹, M.G. Vincter ³³,
 V.B. Vinogradov ⁷⁷, A. Vishwakarma ⁴⁴, C. Vittori ^{23b,23a}, I. Vivarelli ¹⁵³, S. Vlachos ¹⁰, M. Vogel ¹⁷⁹,
 P. Vokac ¹³⁹, G. Volpi ¹⁴, S.E. von Buddenbrock ^{32c}, E. Von Toerne ²⁴, V. Vorobel ¹⁴⁰, K. Vorobev ¹¹⁰,
 M. Vos ¹⁷¹, J.H. Vossebeld ⁸⁸, N. Vranjes ¹⁶, M. Vranjes Milosavljevic ¹⁶, V. Vrba ¹³⁹, M. Vreeswijk ¹¹⁸,
 T. Šfiligoj ⁸⁹, R. Vuillermet ³⁵, I. Vukotic ³⁶, T. Ženiš ^{28a}, L. Živković ¹⁶, P. Wagner ²⁴, W. Wagner ¹⁷⁹,
 J. Wagner-Kuhr ¹¹², H. Wahlberg ⁸⁶, S. Wahrmund ⁴⁶, K. Wakamiya ⁸⁰, V.M. Walbrecht ¹¹³, J. Walder ⁸⁷,
 R. Walker ¹¹², S.D. Walker ⁹¹, W. Walkowiak ¹⁴⁸, V. Wallangen ^{43a,43b}, A.M. Wang ⁵⁷, C. Wang ^{58b,e},
 F. Wang ¹⁷⁸, H. Wang ¹⁸, H. Wang ³, J. Wang ¹⁵⁴, J. Wang ^{59b}, P. Wang ⁴¹, Q. Wang ¹²⁵, R.-J. Wang ¹³³,
 R. Wang ^{58a}, R. Wang ⁶, S.M. Wang ¹⁵⁵, W.T. Wang ^{58a}, W. Wang ^{15c,af}, W.X. Wang ^{58a,af}, Y. Wang ^{58a,am},
 Z. Wang ^{58c}, C. Wanotayaroj ⁴⁴, A. Warburton ¹⁰¹, C.P. Ward ³¹, D.R. Wardrobe ⁹², A. Washbrook ⁴⁸,
 P.M. Watkins ²¹, A.T. Watson ²¹, M.F. Watson ²¹, G. Watts ¹⁴⁵, S. Watts ⁹⁸, B.M. Waugh ⁹², A.F. Webb ¹¹,
 S. Webb ⁹⁷, C. Weber ¹⁸⁰, M.S. Weber ²⁰, S.A. Weber ³³, S.M. Weber ^{59a}, A.R. Weidberg ¹³², B. Weinert ⁶³,
 J. Weingarten ⁴⁵, M. Weirich ⁹⁷, C. Weiser ⁵⁰, P.S. Wells ³⁵, T. Wenaus ²⁹, T. Wengler ³⁵, S. Wenig ³⁵,
 N. Wermes ²⁴, M.D. Werner ⁷⁶, P. Werner ³⁵, M. Wessels ^{59a}, T.D. Weston ²⁰, K. Whalen ¹²⁸,
 N.L. Whallon ¹⁴⁵, A.M. Wharton ⁸⁷, A.S. White ¹⁰³, A. White ⁸, M.J. White ¹, R. White ^{144b}, D. Whiteson ¹⁶⁸,
 B.W. Whitmore ⁸⁷, F.J. Wickens ¹⁴¹, W. Wiedenmann ¹⁷⁸, M. Wielers ¹⁴¹, C. Wiglesworth ³⁹,
 L.A.M. Wiik-Fuchs ⁵⁰, A. Wildauer ¹¹³, F. Wilk ⁹⁸, H.G. Wilkens ³⁵, L.J. Wilkins ⁹¹, H.H. Williams ¹³⁴,
 S. Williams ³¹, C. Willis ¹⁰⁴, S. Willocq ¹⁰⁰, J.A. Wilson ²¹, I. Wingerter-Seez ⁵, E. Winkels ¹⁵³,
 F. Winkelmeier ¹²⁸, O.J. Winston ¹⁵³, B.T. Winter ²⁴, M. Wittgen ¹⁵⁰, M. Wobisch ⁹³, A. Wolf ⁹⁷,
 T.M.H. Wolf ¹¹⁸, R. Wolff ⁹⁹, M.W. Wolter ⁸², H. Wolters ^{137a,137c}, V.W.S. Wong ¹⁷², N.L. Woods ¹⁴³,
 S.D. Worm ²¹, B.K. Wosiek ⁸², K.W. Woźniak ⁸², K. Wraight ⁵⁵, M. Wu ³⁶, S.L. Wu ¹⁷⁸, X. Wu ⁵², Y. Wu ^{58a},
 T.R. Wyatt ⁹⁸, B.M. Wynne ⁴⁸, S. Xella ³⁹, Z. Xi ¹⁰³, L. Xia ¹⁷⁵, D. Xu ^{15a}, H. Xu ^{58a,e}, L. Xu ²⁹, T. Xu ¹⁴²,
 W. Xu ¹⁰³, B. Yabsley ¹⁵⁴, S. Yacoob ^{32a}, K. Yajima ¹³⁰, D.P. Yallup ⁹², D. Yamaguchi ¹⁶², Y. Yamaguchi ¹⁶²,
 A. Yamamoto ⁷⁹, T. Yamanaka ¹⁶⁰, F. Yamane ⁸⁰, M. Yamatani ¹⁶⁰, T. Yamazaki ¹⁶⁰, Y. Yamazaki ⁸⁰, Z. Yan ²⁵,
 H.J. Yang ^{58c,58d}, H.T. Yang ¹⁸, S. Yang ⁷⁵, Y. Yang ¹⁶⁰, Z. Yang ¹⁷, W.-M. Yao ¹⁸, Y.C. Yap ⁴⁴, Y. Yasu ⁷⁹,
 E. Yatsenko ^{58c,58d}, J. Ye ⁴¹, S. Ye ²⁹, I. Yeletskikh ⁷⁷, E. Yigitbasi ²⁵, E. Yildirim ⁹⁷, K. Yorita ¹⁷⁶,
 K. Yoshihara ¹³⁴, C.J.S. Young ³⁵, C. Young ¹⁵⁰, J. Yu ⁸, J. Yu ⁷⁶, X. Yue ^{59a}, S.P.Y. Yuen ²⁴, B. Zabinski ⁸²,
 G. Zacharis ¹⁰, E. Zaffaroni ⁵², R. Zaidan ¹⁴, A.M. Zaitsev ^{121,ao}, T. Zakareishvili ^{156b}, N. Zakharchuk ⁴⁴,
 J. Zalieckas ¹⁷, S. Zambito ⁵⁷, D. Zanzi ³⁵, D.R. Zaripovas ⁵⁵, S.V. Zeißner ⁴⁵, C. Zeitnitz ¹⁷⁹, G. Zemaityte ¹³²,
 J.C. Zeng ¹⁷⁰, Q. Zeng ¹⁵⁰, O. Zenin ¹²¹, D. Zerwas ¹²⁹, M. Zgubić ¹³², D.F. Zhang ^{58b}, D. Zhang ¹⁰³,
 F. Zhang ¹⁷⁸, G. Zhang ^{58a}, H. Zhang ^{15c}, J. Zhang ⁶, L. Zhang ^{15c}, L. Zhang ^{58a}, M. Zhang ¹⁷⁰, P. Zhang ^{15c},
 R. Zhang ^{58a}, R. Zhang ²⁴, X. Zhang ^{58b}, Y. Zhang ^{15d}, Z. Zhang ¹²⁹, P. Zhao ⁴⁷, X. Zhao ⁴¹, Y. Zhao ^{58b,129,ak},
 Z. Zhao ^{58a}, A. Zhemchugov ⁷⁷, B. Zhou ¹⁰³, C. Zhou ¹⁷⁸, L. Zhou ⁴¹, M.S. Zhou ^{15d}, M. Zhou ¹⁵², N. Zhou ^{58c},
 Y. Zhou ⁷, C.G. Zhu ^{58b}, H.L. Zhu ^{58a}, H. Zhu ^{15a}, J. Zhu ¹⁰³, Y. Zhu ^{58a}, X. Zhuang ^{15a}, K. Zhukov ¹⁰⁸,
 V. Zhulanov ^{120b,120a}, A. Zibell ¹⁷⁴, D. Ziemska ⁶³, N.I. Zimine ⁷⁷, S. Zimmermann ⁵⁰, Z. Zinonos ¹¹³,

M. Zinser⁹⁷, M. Ziolkowski¹⁴⁸, G. Zobernig¹⁷⁸, A. Zoccoli^{23b,23a}, K. Zoch⁵¹, T.G. Zorbas¹⁴⁶, R. Zou³⁶,
M. Zur Nedden¹⁹, L. Zwaliński³⁵

¹ Department of Physics, University of Adelaide, Adelaide, Australia

² Physics Department, SUNY Albany, Albany, NY, United States of America

³ Department of Physics, University of Alberta, Edmonton, AB, Canada

⁴ (a) Department of Physics, Ankara University, Ankara; (b) Istanbul Aydin University, Istanbul; (c) Division of Physics, TOBB University of Economics and Technology, Ankara, Turkey

⁵ LAPP, Université Grenoble Alpes, Université Savoie Mont Blanc, CNRS/IN2P3, Annecy, France

⁶ High Energy Physics Division, Argonne National Laboratory, Argonne, IL, United States of America

⁷ Department of Physics, University of Arizona, Tucson, AZ, United States of America

⁸ Department of Physics, University of Texas at Arlington, Arlington, TX, United States of America

⁹ Physics Department, National and Kapodistrian University of Athens, Athens, Greece

¹⁰ Physics Department, National Technical University of Athens, Zografou, Greece

¹¹ Department of Physics, University of Texas at Austin, Austin, TX, United States of America

¹² (a) Bahcesehir University, Faculty of Engineering and Natural Sciences, Istanbul; (b) Istanbul Bilgi University, Faculty of Engineering and Natural Sciences, Istanbul; (c) Department of Physics, Bogazici University, Istanbul; (d) Department of Physics Engineering, Gaziantep University, Gaziantep, Turkey

¹³ Institute of Physics, Azerbaijan Academy of Sciences, Baku, Azerbaijan

¹⁴ Institut de Física d'Altes Energies (IFAE), Barcelona Institute of Science and Technology, Barcelona, Spain

¹⁵ (a) Institute of High Energy Physics, Chinese Academy of Sciences, Beijing; (b) Physics Department, Tsinghua University, Beijing; (c) Department of Physics, Nanjing University, Nanjing; (d) University of Chinese Academy of Science (UCAS), Beijing, China

¹⁶ Institute of Physics, University of Belgrade, Belgrade, Serbia

¹⁷ Department for Physics and Technology, University of Bergen, Bergen, Norway

¹⁸ Physics Division, Lawrence Berkeley National Laboratory and University of California, Berkeley, CA, United States of America

¹⁹ Institut für Physik, Humboldt Universität zu Berlin, Berlin, Germany

²⁰ Albert Einstein Center for Fundamental Physics and Laboratory for High Energy Physics, University of Bern, Bern, Switzerland

²¹ School of Physics and Astronomy, University of Birmingham, Birmingham, United Kingdom

²² Centro de Investigaciones, Universidad Antonio Nariño, Bogota, Colombia

²³ (a) Dipartimento di Fisica e Astronomia, Università di Bologna, Bologna; (b) INFN Sezione di Bologna, Italy

²⁴ Physikalisches Institut, Universität Bonn, Bonn, Germany

²⁵ Department of Physics, Boston University, Boston, MA, United States of America

²⁶ Department of Physics, Brandeis University, Waltham, MA, United States of America

²⁷ (a) Transilvania University of Brasov, Brasov; (b) Horia Hulubei National Institute of Physics and Nuclear Engineering, Bucharest; (c) Department of Physics, Alexandru Ioan Cuza University of Iasi, Iasi; (d) National Institute for Research and Development of Isotopic and Molecular Technologies, Physics Department, Cluj-Napoca; (e) University Politehnica Bucharest, Bucharest; (f) West University in Timisoara, Timisoara, Romania

²⁸ (a) Faculty of Mathematics, Physics and Informatics, Comenius University, Bratislava; (b) Department of Subnuclear Physics, Institute of Experimental Physics of the Slovak Academy of Sciences, Kosice, Slovak Republic

²⁹ Physics Department, Brookhaven National Laboratory, Upton, NY, United States of America

³⁰ Departamento de Física, Universidad de Buenos Aires, Buenos Aires, Argentina

³¹ Cavendish Laboratory, University of Cambridge, Cambridge, United Kingdom

³² (a) Department of Physics, University of Cape Town, Cape Town; (b) Department of Mechanical Engineering Science, University of Johannesburg, Johannesburg; (c) School of Physics, University of the Witwatersrand, Johannesburg, South Africa

³³ Department of Physics, Carleton University, Ottawa, ON, Canada

³⁴ (a) Faculté des Sciences Ain Chock, Réseau Universitaire de Physique des Hautes Energies – Université Hassan II, Casablanca; (b) Centre National de l'Energie des Sciences Techniques Nucléaires (CNESTEN), Rabat; (c) Faculté des Sciences Semlalia, Université Cadi Ayyad, LPHEA, Marrakech; (d) Faculté des Sciences, Université Mohamed Premier and LPTPM, Oujda; (e) Faculté des sciences, Université Mohammed V, Rabat, Morocco

³⁵ CERN, Geneva, Switzerland

³⁶ Enrico Fermi Institute, University of Chicago, Chicago, IL, United States of America

³⁷ LPC, Université Clermont Auvergne, CNRS/IN2P3, Clermont-Ferrand, France

³⁸ Nevis Laboratory, Columbia University, Irvington, NY, United States of America

³⁹ Niels Bohr Institute, University of Copenhagen, Copenhagen, Denmark

⁴⁰ (a) Dipartimento di Fisica, Università della Calabria, Rende; (b) INFN Gruppo Collegato di Cosenza, Laboratori Nazionali di Frascati, Italy

⁴¹ Physics Department, Southern Methodist University, Dallas, TX, United States of America

⁴² Physics Department, University of Texas at Dallas, Richardson, TX, United States of America

⁴³ (a) Department of Physics, Stockholm University; (b) Oskar Klein Centre, Stockholm, Sweden

⁴⁴ Deutsches Elektronen-Synchrotron DESY, Hamburg and Zeuthen, Germany

⁴⁵ Lehrstuhl für Experimentelle Physik IV, Technische Universität Dortmund, Dortmund, Germany

⁴⁶ Institut für Kern- und Teilchenphysik, Technische Universität Dresden, Dresden, Germany

⁴⁷ Department of Physics, Duke University, Durham, NC, United States of America

⁴⁸ SUPA – School of Physics and Astronomy, University of Edinburgh, Edinburgh, United Kingdom

⁴⁹ INFN e Laboratori Nazionali di Frascati, Frascati, Italy

⁵⁰ Physikalisches Institut, Albert-Ludwigs-Universität Freiburg, Freiburg, Germany

⁵¹ II. Physikalisches Institut, Georg-August-Universität Göttingen, Göttingen, Germany

⁵² Département de Physique Nucléaire et Corpusculaire, Université de Genève, Genève, Switzerland

⁵³ (a) Dipartimento di Fisica, Università di Genova, Genova; (b) INFN Sezione di Genova, Italy

⁵⁴ II. Physikalisches Institut, Justus-Liebig-Universität Giessen, Giessen, Germany

⁵⁵ SUPA – School of Physics and Astronomy, University of Glasgow, Glasgow, United Kingdom

⁵⁶ LPSC, Université Grenoble Alpes, CNRS/IN2P3, Grenoble INP, Grenoble, France

⁵⁷ Laboratory for Particle Physics and Cosmology, Harvard University, Cambridge, MA, United States of America

⁵⁸ (a) Department of Modern Physics and State Key Laboratory of Particle Detection and Electronics, University of Science and Technology of China, Hefei; (b) Institute of Frontier and Interdisciplinary Science and Key Laboratory of Particle Physics and Particle Irradiation (MOE), Shandong University, Qingdao; (c) School of Physics and Astronomy, Shanghai Jiao Tong University, KLPPAC-MoE, SKLPPC, Shanghai; (d) Tsung-Dao Lee Institute, Shanghai, China

⁵⁹ (a) Kirchhoff-Institut für Physik, Ruprecht-Karls-Universität Heidelberg, Heidelberg; (b) Physikalisches Institut, Ruprecht-Karls-Universität Heidelberg, Heidelberg, Germany

⁶⁰ Faculty of Applied Information Science, Hiroshima Institute of Technology, Hiroshima, Japan

⁶¹ (a) Department of Physics, Chinese University of Hong Kong, Shatin, N.T., Hong Kong; (b) Department of Physics, University of Hong Kong, Hong Kong; (c) Department of Physics and Institute for Advanced Study, Hong Kong University of Science and Technology, Clear Water Bay, Kowloon, Hong Kong, China

⁶² Department of Physics, National Tsing Hua University, Hsinchu, Taiwan

⁶³ Department of Physics, Indiana University, Bloomington, IN, United States of America

⁶⁴ (a) INFN Gruppo Collegato di Udine, Sezione di Trieste, Udine; (b) ICTP, Trieste; (c) Dipartimento di Chimica, Fisica e Ambiente, Università di Udine, Udine, Italy

- 65 ^(a) INFN Sezione di Lecce; ^(b) Dipartimento di Matematica e Fisica, Università del Salento, Lecce, Italy
 66 ^(a) INFN Sezione di Milano; ^(b) Dipartimento di Fisica, Università di Milano, Milano, Italy
 67 ^(a) INFN Sezione di Napoli; ^(b) Dipartimento di Fisica, Università di Napoli, Napoli, Italy
 68 ^(a) INFN Sezione di Pavia; ^(b) Dipartimento di Fisica, Università di Pavia, Pavia, Italy
 69 ^(a) INFN Sezione di Pisa; ^(b) Dipartimento di Fisica E. Fermi, Università di Pisa, Pisa, Italy
 70 ^(a) INFN Sezione di Roma; ^(b) Dipartimento di Fisica, Sapienza Università di Roma, Roma, Italy
 71 ^(a) INFN Sezione di Roma Tor Vergata; ^(b) Dipartimento di Fisica, Università di Roma Tor Vergata, Roma, Italy
 72 ^(a) INFN Sezione di Roma Tre; ^(b) Dipartimento di Matematica e Fisica, Università Roma Tre, Roma, Italy
 73 ^(a) INFN-TIFPA; ^(b) Università degli Studi di Trento, Trento, Italy
 74 Institut für Astro- und Teilchenphysik, Leopold-Franzens-Universität, Innsbruck, Austria
 75 University of Iowa, Iowa City, IA, United States of America
 76 Department of Physics and Astronomy, Iowa State University, Ames, IA, United States of America
 77 Joint Institute for Nuclear Research, Dubna, Russia
 78 ^(a) Departamento de Engenharia Elétrica, Universidade Federal de Juiz de Fora (UFJF), Juiz de Fora; ^(b) Universidade Federal do Rio De Janeiro COPPE/EE/IF, Rio de Janeiro;
^(c) Universidade Federal de São João del Rei (UFSJ), São João del Rei; ^(d) Instituto de Física, Universidade de São Paulo, São Paulo, Brazil
 79 KEK, High Energy Accelerator Research Organization, Tsukuba, Japan
 80 Graduate School of Science, Kobe University, Kobe, Japan
 81 ^(a) AGH University of Science and Technology, Faculty of Physics and Applied Computer Science, Krakow; ^(b) Marian Smoluchowski Institute of Physics, Jagiellonian University, Krakow, Poland
 82 Institute of Nuclear Physics Polish Academy of Sciences, Krakow, Poland
 83 Faculty of Science, Kyoto University, Kyoto, Japan
 84 Kyoto University of Education, Kyoto, Japan
 85 Research Center for Advanced Particle Physics and Department of Physics, Kyushu University, Fukuoka, Japan
 86 Instituto de Física La Plata, Universidad Nacional de La Plata and CONICET, La Plata, Argentina
 87 Physics Department, Lancaster University, Lancaster, United Kingdom
 88 Oliver Lodge Laboratory, University of Liverpool, Liverpool, United Kingdom
 89 Department of Experimental Particle Physics, Józef Stefan Institute and Department of Physics, University of Ljubljana, Ljubljana, Slovenia
 90 School of Physics and Astronomy, Queen Mary University of London, London, United Kingdom
 91 Department of Physics, Royal Holloway University of London, Egham, United Kingdom
 92 Department of Physics and Astronomy, University College London, London, United Kingdom
 93 Louisiana Tech University, Ruston, LA, United States of America
 94 Fysiska institutionen, Lunds universitet, Lund, Sweden
 95 Centre de Calcul de l'Institut National de Physique Nucléaire et de Physique des Particules (IN2P3), Villeurbanne, France
 96 Departamento de Física Teorica C-15 and CIAFF, Universidad Autónoma de Madrid, Madrid, Spain
 97 Institut für Physik, Universität Mainz, Mainz, Germany
 98 School of Physics and Astronomy, University of Manchester, Manchester, United Kingdom
 99 CPPM, Aix-Marseille Université, CNRS/IN2P3, Marseille, France
 100 Department of Physics, University of Massachusetts, Amherst, MA, United States of America
 101 Department of Physics, McGill University, Montreal, QC, Canada
 102 School of Physics, University of Melbourne, Victoria, Australia
 103 Department of Physics, University of Michigan, Ann Arbor, MI, United States of America
 104 Department of Physics and Astronomy, Michigan State University, East Lansing, MI, United States of America
 105 B.I. Stepanov Institute of Physics, National Academy of Sciences of Belarus, Minsk, Belarus
 106 Research Institute for Nuclear Problems of Byelorussian State University, Minsk, Belarus
 107 Group of Particle Physics, University of Montreal, Montreal, QC, Canada
 108 P.N. Lebedev Physical Institute of the Russian Academy of Sciences, Moscow, Russia
 109 Institute for Theoretical and Experimental Physics (ITEP), Moscow, Russia
 110 National Research Nuclear University MEPhI, Moscow, Russia
 111 D.V. Skobeltsyn Institute of Nuclear Physics, M.V. Lomonosov Moscow State University, Moscow, Russia
 112 Fakultät für Physik, Ludwig-Maximilians-Universität München, München, Germany
 113 Max-Planck-Institut für Physik (Werner-Heisenberg-Institut), München, Germany
 114 Nagasaki Institute of Applied Science, Nagasaki, Japan
 115 Graduate School of Science and Kobayashi-Maskawa Institute, Nagoya University, Nagoya, Japan
 116 Department of Physics and Astronomy, University of New Mexico, Albuquerque, NM, United States of America
 117 Institute for Mathematics, Astrophysics and Particle Physics, Radboud University Nijmegen/Nikhef, Nijmegen, Netherlands
 118 Nikhef National Institute for Subatomic Physics and University of Amsterdam, Amsterdam, Netherlands
 119 Department of Physics, Northern Illinois University, DeKalb, IL, United States of America
 120 ^(a) Budker Institute of Nuclear Physics and NSU, SB RAS, Novosibirsk; ^(b) Novosibirsk State University, Novosibirsk, Russia
 121 Institute for High Energy Physics of the National Research Centre Kurchatov Institute, Protvino, Russia
 122 Department of Physics, New York University, New York, NY, United States of America
 123 Ohio State University, Columbus, OH, United States of America
 124 Faculty of Science, Okayama University, Okayama, Japan
 125 Homer L. Dodge Department of Physics and Astronomy, University of Oklahoma, Norman, OK, United States of America
 126 Department of Physics, Oklahoma State University, Stillwater, OK, United States of America
 127 Palacký University, RCPTM, Joint Laboratory of Optics, Olomouc, Czech Republic
 128 Center for High Energy Physics, University of Oregon, Eugene, OR, United States of America
 129 LAL, Université Paris-Sud, CNRS/IN2P3, Université Paris-Saclay, Orsay, France
 130 Graduate School of Science, Osaka University, Osaka, Japan
 131 Department of Physics, University of Oslo, Oslo, Norway
 132 Department of Physics, Oxford University, Oxford, United Kingdom
 133 LPNHE, Sorbonne Université, Paris Diderot Sorbonne Paris Cité, CNRS/IN2P3, Paris, France
 134 Department of Physics, University of Pennsylvania, Philadelphia, PA, United States of America
 135 Konstantinov Nuclear Physics Institute of National Research Centre "Kurchatov Institute", PNPI, St. Petersburg, Russia
 136 Department of Physics and Astronomy, University of Pittsburgh, Pittsburgh, PA, United States of America
 137 ^(a) Laboratório de Instrumentação e Física Experimental de Partículas – LIP; ^(b) Departamento de Física, Faculdade de Ciências, Universidade de Lisboa, Lisboa; ^(c) Departamento de Física, Universidade de Coimbra, Coimbra; ^(d) Centro de Física Nuclear da Universidade de Lisboa, Lisboa; ^(e) Departamento de Física, Universidade do Minho, Braga; ^(f) Departamento de Física Teórica y del Cosmos, Universidad de Granada, Granada (Spain); ^(g) Dep Física and CEFITEC of Faculdade de Ciências e Tecnologia, Universidade Nova de Lisboa, Caparica, Portugal
 138 Institute of Physics, Academy of Sciences of the Czech Republic, Prague, Czech Republic
 139 Czech Technical University in Prague, Prague, Czech Republic

- 140 Charles University, Faculty of Mathematics and Physics, Prague, Czech Republic
 141 Particle Physics Department, Rutherford Appleton Laboratory, Didcot, United Kingdom
 142 IRFU, CEA, Université Paris-Saclay, Gif-sur-Yvette, France
 143 Santa Cruz Institute for Particle Physics, University of California Santa Cruz, Santa Cruz, CA, United States of America
 144 ^(a) Departamento de Física, Pontificia Universidad Católica de Chile, Santiago; ^(b) Departamento de Física, Universidad Técnica Federico Santa María, Valparaíso, Chile
 145 Department of Physics, University of Washington, Seattle, WA, United States of America
 146 Department of Physics and Astronomy, University of Sheffield, Sheffield, United Kingdom
 147 Department of Physics, Shinshu University, Nagano, Japan
 148 Department Physik, Universität Siegen, Siegen, Germany
 149 Department of Physics, Simon Fraser University, Burnaby, BC, Canada
 150 SLAC National Accelerator Laboratory, Stanford, CA, United States of America
 151 Physics Department, Royal Institute of Technology, Stockholm, Sweden
 152 Departments of Physics and Astronomy, Stony Brook University, Stony Brook, NY, United States of America
 153 Department of Physics and Astronomy, University of Sussex, Brighton, United Kingdom
 154 School of Physics, University of Sydney, Sydney, Australia
 155 Institute of Physics, Academia Sinica, Taipei, Taiwan
 156 ^(a) E. Andronikashvili Institute of Physics, Iv. Javakhishvili Tbilisi State University, Tbilisi; ^(b) High Energy Physics Institute, Tbilisi State University, Tbilisi, Georgia
 157 Department of Physics, Technion, Israel Institute of Technology, Haifa, Israel
 158 Raymond and Beverly Sackler School of Physics and Astronomy, Tel Aviv University, Tel Aviv, Israel
 159 Department of Physics, Aristotle University of Thessaloniki, Thessaloniki, Greece
 160 International Center for Elementary Particle Physics and Department of Physics, University of Tokyo, Tokyo, Japan
 161 Graduate School of Science and Technology, Tokyo Metropolitan University, Tokyo, Japan
 162 Department of Physics, Tokyo Institute of Technology, Tokyo, Japan
 163 Tomsk State University, Tomsk, Russia
 164 Department of Physics, University of Toronto, Toronto, ON, Canada
 165 ^(a) TRIUMF, Vancouver, BC; ^(b) Department of Physics and Astronomy, York University, Toronto, ON, Canada
 166 Division of Physics and Tomonaga Center for the History of the Universe, Faculty of Pure and Applied Sciences, University of Tsukuba, Tsukuba, Japan
 167 Department of Physics and Astronomy, Tufts University, Medford, MA, United States of America
 168 Department of Physics and Astronomy, University of California Irvine, Irvine, CA, United States of America
 169 Department of Physics and Astronomy, University of Uppsala, Uppsala, Sweden
 170 Department of Physics, University of Illinois, Urbana, IL, United States of America
 171 Instituto de Física Corpuscular (IFIC), Centro Mixto Universidad de Valencia – CSIC, Valencia, Spain
 172 Department of Physics, University of British Columbia, Vancouver, BC, Canada
 173 Department of Physics and Astronomy, University of Victoria, Victoria, BC, Canada
 174 Fakultät für Physik und Astronomie, Julius-Maximilians-Universität Würzburg, Würzburg, Germany
 175 Department of Physics, University of Warwick, Coventry, United Kingdom
 176 Waseda University, Tokyo, Japan
 177 Department of Particle Physics, Weizmann Institute of Science, Rehovot, Israel
 178 Department of Physics, University of Wisconsin, Madison, WI, United States of America
 179 Fakultät für Mathematik und Naturwissenschaften, Fachgruppe Physik, Bergische Universität Wuppertal, Wuppertal, Germany
 180 Department of Physics, Yale University, New Haven, CT, United States of America
 181 Yerevan Physics Institute, Yerevan, Armenia

^a Also at Borough of Manhattan Community College, City University of New York, NY; United States of America.

^b Also at California State University, East Bay; United States of America.

^c Also at Centre for High Performance Computing, CSIR Campus, Rosebank, Cape Town; South Africa.

^d Also at CERN, Geneva; Switzerland.

^e Also at CPPM, Aix-Marseille Université, CNRS/IN2P3, Marseille; France.

^f Also at Département de Physique Nucléaire et Corpusculaire, Université de Genève, Genève; Switzerland.

^g Also at Departament de Física de la Universitat Autònoma de Barcelona, Barcelona; Spain.

^h Also at Departamento de Física Teórica y del Cosmos, Universidad de Granada, Granada (Spain); Spain.

ⁱ Also at Departamento de Física, Instituto Superior Técnico, Universidade de Lisboa, Lisboa; Portugal.

^j Also at Department of Applied Physics and Astronomy, University of Sharjah, Sharjah; United Arab Emirates.

^k Also at Department of Financial and Management Engineering, University of the Aegean, Chios; Greece.

^l Also at Department of Physics and Astronomy, University of Louisville, Louisville, KY; United States of America.

^m Also at Department of Physics and Astronomy, University of Sheffield, Sheffield; United Kingdom.

ⁿ Also at Department of Physics, California State University, Fresno CA; United States of America.

^o Also at Department of Physics, California State University, Sacramento CA; United States of America.

^p Also at Department of Physics, King's College London, London; United Kingdom.

^q Also at Department of Physics, St. Petersburg State Polytechnical University, St. Petersburg; Russia.

^r Also at Department of Physics, Stanford University; United States of America.

^s Also at Department of Physics, University of Fribourg, Fribourg; Switzerland.

^t Also at Department of Physics, University of Michigan, Ann Arbor MI; United States of America.

^u Also at Dipartimento di Fisica E. Fermi, Università di Pisa, Pisa; Italy.

^v Also at Giresun University, Faculty of Engineering, Giresun; Turkey.

^w Also at Graduate School of Science, Osaka University, Osaka; Japan.

^x Also at Hellenic Open University, Patras; Greece.

^y Also at Horia Hulubei National Institute of Physics and Nuclear Engineering, Bucharest; Romania.

^z Also at II. Physikalisches Institut, Georg-August-Universität Göttingen, Göttingen; Germany.

^{aa} Also at Institució Catalana de Recerca i Estudis Avancats, ICREA, Barcelona; Spain.

^{ab} Also at Institut für Experimentalphysik, Universität Hamburg, Hamburg; Germany.

^{ac} Also at Institute for Mathematics, Astrophysics and Particle Physics, Radboud University Nijmegen/Nikhef, Nijmegen; Netherlands.

^{ad} Also at Institute for Particle and Nuclear Physics, Wigner Research Centre for Physics, Budapest; Hungary.

^{ae} Also at Institute of Particle Physics (IPP); Canada.

^{af} Also at Institute of Physics, Academia Sinica, Taipei; Taiwan.

^{ag} Also at Institute of Physics, Azerbaijan Academy of Sciences, Baku; Azerbaijan.

- ah* Also at Institute of Theoretical Physics, Ilia State University, Tbilisi; Georgia.
ai Also at Instituto de Física Teórica de la Universidad Autónoma de Madrid; Spain.
aj Also at İstanbul University, Dept. of Physics, İstanbul; Turkey.
ak Also at LAL, Université Paris-Sud, CNRS/IN2P3, Université Paris-Saclay, Orsay; France.
al Also at Louisiana Tech University, Ruston LA; United States of America.
am Also at LPNHE, Sorbonne Université, Paris Diderot Sorbonne Paris Cité, CNRS/IN2P3, Paris; France.
an Also at Manhattan College, New York NY; United States of America.
ao Also at Moscow Institute of Physics and Technology State University, Dolgoprudny; Russia.
ap Also at National Research Nuclear University MEPhI, Moscow; Russia.
aq Also at Physikalisches Institut, Albert-Ludwigs-Universität Freiburg, Freiburg; Germany.
ar Also at School of Physics, Sun Yat-sen University, Guangzhou; China.
as Also at The City College of New York, New York NY; United States of America.
at Also at The Collaborative Innovation Center of Quantum Matter (CICQM), Beijing; China.
au Also at Tomsk State University, Tomsk, and Moscow Institute of Physics and Technology State University, Dolgoprudny; Russia.
av Also at TRIUMF, Vancouver BC; Canada.
aw Also at Università di Napoli Parthenope, Napoli; Italy.
* Deceased.